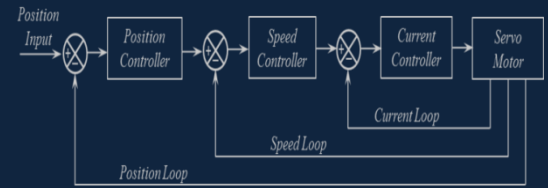




e-ISSN: 2618-575X



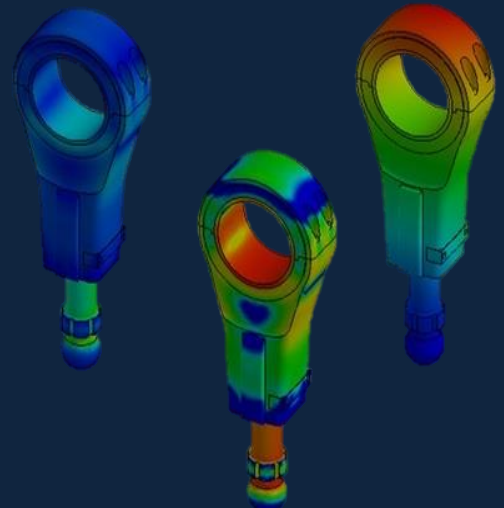
International Advanced Researches and Engineering Journal

Aerospace Engineering,
Aquaculture and Fisheries Engineering,
Architecture,
Bioengineering,
Chemical Engineering,
Civil Engineering,
Computer Engineering,
Electrical and Electronics,
Energy,
Environmental Engineering,
Food Engineering,
Geomatics Engineering,
Industrial Engineering,
Industrial Applications,
Machine Theory and Dynamics,
Manufacturing,
Mechanical Engineering,
Mechanics,
Mechatronics,
Medical,
Modeling and Simulation,
Physics Engineering,
Robotics,
Textile Engineering
Health in Engineering

$$F=ma$$

$$E=mc^2$$

$$\int \frac{dy}{dx} dt$$



Volume: 03 / Issue: 02 / August 2019



e-ISSN: 2618-575X

Available online at www.dergipark.gov.tr

INTERNATIONAL ADVANCED RESEARCHES
and
ENGINEERING JOURNAL

Journal homepage: www.dergipark.gov.tr/iarej

International
Open Access



Volume 03
Issue 02

August, 2019

International Advanced Researches and Engineering Journal (IAREJ) is a double-blind peer-reviewed and publicly available online journal that has Editorial Board (<http://dergipark.gov.tr/iarej/board>). The editor in chief of IAREJ welcomes the submissions that cover theoretical and/or applied researches on **Engineering** and related science with Engineering. The publication language of the Journal is **English**. **Writing Rules** are given in Author Guidelines (<http://dergipark.gov.tr/iarej/writing-rules>). IAREJ publishes **original papers** that are research papers and technical review papers.

IAREJ publication, which is **open access**, is **free of charge**. There is no article submission and processing charges (APCs).

IAREJ is indexed & abstracted in:

Crossref (Doi beginning: 10.35860/iarej.xxxxxx)
Directory of Open Access Scholarly Researches (ROAD)
Directory of Research Journals Indexing (DRJI)
Google Scholar
Journal Factor
J-Gate
Index Copernicus
Rootindexing
Scientific Indexing Services (SIS)

Authors are responsible from the copyrights of the figures and the contents of the manuscripts, accuracy of the references, quotations and proposed ideas and the Publication Ethics (<http://dergipark.gov.tr/iarej/page/4240>).

All rights of the issue are reserved by International Advanced Researches and Engineering Journal (IAREJ). IAREJ also allows the author(s) to hold the copyright of own articles.

©

IAREJ

15 August 2019



This is an open access issue under the CC BY-NC license (<http://creativecommons.org/licenses/by-nc/4.0/>).




e-ISSN: 2618-575X

Available online at www.dergipark.gov.tr

INTERNATIONAL ADVANCED RESEARCHES
and
ENGINEERING JOURNAL

Journal homepage: www.dergipark.gov.tr/iarej

International
Open Access 

Volume 03
Issue 02

August, 2019

Table of Contents

| Research Articles | Pages |
|--|--------------|
| Synthesis and stability analysis of folic acid-graphene oxide nanoparticles for drug delivery and targeted cancer therapies <i>Neşe Keklikcioğlu Çakmak, Mustafa Küçük yazıcı and Atakan Eroğlu</i> | 81-85 |
| Electrophoretic characterization of inbred maize lines <i>Gülsemin Savaş Tuna, Burak Uyanık, Elif Eymen Özdemir, Görkem Dalgıç, Yaren Mengi and Kayıhan Z. Korkut</i> | 86-92 |
| Production of bioplastic from potato peel waste and investigation of its biodegradability <i>Ezgi Bezirhan Arıkan and H. Duygu Bilgen</i> | 93-97 |
| Determination of heat transfer coefficient and electromagnetic directional analysis of pomegranate seed <i>İsmail Üstün, Yıldız Koç, Hüseyin Yağlı, Özkan Köse, M. Tunahan Başar, Cuma Karakuş, Oğuzhan Akgöl and Ali Koç</i> | 98-104 |
| Experimental investigation of thermal coefficient of the graphene used concrete <i>Özkan Köse, Yıldız Koç, Hüseyin Yağlı, İsmail Üstün, Furkan Kasap, Nurhan Adil Öztürk and Ali Koç</i> | 105-110 |
| Experimental investigation of the effect of compression pressure on mechanical properties in glass fiber reinforced organic material-based brake pads production <i>Sait Aras and Necmettin Tarakçıoğlu</i> | 111-115 |
| Performance analysis of SRF-PLL and DDSRF-PLL algorithms for grid interactive inverters <i>Fehmi Sevilmiş and Hulusi Karaca</i> | 116-122 |
| Optimization of assignment problems in production lines with different skilled labor levels <i>Hazel Durmaz and Melik Koyuncu</i> | 123-136 |

**Research Article****Synthesis and stability analysis of folic acid-graphene oxide nanoparticles for drug delivery and targeted cancer therapies**Neşe Keklikcioğlu Çakmak ^{a,*} , Mustafa Küçük yazıcı ^a and Atakan Eroğlu ^a ^a Department of Chemical Engineering, Cumhuriyet University, Sivas 58140, Turkey

ARTICLE INFO

Article history:

Received 02 April 2018

Revised 01 September 2018

Accepted 10 September 2018

Keywords:

Cancer

Nano-graphene oxide

Folic acid

Nano-drug delivery systems

Zeta potential

ABSTRACT

Cancer is the growth and proliferation of damage-ending cells in an uncontrolled or abnormal way. Today, it takes place among the most important health problems around the world and in our country. Surgery, radiotherapy, and chemotherapy are the main treatment methods in cancer treatment. The development of resistance to chemotherapeutic medicines has led scientists to investigate this issue as well as the drug's ability to reach the targeted tumor site and destroying cancer cells in addition to normal cells. The production of various nanostructures for anticancer drug development has been one of the most important areas of nanomedicine. Thus, in the present research, the improved Hummers' method was employed for the synthesis of graphene oxide nanoparticle (NGO), and it was activated by the folic acid (FA) antibody to increase targeting ability after attachment of the drug to the nanostructure systems. SEM, FTIR, XRD, UV/Vis spectroscopy, and zeta potential analysis were performed for characterization of the products. The highest absorbance of the FA-NGO/DIW nanostructures produced at the concentration of 0.01 mg/ml-0.05 mg/ml synthesized by the Hummers' method and in the UV/Vis spectra, peaks at 232 nm and 270 nm corresponds to NGO-DIW and FA-NGO/DIW, respectively. The zeta potential value above 35 mV was obtained in all measurements, and the NGO-DIW and NGO-FA-DIW samples maintained stability for days. These findings are consistent with the few studies in the literature, and this study will guide future studies in which nanoparticle systems will be directed to the target by binding chemotherapeutic drugs.

© 2019, Advanced Researches and Engineering Journal (IAREJ) and the Author(s).

1. Introduction

Nanoparticles (NPS) represent particles between 1 and 100 nanometers in size. In nanotechnology, nanoparticles are described as small objects acting as a whole unit with regard to their features and transport [1,2]. Graphene-based nanoparticles, because of their exceptional physicochemical characteristics, various surface functionalization, good biocompatibility area, and ultra-high surface, have drawn great attention in biomedical applications, including drug delivery, biosensors, theranostics, bioimaging, etc. Two-dimensional nanomaterial - graphene was revealed for the first time in 2004 [3,4]. Graphene, which consists of a single-atom-thick sheet of sp² bonded carbon atoms that are hexagonally arrayed, presents various applications from

composite materials to quantum dots [5-10]. Graphene is present in different forms, including graphene oxide (GO), graphene sheets, and reduced graphene oxide (rGO) [11-13]. Its biodegradability and biocompatibility are the features that make GO be preferred in the area of biomedicine, particularly theranostics [14-15]. A lot of endeavors have been recently made to the nanosized materials' abilities with controlled drug delivery properties because they enable targeted delivery, efficient loading and the release of drugs in a controlled manner, and thus may be used successfully in biomedical practices.

The research conducted recently has shown that the use of low molecular weight targeting agents including folic acid as surface coatings is very promising for the specific cancer cell recognition and enhancement in the intracellular

* Corresponding author. Tel.: +90 346 219 10 10 (Ext:2232)

E-mail addresses: nkeklikcioğlu@cumhuriyet.edu.tr (N. Keklikcioğlu), mkckyzc@gmail.com (M. Küçük yazıcı), atankovv.eroğlu@gmail.com (A. Eroğlu)

ORCID: 0000-0002-8634-9232 (N. Keklikcioğlu Çakmak), 0000-0002-4030-9147 (M. Küçük yazıcı), 0000-0003-4544-5225 (A. Eroğlu)

DOI: 10.35860/iarej.411717

uptake of nanoparticles [16]. FA has short chains and a small size and thus will facilitate the internalization of nanoparticles. For example, Deb and Vimala [17] synthesized a graphene-oxide-polyethylene glycol-folic acid-camptothecin (GO-PEG-FA-CPT) drug delivery system, and this system was investigated by MTT assay by utilizing MCF-7 breast cancer cell lines. Improved anticancer activity was exhibited by the conjugate, and therefore, it might be utilized as a possible candidate for drug delivery. Folic acid-conjugated GO loaded Ce6 was determined to be a powerful candidate for active drug delivery in photodynamic therapy (PDT) [18]. The non-immunogenic, non-toxic, and stable features of folic acid turn it into an appropriate candidate for conjugation with nanocomposites [19]. Folic acid that is conjugated with nanographene oxide and polyvinylpyrrolidone (PVP) has been indicated as an advantageous nanocomposite for chemo-photothermal therapy [20].

In this research, the improved Hummers' method was employed for the synthesis of graphene oxide nanoparticle (NGO), which was activated by the folic acid antibody to increase the targeting ability after attachment of the drug to the nanostructure systems. In our aim, firstly, nano-graphene oxide was synthesized and then activated by the folic acid antibody, because of which sulfonic acid groups were embedded to NGO, bringing it to a stable state under physiological conditions.

2. Material and Method

2.1. Synthesis of NGO

The improved Hummers' method with minor modification was employed for the synthesis of GO [21-24]. For the purpose of acquiring NGO, GO was broken by the ultrasonic probe at 750W for a period of 100 min. SEM, FTIR, XRD, UV/Vis spectroscopy, and zeta potential analysis were performed for characterization of the products.

2.2. Conjugation of FA with NGO

FA-NGO was prepared in a manner described by Zhang et al. [23]. UV/Vis spectroscopy and zeta potential analysis were performed for characterization of FA-NGO.

2.3. Characterization

A scanning electron microscope (TESCAN MIRA3 XMU) was used to measure the morphologies of NGO. The FT-IR spectra of NGO were characterized by an FT-IR spectrophotometer (Bruker: Tensor II) in the 400–4000 cm^{-1} range. A diffractometer (Rigaku DMAX IIIC) was used for the purpose of obtaining X-ray diffraction (XRD) data. A UV-Vis spectrophotometer (UV-1280, Shimadzu, Japan) was used for recording the spectra of the prepared specimens in the 200 - 800 nm range. A Malvern Zetasizer Nano Z was utilized for the measurement of the

specimens' zeta potentials. In the end, for the purpose of the homogeneous dispersion of NGO particles in DIW, a probe sonicator (Sonics & amp; materials INC, USA) with 750W power was utilized.

3. Results and Discussion

An image of scanning electron microscopy (SEM) (Figure 1) provides morphological information on NGO. NGO has the appearance of black powder, is 3.1–6.8 nm in thickness, has purity > 99 wt % and lateral dimension of 15–40 μm . As a result of technical analysis, it was demonstrated that NGO has the following metal contents: C-62.39%; O-36.11%; S-1.18%; H-0.32%.

FT-IR tests showed the presence of OH ($\sim 3300 \text{ cm}^{-1}$), C=C ($\sim 1634 \text{ cm}^{-1}$) [25] functional groups in NGO (Figure. 2).

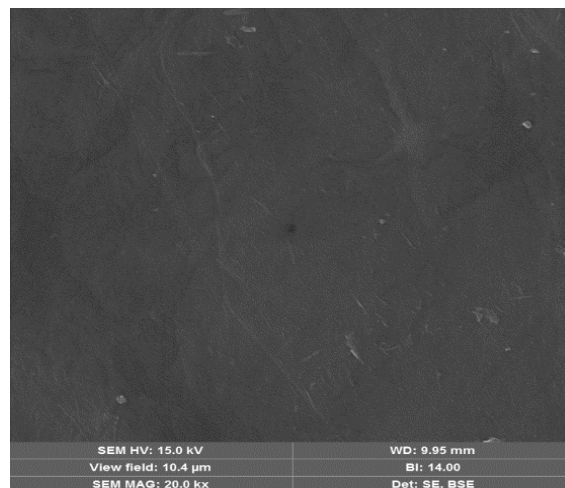


Figure 1. SEM image of NGO

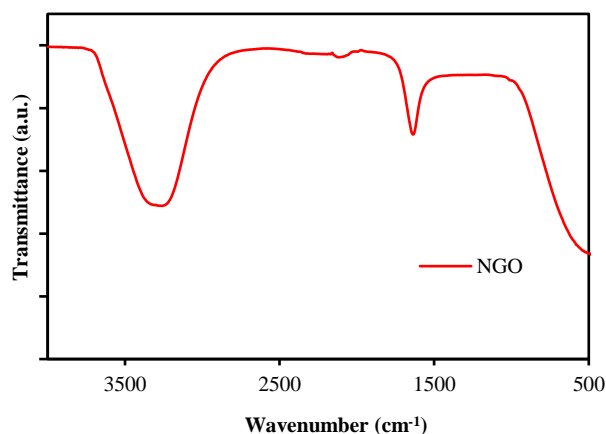


Figure 2. FT-IR spectra of NGO

Figure. 3 presents the X-ray diffraction patterns of graphite and nano-graphene oxide. Graphite shows a very strong and sharp peak at $2\theta = 26.40^\circ$, corresponding to the diffraction of the (002) plane. Following graphite oxidation to GO, the (002) reflection of graphite vanishes and a diffraction peak at $2\theta = 10.21^\circ$ exists, which

corresponds to the diffraction of the (001) plane, indicating the oxidation of graphite in a successful way [26,27].

Figure. 4 shows the UV-Vis spectra of nano-graphene oxide. The optical absorption peak at 232 nm, which originated from the π -plasmon of carbon [28], stayed without changes to a significant extent. The absorption peaks in the spectra at 232 nm and a small shoulder at 300 nm correspond to the π - π^* transition of aromatic C–C bonds and the n - π^* transition of C=O bonds, respectively.

As is seen from the UV/Vis spectra (Figure 5), a peak at 232 nm vanishes, whereas a new peak at 270nm emerges because of the existence of FA in NGO.

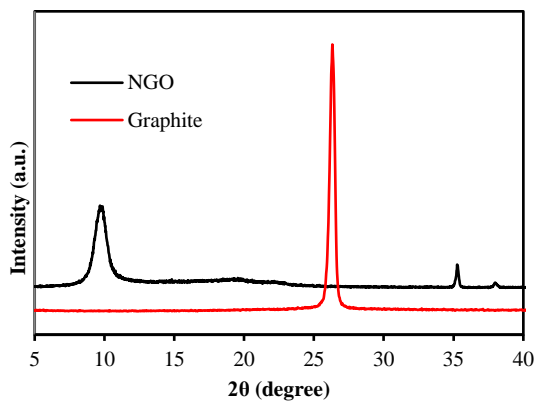


Figure 3. XRD patterns of NGO and graphite

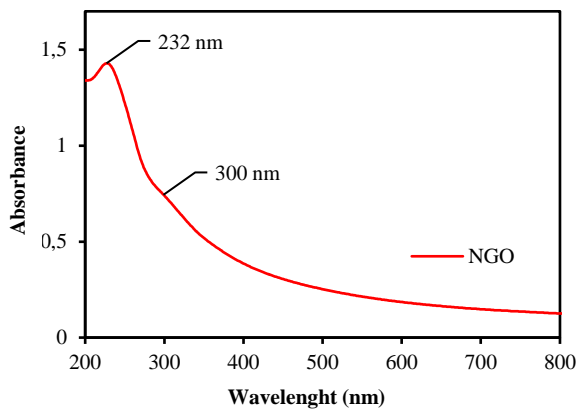


Figure 4. UV-Vis absorption spectra of NGO in DIW

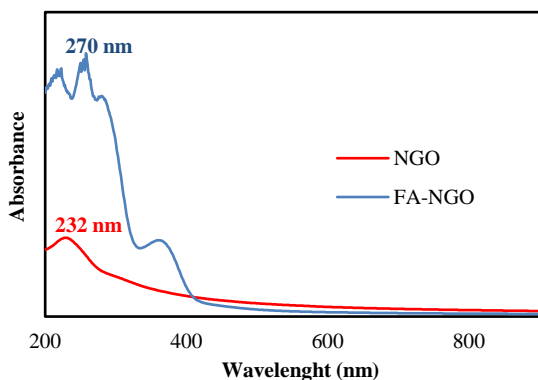


Figure 5. UV-Vis absorption spectra of NGO and FA-NGO in DIW

The stability of NGO-DIW was determined as a result of the measurement of its zeta potential values. Zeta potential represents the electrical potential between the nanoparticle surface and the base fluid, and there is a relationship between the zeta potential absolute value and nanoparticle stability. In case the measured zeta potential absolute value is above 25 mV, it is possible to say that the nanofluid produced is stable. If all the particles in suspension have a large negative or positive zeta potential, there will be a tendency for them to repel each other, but they will not tend to aggregate. The zeta potential value above 35 mV in all measurements is shown in Figure. 6 and Figure. 7, and at the same concentration, the zeta potential value of FA-NGO is quite high compared to NGO. Therefore, dispersibility of NGO in water has been improved by the bonding of FA on NGO.

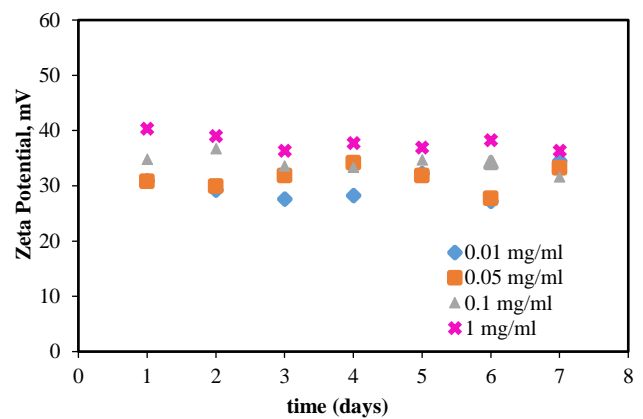


Figure 6. Stability of NGO in aqueous solutions

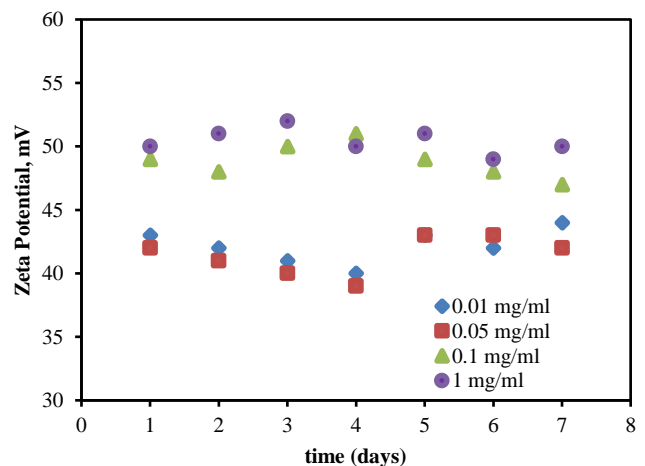


Figure 7. Stability of FA-NGO in aqueous solutions

4. Conclusions

In this study, synthesis of graphene oxide nanoparticles was performed by employing the improved Hummers' method, and it was activated by the folic acid antibody to increase the targeting ability after attachment of the drug to

the nanostructure systems. SEM, FTIR, XRD, UV/Vis spectroscopy, and zeta potential analysis were performed for characterization of the products. The highest absorbance of the FA-NGO/DIW nanostructures produced at the concentration of 0.01 mg/ml-0.05 mg/ml synthesized by the Hummers' method and in the UV/Vis spectra, peaks at 232 nm and 270 nm corresponds to NGO-DIW and FA-NGO/DIW, respectively. The NGO-DIW and NGO-FA-DIW samples maintained stability for days. There is a direct correlation between zeta potential and the stability period of nanomaterials in aqueous solutions, i.e., with an increase in the absolute value of zeta potential, the stability period increases. Consequently, it is determined that the stability of the prepared samples is preserved for days. It is possible to develop a new drug delivery system which is based on FA-conjugated NGO for the loading and targeted delivery of anticancer drugs in future studies. Furthermore, loading in a controlled manner and targeted delivery of mixed anticancer drugs by utilizing the graphene-based nanocarriers in question can be implemented in biomedicine in a widespread way.

Acknowledgment

This study is supported by TÜBİTAK BİDEB Authority under the project numbered 2209/A program 1919B011602924. We would like to thank TUBITAK Scientific Human Resource Support Program for their support in conducting this research..

Nomenclature

NGO : Graphene oxide nanoparticle
 FA : Folic acid
 DIW : Deionized water

References

- Warheit, D. B., Sayes, C. M., Reed, K. L., & Swain, K. A. Health effects related to nanoparticle exposures: environmental, health and safety considerations for assessing hazards and risks. *Pharmacology & therapeutics*, 2008, 120 (1), 35-42.
- Gonzalez, L., Lison, D., & Kirsch-Volders, M. Genotoxicity of engineered nanomaterials: a critical review. *Nanotoxicology*, 2008, 2(4), 252-273.
- Geim, Andre K., and Konstantin S. Novoselov. The rise of graphene, *Nature materials*, 2007, 6.3, 183.
- Neto, A. C., Guinea, F., Peres, N. M., Novoselov, K. S., & Geim, A. K. The electronic properties of graphene. *Reviews of modern physics*, 2009, 81(1), 109.
- Becerril, H. A., Mao, J., Liu, Z., Stoltenberg, R. M., Bao, Z., & Chen, Y. Evaluation of solution-processed reduced graphene oxide films as transparent conductors. *ACS nano*, 2008, 2(3), 463-470.
- Stankovich, S., Dikin, D. A., Dommett, G. H., Kohlhaas, K. M., Zimney, E. J., Stach, E. A., ... & Ruoff, R. S. Graphene-based composite materials. *nature*, 2006, 442(7100), 282.
- Wang, C., Li, D., Too, C. O., & Wallace, G. G. Electrochemical properties of graphene paper electrodes used in lithium batteries. *Chemistry of Materials*, 2009, 21(13), 2604-2606.
- Pasricha, R., Gupta, S., & Srivastava, A. K. A Facile and Novel Synthesis of Ag-Graphene-Based Nanocomposites. *Small*, 2009, 5(20), 2253-2259.
- Shi, Y., Fang, W., Zhang, K., Zhang, W., & Li, L. J. Photoelectrical Response in Single-Layer Graphene Transistors. *Small*, 2009, 5(17), 2005-2011.
- Lv, X., Huang, Y., Liu, Z., Tian, J., Wang, Y., Ma, Y., ... & Chen, Y. Photoconductivity of Bulk-Film-Based Graphene Sheets. *Small*, 2009, 5(14), 1682-1687.
- Dhand, V., Rhee, K. Y., Kim, H. J., & Jung, D. H. A comprehensive review of graphene nanocomposites: research status and trends. *Journal of Nanomaterials*, 2013, 158.
- Marcano, D. C., Kosynkin, D. V., Berlin, J. M., Sinitskii, A., Sun, Z., Slesarev, A., ... & Tour, J. M. Improved synthesis of graphene oxide. *ACS nano*, 2010, 4(8), 4806-4814.
- Sun, Z., Yan, Z., Yao, J., Beitler, E., Zhu, Y., & Tour, J. M. Growth of graphene from solid carbon sources. *Nature*, 2010, 468(7323), 549.
- Urbas, K., Aleksandrak, M., Jedrzejczak, M., Jedrzejczak, M., Rakoczy, R., Chen, X., & Mijowska, E. Chemical and magnetic functionalization of graphene oxide as a route to enhance its biocompatibility. *Nanoscale research letters*, 2014, 9(1), 656.
- Yang, K., Feng, L., Hong, H., Cai, W., & Liu, Z. Preparation and functionalization of graphene nanocomposites for biomedical applications. *Nature protocols*, 2013, 8(12), 2392.
- Zhang, Y., Sun, C., Kohler, N., & Zhang, M. Self-assembled coatings on individual monodisperse magnetite nanoparticles for efficient intracellular uptake. *Biomedical microdevices*, 2004, 6(1), 33-40.
- Deb, A., & Vimala, R. Camptothecin loaded graphene oxide nanoparticle functionalized with polyethylene glycol and folic acid for anticancer drug delivery. *Journal of Drug Delivery Science and Technology*, 2018, 43, 333-342.
- Huang, Peng, et al. Folic acid-conjugated graphene oxide loaded with photosensitizers for targeting photodynamic therapy. *Theranostics*, 2011, 1: 240.
- Low, Philip S.; Henne, Walter A.; Doornweerd, Derek D. Discovery and development of folic-acid-based receptor targeting for imaging and therapy of cancer and inflammatory diseases. *Accounts of chemical research*, 2007, 41.1: 120-129.
- Qin, X. C., Guo, Z. Y., Liu, Z. M., Zhang, W., Wan, M. M., & Yang, B. W. Folic acid-conjugated graphene oxide for cancer targeted chemo-photothermal therapy. *Journal of photochemistry and photobiology B: Biology*, 2013, 120, 156-162.
- Hummers Jr, W. S., & Offeman, R. E. Preparation of graphitic oxide. *Journal of the American chemical society*, 1958, 80(6), 1339-1339.
- Kovtyukhova, N. I., Ollivier, P. J., Martin, B. R., Mallouk, T. E., Chizhik, S. A., Buzaneva, E. V., & Gorchinskiy, A. D. Layer-by-layer assembly of ultrathin composite films from micron-sized graphite oxide sheets and polycations. *Chemistry of materials*, 1999, 11(3), 771-778.
- Zhang, L., Xia, J., Zhao, Q., Liu, L., & Zhang, Z. Functional graphene oxide as a nanocarrier for controlled loading and targeted delivery of mixed anticancer drugs. *Small*, 2010, 6(4), 537-544.
- Keklikcioğlu Çakmak, N., Temel, Ü., Yapıcı, K. Examination Of Rheological Behavior Of Water-Based Graphene Oxide Nanofluids. *Cumhuriyet Science Journal*, 2017, 38 (4), 176-183.
- Szabó, T., Berkesi, O., & Dékány, I. DRIFT study of deuterium-exchanged graphite oxide. *Carbon*, 2005, 43(15), 3186-3189.

26. Pradhan, S. K., Xiao, B., Mishra, S., Killam, A., & Pradhan, A. K. Resistive switching behavior of reduced graphene oxide memory cells for low power nonvolatile device application. *Scientific reports*, 2016, 6, 26763.
27. Angelopoulou, A., Voulgari, E., Diamanti, E. K., Gournis, D., & Avgoustakis, K. Graphene oxide stabilized by PLA–PEG copolymers for the controlled delivery of paclitaxel. *European Journal of Pharmaceutics and Biopharmaceutics*, 2015, 93, 18-26.
28. Reed, B. W., & Sarikaya, M. Electronic properties of carbon nanotubes by transmission electron energy-loss spectroscopy. *Physical Review B*, 2001, 64(19), 195404.



Research Article

Electrophoretic characterization of inbred maize lines

Gülsemin Savaş Tuna ^{a,*} , Burak Uyanık ^a , Elif Eymen Özdemir ^a , Görkem Dalgıç ^a ,
Yaren Mengi ^a  and Kayıhan Z. Korkut ^b 

^a Aden Science High School, Tekirdağ, 59030, Turkey

^b Namık Kemal University, Faculty of Agriculture, Department of Field Crops, Tekirdağ, 59030, Turkey

ARTICLE INFO

Article history:

Received 06 April 2018

Revised 13 November 2018

Accepted 27 November 2018

Keywords:

Zea mays L.

Inbred line

SDS-PAGE

Gliadin electrophoresis,

Electrophoretic character

ABSTRACT

In this study, 50 inbred lines (S₄) of maize (*Zea mays indentata* Sturt.), which were developed by the Department of Field Crops, Faculty of Agriculture, University of Namık Kemal, were used as a material. In the study, the band patterns of the gliadin protein of inbred lines were determined by the SDS – PAGE method, and regarding the ratio density data of the genotypes, the number of the bands and the spreading of them to the gliadin regions were examined. At the end of the electrophoresis examinations, it was revealed that the band number of the gliadin proteins in the inbred maize lines was between 11 and 20, the relative mobility of the genotypes was between 18 and 90 kDA, and according to the gliadin regions, the bands were mainly in the omega, beta and gamma regions, respectively. It was found out that the relative mobility was minimum in the alpha region. As a result of the study, it was determined that some lines were formed by similar populations with the obtained band patterns, and the majority were different. This indicates that genetic diversity exists in the examined lines, and the obtained data can be used in the breeding studies.

© 2019, Advanced Researches and Engineering Journal (IAREJ) and the Author(s).

1. Introduction

Maize is an annual summer-growing cereal included in the Poaceae family. Its origin is America, and it was first cultivated in Rio Balsas region of Mexico about 9000 years ago [1]. It can be grown in tropical and subtropical mild temperate zones and can be cultivated almost everywhere in the world. While grain cropping is carried out in about 712 million hectares of the total 1.5 billion hectares of agricultural land in the world, maize is cultivated in 183 million hectares of this area. Maize is the most cultivated grain after wheat and rice [2]. In our country, according to 2016 data, maize was grown in an area of 6.820.000 decares, and its production was 6.300.000 tons [3]. Under optimum conditions, in Adana, Sakarya and Aydın provinces (under main product conditions), around 1400-1600 kg/da yield is obtained per unit area, and our country is generally above the average of the world and EU countries in terms of maize yield [4].

Maize production has indispensable importance in terms of agriculture and economy of our country. The contribution of grain maize production to Turkey's economy is calculated as approximately 4.05 billion TL according to 2014 data of the TÜİK (Turkish Statistical Institute) [5].

Maize is rich in fat and protein and it is consumed as human food and animal feed. Furthermore, in terms of industry, it is abundantly used in the production of starch, syrup, beer, alcohol and whiskey [6]. The proteins stored in the endosperm of cereals are classified into two main groups as prolamines and glutelins. Prolamines are the proteins that are soluble in alcohol. Maize includes zein from the prolamine group [7]. In the studies carried out by the SDS-PAGE method, it was determined that the zein protein is composed of two different polypeptides. These polypeptides are hordein that is abundant in barley and gliadin that is abundant in wheat [8]. There are many

* Corresponding author. Tel.: +90 505 253 3430

E-mail addresses: glsvs@yahoo.com (G. Savaş Tuna), burakuyanik22@gmail.com (B. Uyanık), elif-eymen@hotmail.com (E. Eymen Özdemir),

grkm.dlgc.242@outlook.com (G. Dalgıç), yarenmengi@hotmail.com (Y. Mengi), kayihankorkut@nku.edu.tr (K.Z. Korkut)

ORCID: 0000-0003-2089-2790 (G. Savaş Tuna), 0000-0002-5576-8581 (B. Uyanık), 0000-0002-2959-6042 (E. Eymen Özdemir),

0000-0003-1258-2733 (G. Dalgıç), 0000-0002-2462-9888 (Y. Mengi), 0000-0002-2536-2791 (K.Z. Korkut)

DOI:10.35860/iarej.413379

studies related to zein in maize in the literature [9-10-11-12 -13]. However, the studies related to gliadin were mostly carried out in wheat [14-15-16-17]. The basic amino acids are disproportionately found in the structure of zein [11]. For this reason, zeins are classified as α , β , γ and δ according to their molecular mass (18). δ -zein (10-kDa) is very rich in terms of methionine, and if it is not available, the quality of maize is negatively affected. It is thought that maize is rich in terms of methionine before it is cultivated, but its high methionine characteristic is lost after it is cultivated [19]. Therefore, while breeders try to improve the grain quality, they attempt to reduce the zein content and thus to facilitate the accumulation of albumins and globulins, which have a more balanced amino acid ratio, or to produce lines containing high lysine, methionine and phenylalanine by obtaining hybrids through using the ancestors of corn [20].

Maize is the plant on which the breeding studies are most intensely performed in the world. Hybrid maize breeding studies started in our country in the 1950s. Along with the breeding studies carried out until today, valuable populations, a large number of inbred lines and hybrid maize varieties have been developed [4]. The basic step in the hybrid variety breeding is to obtain inbred lines. When the studies carried out on maize in our country are examined, it is observed that inbred lines or hybrid maize varieties have been developed; however, there is no study on zein in the content of these materials or gliadin or hordein in the structure of zein. In this study, it was aimed 1- to examine the gliadin band patterns of the inbred lines by the SDS-PAGE method, and 2- to determine the similarities and differences of the lines according to band patterns.

2. Material and Method

2.1 Material

In the study, 50 inbred *Zea mays indentata* Sturt. lines at S₄ generation belonging to the Department of Field Crops, Faculty of Agriculture, University of Namık Kemal, were used as the material (Table 1).

2.2 Method

2.2.1 Planting and cultivation of maize seeds

The seeds of the 50 inbred maize lines at S₄ generation developed by selection and inbreeding in previous years were planted in the trial field of the Faculty of Agriculture, University of Namık Kemal. In the experiment set up with three repetitive, the parcel length was 5.00 m, inter-row spacing was 0.70 m, and intra-row spacing was 0.25 m. In the experiment, each line was manually planted in a single row (three seeds for each line). The germination of the seeds and the growth of the plants were monitored, and irrigation, hoeing, and fertilization were performed if required. During the

harvest-time, the cobs of each line were picked one by one, put into paper bags and stored in the seed chamber of the Department of Field Crops.

2.2.2 SDS-PAGE Method

The SDS-PAGE method was used to reveal the genotypic differences of the lines used in the experiment. Five seeds for each line were examined at this stage. The electrophoresis procedures used in the determination of the protein bands of the genotypes were performed by following the steps below;

- One grain maize was thoroughly crushed and then ground, 0.04 g was taken from the sample and placed into the Eppendorf tube. Then, 500 μ l of 70% ethanol was added on this sample, and it was kept waiting for 2 hours. During waiting, the tubes were mixed in a vortex mixer for 1 minute every 10 minutes. At the end of this period, the tubes were centrifuged at 13.000 rpm for 5 minutes. 100 μ l was taken from the centrifuged sample and transferred to a separate tube.

- 100 μ l of SDS solution, 25 μ l of Mercaptoethanol, 190 μ l of 60% Glycerin, and 190 μ l of 0.005% Bromphenol blue solution were added to the tubes, and they were kept waiting in hot water bath (90 °C) for 2.5 minutes. 10 μ l of sample was taken from the tubes and loaded into the gel.

Two gels (loading gel and running gel) were prepared for electrophoresis. The following stocks were made ready before these gels were prepared.

Water: 4 ml of deionized water was used to prepare 10 ml gel.

Acrylamide-Bisacrylamide mixture: 9 g of acrylamide and 0.24 g of bisacrylamide were weighed and completed to 30 ml with deionized water. After the prepared 30% acrylamide was mixed in the mechanical shaker for an hour, it became ready for use. After the usage, the remaining part can be stored in a dark environment.

SDS (10%): 1g of SDS was taken and completed to 10 ml with deionized water, and it was stirred and allowed to dissolve. The prepared solution was stored at room temperature until use.

1.5 M Tris (pH 8.8): 9.075 g of Tris was weighed and completed to 50 ml with deionized water, and the pH value of the solution was measured. The pH value of the solution was adjusted to 8.8 by using concentrated HCl.

1 M Tris (pH 6.8): 6.055 g of Tris was weighed and completed to 50 ml with deionized water, and the pH value of the solution was measured. Then, the pH value was adjusted to 6.8 by using concentrated HCl.

10% APS: After 1 g of APS (ammonium persulphate) was weighed, it was completed to 10 ml with deionized water to prepare the solution. During the use of this solution, attention was paid to prepare it as fresh.

TEMED: The ready-to-use TEMED solution was used.

Table 1. Inbred Zea mays indentata Sturt. Lines numbers, relative mobility value of bands, band number of gliadin regions (Ω , γ , β , α) and total band numbers used as a material in the experiment

| BN | GR | | | | Relative Mobility (Rm) | | | | | | | | | | | | | | | | | LN | | | | |
|----|----------|---------|----------|----------|------------------------|----|----|----|----|----|----|----|----|----|----|----|----|----|----|----|----|----|----|----|--------|--------|
| | α | β | γ | Ω | | | | | 87 | 82 | 76 | 70 | 60 | 53 | 49 | 46 | 41 | 39 | 37 | 31 | 25 | | 24 | 21 | 19 | |
| | | | | | | | | | 88 | 82 | 77 | 68 | 61 | 57 | 55 | 48 | 47 | 42 | 39 | 37 | 33 | 31 | 26 | 23 | 21 | SM 158 |
| 17 | 1 | 2 | 2 | 12 | | | | | | | | | | | | | | | | | | | | | | SM 21 |
| 14 | - | 3 | 1 | 10 | | | | | | | 83 | 81 | 76 | 69 | 59 | 53 | 49 | 45 | 40 | 37 | 30 | 26 | 24 | 19 | SM 191 | |
| 14 | 1 | 2 | 2 | 9 | | | | | | | 87 | 83 | 76 | 73 | 62 | 59 | 57 | 54 | 42 | 38 | 33 | 27 | 24 | 21 | SM 140 | |
| 15 | - | 2 | 4 | 9 | | | | | | | 81 | 76 | 74 | 70 | 61 | 60 | 53 | 50 | 47 | 42 | 40 | 37 | 31 | 25 | 24 | SM 252 |
| 17 | 1 | 2 | 3 | 11 | | | | | 88 | 83 | 76 | 73 | 68 | 61 | 57 | 51 | 48 | 47 | 41 | 37 | 35 | 32 | 26 | 23 | 21 | SM 143 |
| 12 | 1 | 3 | 2 | 6 | | | | | | | | | | 86 | 83 | 79 | 75 | 71 | 60 | 55 | 45 | 40 | 37 | 32 | 24 | SM 34 |
| 11 | 1 | 1 | 3 | 6 | | | | | | | | | | | 87 | 83 | 72 | 66 | 61 | 52 | 46 | 41 | 38 | 30 | 26 | SM 247 |
| 14 | 1 | 3 | 2 | 8 | | | | | | | 87 | 84 | 81 | 75 | 69 | 60 | 51 | 47 | 42 | 38 | 36 | 32 | 29 | 24 | SM 206 | |
| 16 | - | 3 | 3 | 10 | | | | | 84 | 80 | 77 | 73 | 68 | 60 | 57 | 53 | 49 | 48 | 46 | 41 | 38 | 36 | 33 | 26 | SM 17 | |
| 16 | - | 4 | 2 | 10 | | | | | 85 | 82 | 76 | 75 | 72 | 62 | 56 | 52 | 48 | 43 | 41 | 38 | 35 | 32 | 27 | 23 | SM 60 | |
| 13 | - | 4 | 2 | 7 | | | | | | | | 85 | 81 | 77 | 76 | 70 | 62 | 58 | 51 | 47 | 42 | 38 | 32 | 27 | SM 107 | |
| 15 | - | 3 | 3 | 9 | | | | | | 85 | 82 | 76 | 74 | 69 | 61 | 58 | 53 | 46 | 41 | 38 | 33 | 31 | 27 | 23 | SM 243 | |
| 14 | - | 3 | 2 | 9 | | | | | | | 85 | 82 | 76 | 70 | 61 | 58 | 51 | 48 | 43 | 39 | 37 | 33 | 26 | 22 | SM 31 | |
| 13 | - | 4 | 1 | 8 | | | | | | | | 85 | 82 | 77 | 75 | 62 | 58 | 50 | 47 | 44 | 41 | 37 | 26 | 24 | SM 61 | |
| 14 | - | 3 | 2 | 9 | | | | | | | 83 | 81 | 76 | 71 | 62 | 59 | 54 | 50 | 47 | 43 | 39 | 35 | 32 | 25 | SM 12 | |
| 15 | - | 3 | 3 | 9 | | | | | | 84 | 81 | 76 | 72 | 68 | 61 | 55 | 52 | 48 | 42 | 39 | 35 | 30 | 25 | 23 | SM 8 | |
| 14 | - | 3 | 2 | 9 | | | | | | | 83 | 80 | 76 | 72 | 61 | 53 | 49 | 47 | 41 | 38 | 35 | 33 | 27 | 24 | SM 59 | |
| 13 | - | 3 | 1 | 9 | | | | | | | | 83 | 80 | 75 | 60 | 52 | 49 | 47 | 41 | 37 | 31 | 27 | 24 | 22 | SM 48 | |
| 14 | - | 3 | 2 | 9 | | | | | | | 83 | 80 | 75 | 72 | 64 | 59 | 53 | 49 | 45 | 41 | 37 | 33 | 26 | 23 | SM 59 | |
| 15 | - | 4 | 2 | 9 | | | | | | 85 | 80 | 79 | 78 | 67 | 60 | 55 | 53 | 48 | 40 | 38 | 35 | 31 | 27 | 25 | SM 68 | |
| 14 | 1 | 3 | 2 | 8 | | | | | | | 86 | 84 | 79 | 75 | 67 | 63 | 54 | 48 | 44 | 39 | 35 | 30 | 27 | 25 | SM 30 | |
| 15 | 1 | 4 | 2 | 8 | | | | | | 88 | 84 | 81 | 79 | 75 | 67 | 60 | 47 | 44 | 39 | 37 | 34 | 29 | 28 | 26 | SM 4 | |
| 14 | 1 | 3 | 2 | 8 | | | | | | | 89 | 85 | 78 | 75 | 67 | 63 | 56 | 46 | 40 | 35 | 30 | 29 | 26 | 25 | SM 209 | |
| 15 | 1 | 3 | 2 | 9 | | | | | | 88 | 84 | 79 | 78 | 66 | 60 | 55 | 47 | 42 | 36 | 34 | 31 | 28 | 26 | 24 | SM 201 | |
| 12 | - | 2 | 2 | 8 | | | | | | | | | | 85 | 78 | 65 | 60 | 55 | 49 | 38 | 35 | 34 | 29 | 26 | 25 | SM 242 |
| 13 | 1 | 2 | 1 | 9 | | | | | | | | | 90 | 84 | 78 | 65 | 59 | 50 | 45 | 38 | 35 | 29 | 27 | 26 | 24 | SM 214 |
| 13 | - | 3 | 1 | 9 | | | | | | | | | 84 | 79 | 75 | 65 | 58 | 49 | 46 | 42 | 35 | 29 | 27 | 25 | 23 | SM 63 |
| 14 | 1 | 3 | 1 | 9 | | | | | | | 88 | 85 | 78 | 77 | 65 | 58 | 45 | 36 | 35 | 31 | 29 | 26 | 25 | 23 | SM 134 | |
| 15 | 1 | 3 | 2 | 9 | | | | | | 88 | 84 | 80 | 78 | 73 | 67 | 59 | 51 | 46 | 41 | 37 | 34 | 30 | 26 | 24 | SM 193 | |
| 16 | 2 | 2 | 4 | 8 | | | | | 88 | 86 | 81 | 78 | 71 | 68 | 66 | 60 | 52 | 44 | 38 | 34 | 30 | 25 | 23 | 18 | SM 579 | |
| 15 | 1 | 3 | 2 | 9 | | | | | | 88 | 85 | 81 | 79 | 71 | 66 | 58 | 54 | 50 | 43 | 39 | 34 | 27 | 22 | 17 | SM 164 | |
| 14 | 1 | 2 | 1 | 10 | | | | | | | 87 | 83 | 81 | 70 | 58 | 53 | 50 | 44 | 41 | 39 | 34 | 28 | 21 | 19 | SM 245 | |
| 13 | 2 | 1 | 3 | 7 | | | | | | | | | 89 | 87 | 81 | 74 | 70 | 66 | 56 | 50 | 44 | 37 | 33 | 27 | 18 | SM 200 |
| 13 | - | 2 | 2 | 9 | | | | | | | | | 81 | 77 | 70 | 67 | 59 | 56 | 50 | 42 | 37 | 32 | 26 | 20 | 18 | SM 184 |
| 14 | 2 | 2 | 2 | 8 | | | | | | | 88 | 87 | 81 | 76 | 69 | 65 | 57 | 49 | 38 | 32 | 29 | 25 | 21 | 19 | SM 108 | |
| 11 | - | 3 | 1 | 7 | | | | | | | | | | 85 | 81 | 78 | 70 | 59 | 51 | 44 | 36 | 29 | 21 | 18 | SM 223 | |
| 13 | 2 | 2 | 2 | 7 | | | | | | | | 88 | 87 | 81 | 76 | 70 | 61 | 53 | 44 | 38 | 34 | 27 | 21 | 19 | SM 228 | |
| 14 | 1 | 3 | 2 | 8 | | | | | | | 89 | 84 | 81 | 77 | 71 | 68 | 59 | 52 | 44 | 39 | 33 | 27 | 22 | 19 | SM 93 | |
| 14 | - | 3 | 1 | 10 | | | | | | | 85 | 81 | 76 | 70 | 59 | 52 | 46 | 42 | 38 | 34 | 30 | 25 | 22 | 19 | SM 144 | |
| 17 | 2 | 1 | 1 | 13 | | | | | 89 | 88 | 85 | 70 | 59 | 53 | 45 | 41 | 36 | 34 | 30 | 28 | 26 | 25 | 22 | 21 | 18 | SM 104 |
| 17 | 1 | 2 | 3 | 11 | | | | | 86 | 85 | 82 | 74 | 69 | 63 | 57 | 52 | 46 | 41 | 34 | 27 | 26 | 23 | 22 | 21 | 18 | SM 45 |
| 20 | 2 | 3 | 2 | 13 | 88 | 87 | 85 | 81 | 75 | 69 | 63 | 57 | 53 | 50 | 45 | 40 | 35 | 32 | 27 | 26 | 24 | 22 | 20 | 18 | SM 220 | |
| 19 | 2 | 3 | 2 | 12 | | 88 | 86 | 85 | 78 | 75 | 71 | 62 | 53 | 50 | 45 | 42 | 37 | 33 | 29 | 28 | 26 | 23 | 22 | 20 | SM 242 | |
| 18 | 2 | 2 | 2 | 12 | | | 89 | 88 | 85 | 82 | 71 | 69 | 58 | 53 | 49 | 45 | 41 | 33 | 30 | 28 | 26 | 25 | 22 | 18 | SM 79 | |
| 17 | 1 | 3 | 1 | 12 | | | | 89 | 85 | 83 | 78 | 70 | 57 | 53 | 44 | 41 | 36 | 33 | 29 | 27 | 26 | 24 | 22 | 20 | SM 15 | |
| 17 | 2 | 2 | 2 | 11 | | | | 89 | 86 | 83 | 79 | 72 | 67 | 58 | 52 | 47 | 40 | 34 | 33 | 29 | 27 | 26 | 23 | 20 | SM 132 | |
| 17 | 2 | 1 | 2 | 12 | | | | 88 | 86 | 83 | 73 | 68 | 57 | 53 | 47 | 43 | 41 | 36 | 28 | 26 | 25 | 23 | 21 | 20 | SM 246 | |
| 16 | 1 | 2 | 2 | 11 | | | | | 89 | 85 | 79 | 73 | 67 | 58 | 51 | 46 | 43 | 40 | 32 | 27 | 26 | 24 | 22 | 20 | SM 55 | |
| 16 | 1 | 2 | 2 | 11 | | | | | 89 | 85 | 80 | 72 | 61 | 49 | 46 | 40 | 35 | 31 | 28 | 27 | 25 | 24 | 22 | 20 | SM 118 | |

LN: Line number GR: Gliadin regions BN: Band numbers Ω : Omega γ : Gamma β : Beta α : Alpha

For the preparation of 10 ml of 10% running gel, 4 ml of water, 3.3 ml of acrylamide, 2.5 ml of Tris (pH 8.8), 0.100 ml of SDS and 0.100 ml of APS were taken from the above stocks, and they were thoroughly mixed in a suitable container. The prepared gel was mixed with an addition of 10 μ l of TEMED immediately before being poured, and the gel (sub-gel= running gel) was quickly poured between the glass plates of the electrophoresis apparatus so that the gel would not be solidified (Figure 1A).

For the preparation of 5 ml of loading gel, 3.4 ml of water, 0.830 ml of acrylamide mixture, 0.625 ml of 1 M Tris (pH 6.8), 0.050 ml of SDS and 0.050 ml of APS were taken from the above stocks, and they were thoroughly mixed in a suitable container. Before the obtained gel was poured on the running gel, 5 μ l of TEMED (0.005 ml of TEMED) was added and quickly mixed. After the gels were poured, the combs were placed between the glass plates (Figure 1B, 1C).

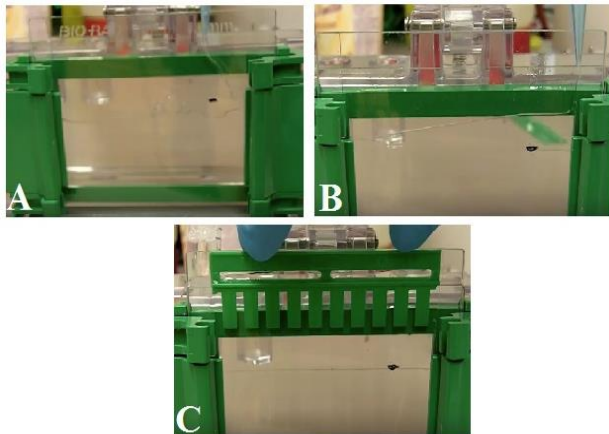


Figure 1. A: Running gel was poured between the glass plates of the electrophoresis apparatus B: Loading gel was poured between the glass plates C: The combs were placed between the glass plates

After waiting for 1 to 1.5 hours for the freezing of gels, the gels were fixed to their place in the electrophoresis apparatus and added solution (Figure 2A and 2B). By using micro-injector, 0.005 ml of sample liquid was injected from previously prepared samples into the comb housing (Figure 2C and 2D). The electrophoresis apparatus was capped and run at 10 amperes for 15 minutes and then it was run at 16 amperes until the end of the process. When the process was completed, the gels were taken out and put into the dye solution. 2% Coomassie-blue R was used for the dyeing of gels. 24 ml of glacial acetic acid and 16 ml of ethyl alcohol were added to 400 mg % Coomassie-blue R to prepare 200 ml of the dye solution. The solution was completed to 200 ml with deionized water and thoroughly mixed.

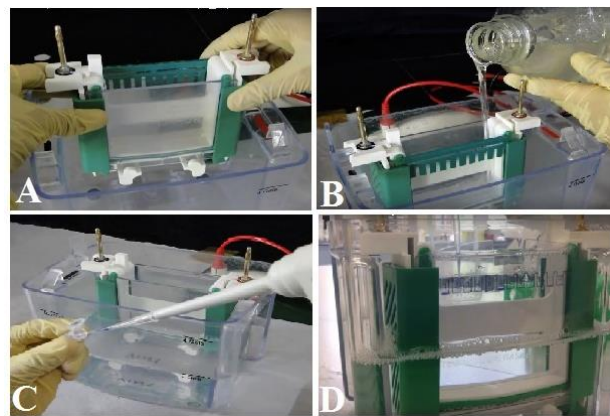


Figure 2. A and B: The gels were fixed to their place in the electrophoresis apparatus and added solution, C and D: Sample liquid was injected into the comb housing by using micro-injector

The gel taken from the electrophoresis apparatus was left in the dye solution, which was poured into a container, it was waited overnight, and through this way, the gel was ensured to be dyed. During the dyeing, the container was shaken in a magnetic stirrer. The dye removal solution was prepared to remove dye from the dyed gels. While preparing the solution, 24 ml of glacial acetic acid, 16 ml of ethyl alcohol and 160 ml of deionized water were used. The gels taken from dyeing process were placed into the dye removal solution and washed. This process was repeated 3 times with 15-minute intervals. The gels taken from there were fixed in 5% glycerol.

2.2.3 Calculation of the relative mobility values of the genotypes of the inbred maize lines

The electrophoregrams were evaluated on 9 x 13 cm size photographs [21]. While calculating the relative mobility values of the protein bands, the Low Molecular Weight Standard M 5630 was used as the standard. The protein types and molecular weights in the structure of the standard are presented in Table 2.

Using the molecular weight values of this standard type, the relative mobility values of the genotypes of the inbred maize lines were calculated with the UviPhotoMW software.

Table 2. Protein types and molecular weights in the standard used.

| Protein | Molecular weight |
|--|------------------|
| Aprotinin | 6500 |
| Alfa-Lactalbumin | 14200 |
| Trypsinogen Inhibitor | 20000 |
| Trypsinogen | 24000 |
| Carbonic Anhydrase | 29000 |
| Glyceraldehyde- 3- phosphate Dehydrogenase | 36000 |
| Ovarbumin | 45000 |
| Albumin | 66000 |

2.2.4 Evaluation of gliadin band patterns:

In the evaluation of gliadin band patterns, the genotype formulas were obtained by tabulating the relative mobility (Rm) values calculated for each inbred line genotype. By benefiting the relative mobility values of the bands in the genotype formula and according to the French system also used by Bushuk and Zilman (1978), it was accepted that the Rm values between 0-59 were Ω (Omega) gliadin region, between 59-74 were γ (gamma) gliadin region, between 74-85 were β (Beta) gliadin region, and between 85-100 were α (alpha) gliadin region. The distribution patterns of the gliadin bands of the relevant sample were determined by using this information [23- 24].

3. Results and Discussion

In this study, the gliadin protein bands of the 50 inbred maize lines at S₄ generation that were included in the experiment were examined by the electrophoresis method, and their genotypes were investigated. The gliadin band patterns obtained for these lines are presented in Figure 3. The end band belongs to the standard.

When the obtained values for the gliadin protein bands of the maize lines were examined (Table 1), it was determined that the band number of the gliadin proteins in the inbred maize lines showed variances between 11 and 20. In addition, the relative mobility values of the genotypes varied between 18 and 90 kDa, and according to the gliadin regions, the bands were mainly in the omega region, and it was followed by the beta and gamma regions. It was also found out that the relative mobility values were minimum in the alpha region.

When the genotypes were compared in terms of the gliadin protein band structure, it was observed that the lines SM1, SM3, SM6, SM9, SM13, SM14, SM16, SM17, SM18, SM19, SM20, SM22, SM24, SM25, SM28, SM30, SM32, SM39, SM40, SM42, SM49 and SM50 had similar bands.

When the relative mobility values of the bands of the lines were examined, it was determined that the lines SM1, SM49 and SM50 had 20, 24, 25, and 40 kDa bands, the lines SM3 and SM40 had 19, 30, 59, 76 and 81 kDa bands, the lines SM6 and SM42 had 21, 23, 26, 41, 57 and 88 kDa bands, the lines SM9, SM39, SM22 and SM24 had 39, 67, and 75 kDa bands, the lines SM13 and SM17 had 23, 61, and 76 kDa bands, the lines SM14, SM16, SM18 and SM20 had 26, 33, 38, 50, 76 and 83 kDa bands, the lines SM19 and SM28 had 27, 49, and 75 kDa bands, and the lines SM25, SM30 and SM32 had 26, 34, 66, 79 and 80 kDa bands. It is also determined that the other band values were generally close to each other. The code required for the synthesis of proteins is given from DNA and each living being has its own unique

protein structure. The fact that the lines have similar gliadin band patterns indicates that they are also similar to each other in terms of genotypes.

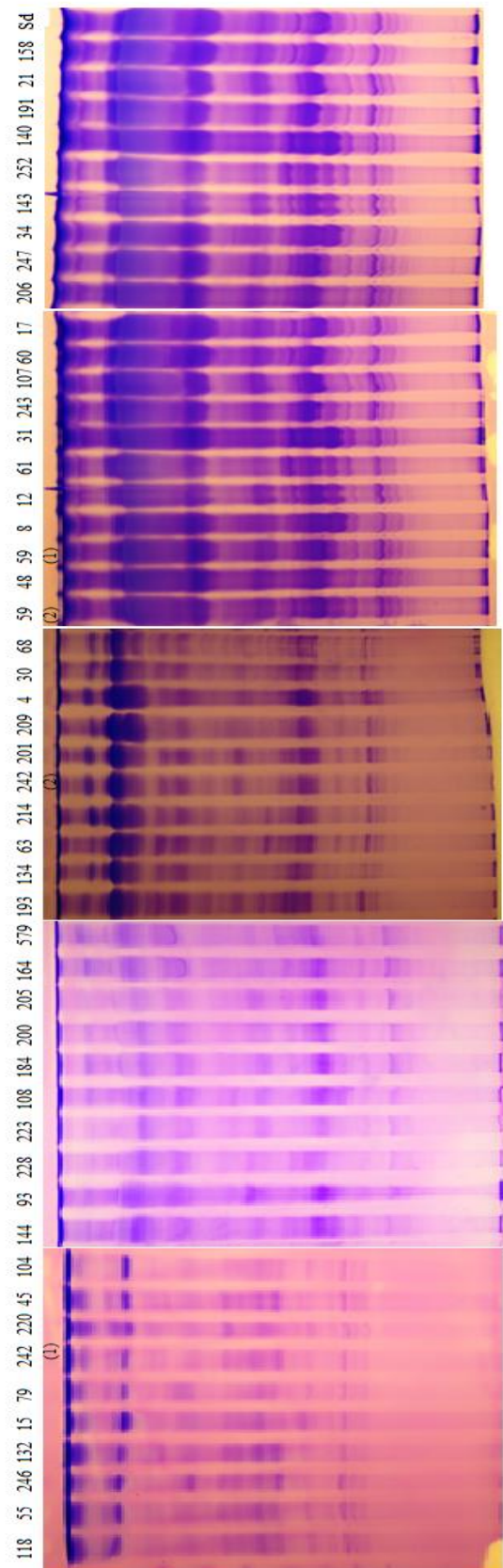


Figure 3. Gliadin protein band patterns of the inbred *Zea mays* indentata Sturt. lines at S₄ generation. Sd: Standard

As a result of the examination, it was determined that the inbred maize lines of SM 247, SM 252, SM 242, SM 61, SM 579, SM 245, SM 200, SM 184 and SM 15 showed significant differences in terms of the gliadin protein band structure compared to other lines. During the study, some morphological characteristics of the maize lines were also examined, and it was attempted to identify the relationship between band patterns and some morphological characteristics. When the morphological characteristics of similar genotypes in terms of the gliadin protein band structure were compared, it was observed that there were significant differences in all characters. Whereas some of the lines taking values far below or above the average in terms of characteristics such as stalk diameter, grain yield, cob length, thousand kernel weight, corncob diameter, diameter weight and leaf area are early-season, some others are late-season, and they have the same band pattern. It was determined that the lines that were found to differ significantly from other lines in terms of the gliadin protein band structure generally took place in the late-season groups in terms of the tasseling period and the ear silking period, and that their the leaf areas, stalk diameters, plant appearances, corncob diameter, and weights were usually above the average. The performance of the lines in terms of cob length, number of grains in the cob, and thousand kernel weight showed significant changes comparing to the general average, and they were usually below the average. In terms of grain yield, it was determined that the lines usually had the values close to the average. The obtained results show that these lines are significantly different from other lines in terms of protein band distribution and various morphological characteristics.

Depending on in which areas (silage, food for people, oil production, grain, etc.) the maize will be used, the desired morphological characteristics vary. Therefore, the lines to be proposed in the breeding studies to be performed will also vary. For example, when the morphological characters of maize lines were examined together with protein band structures, it was determined that SM 30 and SM 68 lines, which had the earliest silking time, carried 25, 27, 35, 48, 67 and 79 kDa bands. For high quality and efficient silage, it is important that the lines are early [25-26]. Corn lines with a lower stove diameter, stove weight and stem diameter are more valuable as silage. It was determined that SM 8, SM 246 and SM 134 lines, which had the lowest stove diameter and stove weight, were carrying 23, 25, 31 and 35 kDa bands. It was also identified that SM 45, SM 245, SM 21 and SM 63 lines with the lowest stem diameter generally carried 21, 23, 27, 34, 41 or 42, 46 or 47, 57 or 58, 82 kDa bands.

In the selection of silage corn lines, the characteristics such as leaf area, plant grain yield, ear length, grain

number on the ear and thousand kernel weight should be above the average [25-26]. It was determined that SM 79 and SM 579 lines, which have the highest leaf area, carried 18, 25, 30, 71, and 88 kDa bands; SM 214 and SM 193 lines, which have the highest grain number on the ear and the highest plant grain yield, carried 24, 26, 59, 78 and 84 kDa bands; SM 61 and SM 184 lines having a maximum of thousand kernel weight carried 26, 37, 50 and 77 kDa bands; and SM 63 and SM 243 lines with the maximum length of the ear carried 23, 27, 46 and 58 kDa bands.. According to these obtained data, in terms of the examined characters, the presence of the bands, whose relative mobility values are same, in the similar lines jointly may explain the effect of these bands on the emerging of the characters. Therefore, these lines, whose band distributions and the common bands they carried were given, can be considered suitable for developing silage corn cultivar in the future.

Gliadin is one of the proteins involved in the gluten structure. The alpha, beta, gamma gliadins cause celiac disease in humans having gluten-sensitive enteropathy. Therefore, it is tried to reduce the amount of gliadin in cereals. In this study, it was found that the amount of lysine increased in gliadin-reduced wheat [27]. Lysine is considered the most important essential amino acid, and because it is not synthesized in animals, it must be acquired through diet. Especially in developing countries where the diet is mainly composed by a single cereal, there is a great interest in increasing the content of lysine in cereal crops since it has both an economic and humanitarian importance [28]. Mutant high-Lys lines have been obtained in maize opaque-2 mutants and opaque-2- derived quality protein maize (QPM) lines [29]. Genetic engineering approaches have been also used to increase the lysine content in maize and rice [30]. Previous studies with opaque-2 mutants and QPM maize lines have demonstrated the enhancement of the nutritional properties in animal (rats, pigs, and chickens) and human nutrition, with higher utilizable protein values as a consequence of the lysine increase and a more balanced amino acid composition [27]. If corn is to be produced as food for humans, lines with a small number of alpha, beta and gamma gliadin bands should be preferred. In this study, it was determined that SM48, SM63, SM144, SM 191 and SM 223 lines did not carry an alpha band. The protein band number in the beta and gamma regions was determined as 4. These lines are recommended for the nutrition of people with celiac disease.

4. Conclusion

As a result of this study, it was determined that whereas some of the examined 50 maize lines had similar gliadin band patterns, the majority of them were different.

This result indicates that the available lines at S4 generation have genetic diversity. The obtained data can be evaluated and used by breeders in the development of new varieties with desired characteristics in terms of silage or grain.

References

- Ranere, A.J., Piperno, D.R., Holst, I., Dickau, R., Iriarte, J. The cultural and chronological context of early Holocene maize and squash domestication in the Central Balsas River Valley, Mexico. *Proc Natl Acad Sci*, 2009. 106: 5014–5018.
- FAO Internet Web Site, FAOSTAT. Database. [cited 2017 1 August]; Available from: www.fao.org
- Ziraat Mühendisleri Odası, [cited 2016 10 August]; Available from: <http://www.zmo.org.tr/genel>
- Cengiz, R. Türkiye’de Kamu Mısır Araştırmaları [Public Maize Investigations in Turkey]. *Tarla Bitkileri Merkez Araştırma Enstitüsü Dergisi*, 2016. 25: 304-310.
- USDA/FAS, cited 2015 21 January]; Available from: <http://www.fas.usda.gov/search/Corn%20production>
- Pingali, P.L. CIMMYT 1999-2000, World Maize Facts and Trends. Meeting World Maize Needs: Technological Opportunities and Priorities for the Public Sector. 2001. Mexico, D.F.: CIMMYT.
- Osborne, T. B., The amount and properties of the proteids of the maize kernel. *J. Amer. Chem. Soc*, 1897. 19: 525-532.
- Dierks-Ventling, C., Cozens, K., Immunochemical Crossreactivity Between Zein, Hordein And Gliadin. *Herbs Letters*, 1982. 14:147-150.
- Valentini, G., Soave, C., Ottaviano, E., Chromosomal location of zein genes in *Zea mays*. *Heredity*, 1979. 42:33–40.
- Esen, A., A proposed nomenclature for the alcohol-soluble proteins (zeins) of maize (*Zea mays* L.). *Journal of Cereal Science*, 1987. 5:117-128.
- Holding, D.R., Larkins, B.A. Zein storage proteins. In *Molecular Genetic Approaches to Maize Improvement*, AL KrizBA Larkins, *Biotechnology in Agriculture and Forestry*, Springer- Verlag Berlin Heidelberg, Germany, 2009. 63: 269–286.
- Krishnan, H.B., Kerley, M.S., Allee, G.L., Jang, S., Kim, W.S. et al. Maize 27 kDa γ -Zein Is a Potential Allergen for Early Weaned Pigs. *J Agric Food Chem*, 2010. 58: 7323–7328.
- Şuteu, D., Băcilă, I., Haş, V., Haş, I., Miclăuş, I., Romanian Maize (*Zea mays*) Inbred Lines as a Source of Genetic Diversity in SE Europe, and Their Potential in Future Breeding Efforts. *Plos One*, 2013. 8:1-13.
- Lookhart, G. and Bean, S., Separation and characterization of wheat protein fractions by high-performance capillary electrophoresis. *Cereal Chem.*, 1995. 72: 527–532.
- Đukić, N., Matic, G., Konjević, R. Biochemical Analysis Of Gliadins Of Wheat Triticum. *Kragujevac J. Sci.*, 2005. 27:131-138.
- Waga, J. and Zientarski, J., Isolation And Purification Of Individual Gliadin Proteins by Preparative Acid Polyacrylamide Gel Electrophoresis (A-Page). *Polish Journal Of Food And Nutrition Sciences*, 2007. 57:91-96.
- Žilić, S., Barać, M., Pešić, M., Dodig, D., Ignjatović-Mičić, D., Characterization Of Proteins From Grain of Different Bread and Durum Wheat Genotypes. *International Journal of Molecular Sciences*, 2011. 12:5878-5894.
- Xu, J.H. and Messing, J., Organization of the prolamin gene family provides insight into the evolution of the maize genome and gene duplications in grass species. *Proc Natl Acad Sci of the USA*, 2008. 105: 14330–14335.
- Swarup, S., Timmermans, M.C., Chaudhuri, S., Messing, J., Determinants of the high-methionine trait in wild and exotic germplasm may have escaped selection during early cultivation of maize. *Plant J*, 1995. 8: 359–368.
- Wang, L., Xu, C., Qu, M., Zhang, J., Kernel amino acid composition and protein content of introgression lines from *Zea mays* ssp. *Mexicana* into cultivated maize. *Journal of Cereal Science*, 2008. 48: 387–393.
- Kosmolak, F. G. et al., A relationship between durum wheat quality and gliadin electrophorograms. *Ca. J. Plant Sci.*, 1980. 60: 427- 432
- Bushuk, W. and Zillman, R.R., Wheat cultivar identification by gliadin electroforegrams. I. Apparatus, method and nomenclature. *Can. J. Plant Sci.*, 1978.58: 505-515.
- Motel, J. S. et al., Zentral Institut für Genetik und Kulturpflanzenforschung der Akademie der Wissenschaften der DDR, Corrensstrasse 3. 434 Gatersleben, DDR. 1981.
- Lookhart et al., An improved method of standardizing polyacrylamide gel electrophoresis of wheat gliadin Proteins, *Cereal Chem.*, 1982. 59: 178-181.
- Güney, E., Tan, M., Dumlugül, Z., Gül, İ. Erzurum Şartlarında Bazı Silajlık Mısır Çeşitlerinin Verim ve Silaj Kalitelerinin Belirlenmesi. *Atatürk Üniversitesi Ziraat Fakültesi Dergisi*, 2011. 41:105-111.
- Özata, E., Öz, A., Kapar, H. Silajlık Hibrit Mısır Çeşit Adaylarının Verim ve Kalite Özelliklerinin Belirlenmesi. *Tarım Bilimleri Araştırma Dergisi*, 2012. 5: 37-41.
- Gil-Humanes, J., Pisto, F., Altamirano-Fortoul, R., Real, A., Comino, I., Sousa, C., Rosell, C.M., Barro, F. Reduced-Gliadin Wheat Bread: An Alternative to the Gluten-Free Diet for Consumers Suffering Gluten-Related Pathologies. *Plos One*, 2014, 9 : 1-9.
- Wenefrida, I., Utomo, H.S., Blanche, S.B., Linscombe, S.D., Enhancing essential amino acids and health benefit components in grain crops for improved nutritional values. *Recent patents on DNA & gene sequences*, 2009. 3: 219–225.
- Glover, D.V. Corn protein-genetics, breeding, and value in foods and feeds. In: Mertz ET, editor. *Quality Protein Maize*. St. Paul, MN: American Association of Cereal Chemist, 1992. 49–78.
- Wu, X.R., Kenzior, A., Willmot, D., Scanlon, S., Chen, Z., et al. Altered expression of plant lysyl tRNA synthetase promotes tRNA misacylation and translational recoding of lysine. *Plant J.*, 2007. 50: 627–636.

**Research Article**

Production of bioplastic from potato peel waste and investigation of its biodegradability

Ezgi Bezirhan Arıkan ^{a,*}  and H. Duygu Bilgen ^a 

^a Faculty of Engineering, Department of Environmental Engineering, Mersin University, Mersin, 33343, Turkey

ARTICLE INFO*Article history:*

Received 03 May 2018

Revised 06 February 2019

Accepted 18 April 2019

Keywords:

Biodegradability

Bioplastic

Food industry

Waste

Water absorption.

ABSTRACT

Recently, environmental problems caused by petroleum-based plastics have been increasing. Therefore, researchers have begun to investigate new materials that may be alternatives to plastics. Bioplastics are considered as green materials alternatives to plastics and they are produced from renewable resources such as corn and potatoes, or microorganisms under certain conditions. In addition, most researchers are concerned with renewable resources for non-food using, such as bioplastic production. For this reason, researchers have been focusing on the utilization of the wastes as bioplastic products. In this study, the bioplastic was produced from potato peel as the food industry waste. Also, some properties of the produced bioplastic such as water absorption capacity and biodegradability were analyzed. Furthermore, water absorption capacity and biodegradability of a commercial bioplastic were also determined in order for the comparison with the one produced from potato peel waste in different conditions. It was found that the produced potato peel bioplastic (PPB) had higher water absorption capacity than commercial bioplastic (CB). Therefore, PPB may not be used in the food service industry but can be used as packing material. Biodegradability tests showed that PPB biodegraded at about 71% in moist soil and 100% in vermicompost within four weeks. On the other hand, it was determined that CB was not degraded in the soil or in the compost in four weeks. Therefore, as a food industry waste, potato peel can be used in biodegradable bioplastic production. In this way, petroleum-based plastic pollution may be decreased both in Turkey and the world.

© 2019, Advanced Researches and Engineering Journal (IAREJ) and the Author(s).

1. Introduction

Plastics are more useful than metals, papers, and other materials because of their properties such as lightness, cheapness and durability. Therefore, they have been being used in almost every industrial field. Worldwide, more than 300 million tons of plastic were consumed in 2015 [1]. The whole world, even the oceans, is full of plastic wastes. In addition, the plastic industry has some disadvantages related to economic and environmental problems [2].

The first disadvantage related to the environment is the shrinking of the landfill capacity because of the increasing of the plastic waste amount in the landfill areas [3]. Increasing of the plastic waste leads to a crisis in the landfill due to the rising costs and strong legislation. On the other hand, oceans are also full of

plastic wastes. The damaging of the marine ecosystem is the second disadvantage. The third disadvantage is that the waste management options are inadequate. Recycling proportion of plastics is very low. On the other hand, toxic emissions such as carbon dioxide and methane are generated because of plastic incineration. These greenhouse gases (GHGs) affect the worldwide climate change negatively [4]. Plastic's non-degradability or durability is the fourth disadvantage. It was known that plastics are not biodegradable and it can remain in the environment for hundreds of years [5]. In addition, it is expected that fossil fuel will become more expensive and the supply will become more volatile [3]. The economic problem is the increasing fossil fuel prices. These environmental/economic disadvantages and social concerns have led to the development of the green

* Corresponding author. Tel.: +90 324 361 00 01; Fax: +90 324 361 00 32.

E-mail addresses: ezgibezirhan@gmail.com (E.B. Arıkan), hduygubilgen@gmail.com (H.D. Bilgen)

ORCID: 0000-0003-4203-165X (E.B. Arıkan), 0000-0002-9510-8131 (H.D. Bilgen)

DOI: 10.35860/iarej.420633

materials, such as bioplastics, in recent years [6]. Today, bioplastics are considered as a promising alternative to plastics [7] since they may diminish the dependency on fossil fuels and the certain environmental problems.

Although there are several definitions, generally, 'Bioplastics' are defined as plastics made from renewable resources such as potato, sugar, corn etc. [8, 9] and produced by a range of microorganisms [10]. Photodegradable, compostable, bio-based and biodegradable bioplastics are types of bioplastics. Photodegradable bioplastics are light sensitive group due to the additives, and UV can disintegrate their polymeric structure. However, they cannot be disintegrated where there is lack of sunlight [5]. Bio-based bioplastics are derived from renewable resources containing starch, protein, and cellulose [11]. The most known bio-based plastic is Polylactic Acid (PLA). Compostable bioplastics are defined as biologically decomposed during a composting process [9] and according to American Society for Testing and Materials (ASTM) D6400 standard, the plant should not be damaged after the composting process. Biodegradable bioplastics are completely biologically degraded by microorganisms. The term "biodegradable" refers to materials that can disintegrate or break down naturally in carbon dioxide and water as a result of being exposed to a microbial environment and humidity [5].

In many countries, bioplastic are mostly used as cutlery, diapers, packing materials etc. in many industrial areas. It is forecasted that bioplastic production will be 7.8 million tons in 2019 in the world [12]. Therefore, it is thought that the future of bioplastics shows great potential. Nevertheless, the cost of the bioplastic produced from microbial resources is still higher [13, 14] than produced from renewable resources. For this reason, most of bioplastic manufacturers have focused on the production via renewable resources.

Among the renewable resources, starch is a potentially useful material for bioplastics because it is inexpensive and easily available [13, 15, 16]. Starch has been used in many industrial areas such as paper, corrugated boards biofuels [17], pharmaceutical, textile [18] and especially food industry. On the other hand, many companies have already begun to use the starch for the production of bioplastic. In spite of its abundance, low cost and natural origin, there is still a major concern about the use of this type of renewable resources for production. Furthermore, many researchers advocates that when there is hunger in the world, renewable sources such as starch should not be used in non-food areas. Also, the bioplastic industry can decrease the land that is available for food production or in order to create more arable land, it can increase the incentives to cut down the forested areas [19]. Recently, in order to ensure the potential competition with

agricultural resources for foods and also to provide additional raw-material sources, utilization of wastes is the current trend [20].

In this study, the overall purpose was to investigate the utilization of the food industry wastes in order for the bioplastic production. To achieve this objective, the production of bioplastics from potato peel waste was investigated. In addition, some properties of the produced bioplastics such as water absorption capacity and biodegradability were analyzed.

2. Materials and Methods

The glycerin used in the experiments was obtained from a firm located in Konya, Turkey. Starch-based bioplastic spoon were purchased from www.amazon.com as market, cleaned up after using and divided into small pieces at about equal size for further use. This purchased bioplastic is called as commercial bioplastic (CB) in this study.

2.1 Bioplastic production

Potatoes were cleaned up and peeled for further studies. Potato peels were granulated and centrifuged at 15000 rpm for 20 min. The supernatant was filtered and the starch was obtained. 13.5 g dried starch was extracted from 330 g wet potato peels. After filtration, starch was dried at 50 °C for 2 h and kept in a zip-locked airtight environment until the processing [21]. After the starch was obtained, 13.5 g of starch was weighed and 135 mL of tap water, 16.2 mL of vinegar, and 10.8 mL of glycerin was added to the starch. This mixture was heated on a hot plate till to 100 °C and kept waiting at that temperature for 20 min. The mixture was led to air dry for about 48 h and the bioplastic was produced in a sheet form (Figure 1).

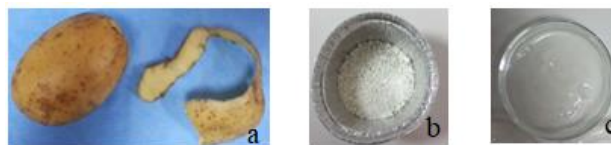


Figure 1. (a) Potato peel; (b) potato starch; (c) bioplastic

This produced bioplastic from potato peel waste is called as PPB at the rest of study.

2.2 Measurements of water absorption

Water absorption of two type of bioplastic (PPB and CB) was measured according to ASTM D570-81. Bioplastics having the same surface-area and weigh were dried in an oven at 50 °C for 24 h and cooled in a desiccator before weighing. Bioplastics were submerged in distilled water at 25 °C. After 2 h, the bioplastics were removed, their surface water dried with a paper towel, they were immediately weighed, and re-submerged into

the water. They were weighed again after another 24 h following the same procedure. Water absorption was calculated as a percentage of initial weight [22, 23]. For the determining of water-soluble content of the samples during soaking, PPB and CB samples were dried at 50 °C for 24 h. At the end of 24 h, samples were weighed again and weight loss of the samples was calculated. The sum of the weight gain following soaking plus the weight loss after drying is defined as the total absorbed water [23]. All water absorption measurements were performed in three replications.

2.3 Biodegradability analysis

The biodegradability of PPB and CB samples were investigated in different controlled environments [24, 25]. After weighing, two different PPB and CB samples also were buried under 50 g of moist soil and 50 g of vermicompost [26] in petri dishes, respectively. Bioplastic samples, whose initial masses were known, were weighed after burying weekly. All experiments were performed in three replications.

According to European Committee for Standardization (CEN), biodegradation is a degradation caused by biological activity, especially by enzymatic action, leading to a significant change in the chemical structure of a material. Also, the weight loss measurement is a standard method for biodegradation of polymer [27]. Amount of biodegradation was calculated by the following Equation 1 [28].

$$WL(\%) = \frac{(W_0 - W)}{W_0} \times 100 \tag{1}$$

W_0 and W are the initial and final weight of bioplastic samples, respectively. Also WL refers to the Weight Loss.

3. Results and Discussion

3.1 Results of the Water absorption measurements

The results of the water absorption experiments showed that PPB absorbed water by 48.46% within two hours and 83.57% within 24 hours. It was also observed that CB absorbed water by 2.04% within two hours and 7.48% within 24 hours (Figure 2).

It was found that CB had higher water resistance than PPB. It is thought that some additives might have been added to commercial bioplastic for increasing water resistance. Because of higher water absorption, PPB may not use in the food services industry but can be used as packing materials. However, mechanical property, tensile strength, hydrostatic pressure, elastic property, and strength property should be identified in order to determine the industrial usage areas.

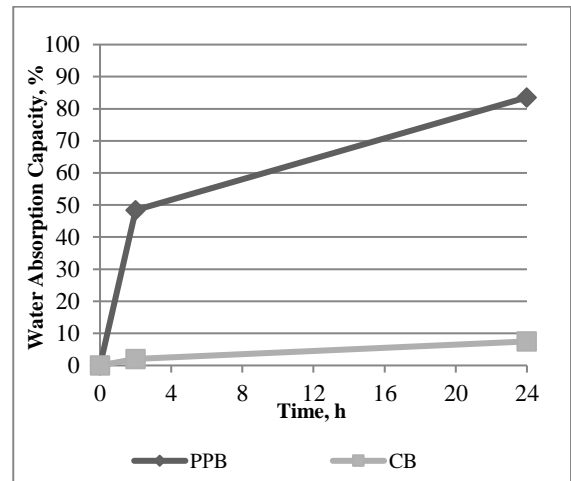


Figure 2. Water absorption capacity of PPB and CB

3.2 Biodegradability analysis results

Biodegradability tests showed that within four weeks, the PPB biodegraded at about 71% in moist soil and 100% in vermicompost (Figure 3). On the other hand, any degradation for CB was not observed in the soil or in the compost within four weeks.

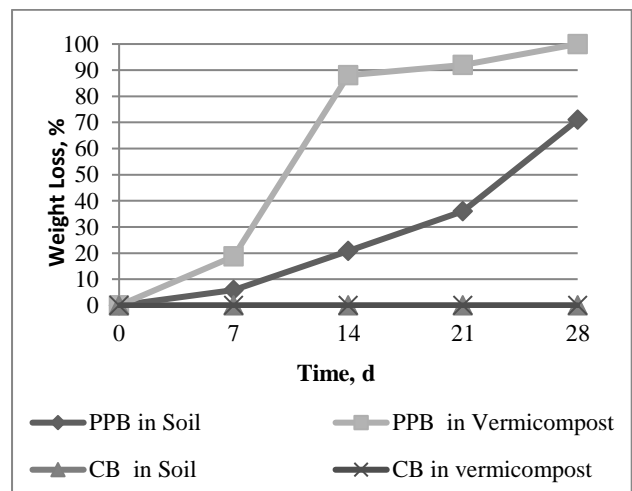


Figure 3. Weight loss of PPB and CB

Biodegradability is strongly dependent on the starch proportion [29]. It is known that PPB consist of 8% starch. But, the starch content of commercial bioplastic is unknown. Therefore it is thought that some additives may have been added to commercial bioplastic for improving mechanical properties such as durability, flexibility and etc. For example, additives used for enhancing antimicrobial properties may reduce or eliminate the biological degradability of bioplastics. Because of this, the structure of commercial bioplastic may have changed and this change may have also affected biological degradability. Furthermore, due to the natural conditions are not controlled, commercial bioplastics can biodegrade within a long time or cannot biodegrade.

4. Conclusions

Since many countries around the world are struggling with food shortages, producing bioplastics from wastes instead of foods is the best way to go. This study concluded that food wastes could be used for bioplastic production. In this study, it was determined that the bioplastics produced from potato peels completely biodegraded within 28 days, and it was suggested that these bioplastics can be used in packaging industry. The development of mechanical properties should be investigated for the utilization of it in different industrial areas. On the other hand, it was observed that the commercial bioplastic did not biodegrade in 28 days. Bioplastics usage has increased in recent years both in the world and Turkey. Therefore, for the sustainability of those called as 'biodegradable', the standards should be developed. In conclusion, a new guide for bioplastics should be developed for production, usage and waste management in Turkey as soon as possible.

References

- Mekonnen, T., P. Mussone, H. Khalil, D. Bressler, *Progress in bio-based plastics and plasticizing modifications*. Journal of Material Chemistry A, 2013. **43**(1): p.13379-13398.
- Zarate-Ramirez, L.S., A. Romero, I. Martinez, C. Bengoeche, P. Partal, A. Guerrero, *Effect of aldehydes on thermomechanical properties of gluten-based bioplastics*. Food and Bioproducts Processing, 2014. **92**: p.20–29.
- Philp, J.C., R.J. Ritchie, K. Guy, *Biobased plastics in a bioeconomy*. Trends in Biotechnology, 2013. **31**(2): p.65–67.
- Barker, T., *In Climate Change 2007: Mitigation. Contribution of Working Group III to the Fourth Assessment, Report of the Intergovernmental Panel on Climate Change*. 2010, USA: Cambridge University Press.
- El Kadi, S., *Bioplastic production form inexpensive sources bacterial biosynthesis, cultivation system, production and biodegradability*. 2010, USA: VDM Publishing House.
- Peelman, N., P. Ragaert, B. De Meulenaer, D. Adons, R. Peeters, L. Cardon, F.V. Impe, F. Devlieghere, *Application of bioplastics for food packaging*. Trends in Food Science and Technology, 2013. **32**(2):p. 128-141.
- Mirel. [cited 2017 03 March]; Available from: <https://pdfs.semanticscholar.org/fa36/d6c497ea7d4d9830682a671ee11cd2746d30.pdf>
- Karana, E., *Characterization of 'natural' and 'high-quality' materials to improve perception of bioplastics*. Journal of Cleaner Production, 2012. **37**: p. 316-325.
- Sarasa, J., J. M. Gracia, C. Javierre, *Study of the biodegradation of a bioplastic material waste*. Bioresource Technology, 2008. **100**(15): p.3764-3768
- Luengo, J. M., B. Garcia, A. Sandoval, G. Naharro, E. R. Olivera, *Bioplastics from microorganisms*. Current Opinion in Microbiology, 2003. **6**(3): p.251–260.
- Alvarez-Chavez, C.R., S. Edward, R. Moure-Eraso, K. Geiser, *Sustainability of bio-based plastics: general comparative analysis and recommendations for improvement*. Journal of Cleaner Production, 2012. **23**(1): p.47–56.
- Schulze, C., M. Juraschek, C. Herrmann, S. Thiede, *Energy Analysis of Bioplastics Processing*. Procedia CIRP 2017. **61**: p. 600-605.
- Kaith, B.S., R. Jindal, A.K. Jana, M. Maiti, *Development of corn starch based green composites reinforced with Saccharum spontaneum L fiber and graft copolymers – Evaluation of thermal, physico-chemical and mechanical properties*. Bioresource Technology, 2009. **101**(17): p. 6843–6851.
- Anjum, A., M. Zuber, K.M. Zia, A. Noreen, M. Naveed Anjum, S. Tabasum, *Microbial production of polyhydroxyalkanoates (PHAs) and its copolymers: A review of recent advancements*. International Journal of Biological Macromolecules, 2016. **89**: p.161–174.
- Roldán-Carrillo, T., R. Rodríguez-Vazqúez, D. Díaz-Cervantes, H. Vázquez-Torres, A. Manzur-Guzmán, A. Torres-Domínguez, *Starch-based plastic polymer degradation by the white rot fungus Phanerochaete chrysosporium grown on sugarcane bagasse pith: enzyme production*. Bioresource Technology, 2003. **86**(1): p.1-5.
- Ma, X., P. R. Chang, J. Yu, M. Stumborg, *Properties of biodegradable citric acid-modified granular starch/thermoplastic pea starch composites*. Carbohydrate Polymers, 2008. **75**(1): p.1–8.
- Naik, S. N., V. V. Goud, P.K. Rout, A.K. Dalai, *Production of first and second generation biofuels: A comprehensive review*. Renewable and Sustainable Energy Reviews, 2010. **14**(2): p.578–597.
- Tupa, M., L. Maldonado, A. Vazquez, M. L. Foresti, *Simple organocatalytic route for the synthesis of starch esters*. Carbohydrate Polymers 2013. **98**(1): p.349– 357.
- [cited 2017 03 March]; Available from: <http://www.carboncommentary.com/2011/09/02/2061>
- Lagaron, J. M., A. Lopez-Rubio, *Nanotechnology For Bioplastics: Opportunities, Challenges and Strategies*. Trends in Food Science & Technology, 2011. **22**(11): p.611-617.
- Singh, S. and A.K. Mohanty, *Wood fiber reinforced bacterial bioplastic composites: Fabrication and performance evaluation*. Composites Science and Technology, 2007. **67**(9): p.1753–1763.
- Paetau, I., C. Zue Chen, and J. lin Jane, *Biodegradable Plastic Made from Soybean Products. 1. Effect of Preparation and Processing on Mechanical Properties and Water Absorption*. Ind. Eng. Chem. Res. 1994. **33**(7): p.1821-1827.
- Liu, W., M. Misra, P. Askeland, L. T. Drzal, A. K. Mohanty, *Green composites from soy based plastic and pineapple leaf fiber: fabrication and properties evaluation*. Polymer, 2005. **46**(8): p.2710–272.
- Maran, J. P., V. Sivakumar, K. Thirugnanasambandham, R. Sridhar, *Degradation behavior of biocomposites based on cassava starch buried under indoor soil conditions*. Carbohydrate polymers, 2014. **30**(101): p.20-28.
- Spaccini, R., D. Todisco, M. Drosos, A. Nebbioso, A. Piccolo, *Decomposition of bio-degradable plastic polymer*

- in a real on farm composting process*. Chemical and Biological Technologies in Agriculture, 2016. **3**(4) DOI 10.1186/s40538-016-0053-9.
26. Ashok A., R. Abhijith, C. R. Rejeesh, *Material characterization of starch derived bio degradable plastics and its mechanical property estimation*. Materials Today: Proceedings, 2018. **5**(1): p.2163–2170.
 27. Mahalakshmi V., *Evaluation of Biodegradation of Plastics*. International Journal Of Innovative Research & Development, 2014. **3**(7): p.185-190.
 28. Ismail, N. A., S. M. Tahir, N. Yahya, M. F.A. Wahid, N. E. Khairuddin, I. Hashim, N. Rosli, M. A. Abdullah, *Synthesis and Characterization of Biodegradable Starch-based Bioplastics*. Materials Science Forum, 2016. **846**: p. 673-678.
 29. Guohua, Z., L. Ya, F. Cuilan, Z. Min, Z. Caiqiong, C. Zongdao, *Water resistance, mechanical properties and biodegradability of methylated-cornstarch/poly(vinyl alcohol) blend film*. Polymer Degradation and Stability, 2006. **91**(4): p.703–711.



Research Article

Determination of heat transfer coefficient and electromagnetic directional analysis of pomegranate seed

İsmail Üstün ^a , Yıldız Koç ^a , Hüseyin Yağlı ^a , Özkan Köse ^a , M. Tunahan Başar ^a 
Cuma Karakuş ^a , Oğuzhan Akgöl ^b  and Ali Koç ^{a,*} 

^aDepartment of Mechanical Engineering, Iskenderun Technical University, Iskenderun, Hatay, 31200, Turkey

^bDepartment of Electrical Engineering, Iskenderun Technical University, Iskenderun, Hatay, 31200, Turkey

ARTICLE INFO

Article history:

Received 03 April 2018

Revised 11 April 2019

Accepted 12 July 2019

Keywords:

Insulation materials

Thermal conductivity coefficient

Electromagnetic field permeability

Energy saving

ABSTRACT

As Turkey uses about 25.7% of energy consumption in residential area and doing this with natural gas imported from the abroad, production of efficient insulation materials is important to decrease energy dependence and deficiency. Due to both waste minimisation and money saving, there are great efforts on developing new environment friendly insulation materials. In the scope of the current study, the heat transfer coefficient was acquired by applying the linear heat conduction coefficient measurement device to find the heat transfer coefficient of the pomegranate seed sample obtained from various processes for the production of insulation material. The sample also have been examined with a two-port vector network analyser to see electromagnetic property. At the end of the experiment, the heat transfer coefficient of the sample produced from pomegranate seeds was calculate as $k = 0.6115 \text{ W/mK}$. Moreover, it has been found that the obtained sample performs better than the other insulation materials in terms of electromagnetic perspective. With this feature of the sample, it has been found that using as insulation material in the areas with the high electro-magnetic field can minimize the effect of the harmful electromagnetism in the place where it is applied.

© 2019, Advanced Researches and Engineering Journal (IAREJ) and the Author(s).

1. Introduction

The fast increase of world population and industrialization have caused incredible energy demand all over the world. Total primary energy consumption is 150,000,000 GWh and it is estimated to rise by 57% until the year 2050 These energy consumptions depend on fossil fuels such as petroleum, natural gas and coal [1-2]. As a result of the utilization of these limited energy resources as energy, there have been many undesirable effects such as the deterioration of ecological balance, climate change and accumulation of greenhouse gases on the ozone layer [3].

The world needs more energy day by day because of increasing population and industrialization and this reached 13,147 billion tons of oil equivalent (TOE) and this energy consumption for Turkey is around 126,9

million (TOE) by end of the 2015 [4,5].

Turkey's energy production, that is totally 148.491 thousand (TOE) and only 35.374 thousand (TOE) with domestic resources in 2016, is not enough to meet increasing energy needs from local sources especially for natural gas and oil [4- 6]. In order to meet these energy needs, Turkey import great amounts of energy from the other countries [7-4]. Turkey's energy dependence rate has started to rise especially since the early 1990 and continue around 70% since the early 2000s [8]. Turkey needs to use its abundant renewable energy to decrease its energy dependence and develop domestic production rather than export [9] in all sector such as isolation materials, food and the important part of renewable energy technologies. In addition to these, increasing the continuity and efficiency of existing systems in industry is important for energy sector and for its planning [10-13].

* Corresponding author. Tel.: +90 (326) 613 56 00; Fax: +90 (326) 613 56 13.

E-mail addresses: ismail.ustun@iste.edu.tr (İ. Üstün), yildiz.koc@iste.edu.tr (Y. Koç), huseyin.yagli@iste.edu.tr (H. Yağlı), ozkan.kose@iste.edu.tr (Ö. Köse),

mustafabasar12@hotmail.com (M.T. Başar), cuma.karakus@iste.edu.tr (C. Karakuş), oguzhan.akgol@iste.edu.tr (O. Akgöl), ali.koc@iste.edu.tr (A. Koç)

ORCID: 0000-0001-8885-5510 (İ. Üstün), 0000-0002-2219-645X (Y. Koç), 0000-0002-9777-0698 (H. Yağlı), 0000-0002-9069-1989 (Ö. Köse),

0000-0002-3108-8995 (M.T. Başar), 0000-0002-3553-9335 (C. Karakuş), 0000-0002-1423-1569 (O. Akgöl), 0000-0002-7388-2628 (A. Koç)

DOI: 10.35860/iarej.412270

Considering 25.7% of residential energy consumption of Turkey which imports a large portion of its energy needs, it is very important to develop isolation materials technologically and decrease their costs [14]. As the technological development is increase, energy demand of the world increases parallelly and alternative energy sources have been taken an importance place such as renewable energy [15].

Because the technological advancements in insulation materials take place, lighter and ergonomic materials can be produced. Thus, loss of life and damage to buildings can be reduced in case of an earthquake. Because natural resources are limited and consumption is increasing rapidly, recycling has been one of the important issues discussed in the world lately [16]. Thanks to the recycling efforts, wastes in many sectors (marble pieces, paper, metal beverage boxes, etc.) can be recovered many times and used with less cost and labour power. Efforts in the world where existing energy resources are using cost effective and efficient way are constantly increasing. However, Studies and operation on recycling in agricultural areas are still insufficient and limited. The recycling of agricultural product and the conversion of lost biological waste into workable forms in different industrial will bring along important development. According to Food and agriculture Organization of the United Nation, 1.3 billion tons of waste from food is takes place per year globally [17]. During Industrial process of organic waste like pomegranate seed, huge volume of this wastes are accumulated, the proportion of which affects the environment badly [18].

In the sense of protecting the energy, the use of these wastes as insulation materials is going to increase the sustainability as well as the energy savings in the world. A number of studies have been conducted on recovery of waste materials.

Dönmez at al. have indicated that the tree bark in our country contains chemically different substances and have worked on its recycling into industry. They have emphasized the importance of increasing the use of wood crusts in different areas such as concrete strengthening, sound insulation and heat insulation in the industrial areas [19].

Ozkan et al. have studied the change in the thermal conductivity of the concrete with the addition of graphene [20].

Binici at al. analysed the heat, sound and radiation transmittance of chipboard panels produced by cotton wool, fly ash and barite. In the experiment of heat insulation, they found the heat transfer coefficient at around 0.0023 kW/mK (containing textile waste) and stated the light building materials and thermal insulation material. They found a better sound insulation in the sample with the textile waste and examined the insulation properties for the radioactive areas in their formed samples [21]. In the sense of the recycling and energy recovery from insulation materials, Kozak investigated solid waste which is obtained from textile industry and also pointed out the energy saving. They predicted that the applicability

of recycling plants in the production of construction and geo-textile equipment can be investigated [22]. Tüccar and Uludamar have studied utilization of pomegranate seed oil biodiesel to find alternative fuel to diesel engine [1].

There are many subjects of study area on pomegranate seed in literature such as; food science and nutrition [23,24], medicine [25] and other areas [26]. As far as literature is examined, we have not encountered much the study about heat conduction coefficient, electromagnetic examination and usability pomegranate seeds as an insulating material.

Mahmoodi and Hosein studied on thermal conductivity of exocarp, mesocarp and seed of pomegranate samples and found heat transfer coefficient between 0.15 to 0.42 W/m°C, 0.15 to 0.45 W/m°C and 0.13 to 0.42 W/m°C in Alan and 0.18 to 0.5 W/m°C, 0.2 to 0.49 W/m°C and 0.18 to 0.51 W/m°C in Aghamad-ali, under different temperature and humidity condition, respectively [27].

Mukama et al. have studied about thermal properties of whole and tissue parts of pomegranate. They determined the thermal conductivity of aril part, mesocarp and epicarp in Acco at 7 °C, 0.419 Wm⁻¹K⁻¹, 0.352 Wm⁻¹K⁻¹, 0.389 Wm⁻¹K⁻¹, respectively [28].

As a result, investigating the recycling of agricultural waste both in the literature and in practice is reasonable and valuable. In this study, the usability of the pomegranate seed as an isolation substance has been investigated. Researches, experiments and analyses were also conducted about the suitability of pomegranate seed which has been passed through some processes, without additive, as an insulation material in industrial and engineering fields.

First of all, the pomegranate seeds that have been separated from the wastes are dried until the biological reactions are finished, and then dried pomegranate seeds are pulverized and pressed in standard heat insulation sample sizes (30 x 30 mm cylindrical form). The pressed samples were then placed in a linear heat transfer coefficient measurement device, coefficient analysis and necessary data were recorded.

Because of the negative effects of electromagnetic radiation, we have been exposed to in almost every part of our lives with developing technology, studies on various types of insulation materials that will prevent electromagnetic radiation are increasing day by day.

In order to determine the electromagnetic characteristics of the proposed sample, measurements were made in the laboratory using with two-port Agilent brand vector network analyser which is capable of operating up to 43 GHz and also using two high gain, wideband, linearly polarized horn antennas operating in the frequency range of 3-18 GHz. The prepared samples were compared with the existing insulation materials and pure concrete in terms of their electromagnetic properties and their transmission characteristics were also compared with reflection. During measurements, s-parameters, also known as scatter parameters, were measured and found to generate significant differences in the 3-18 GHz frequency band.

The s-parameter used for reflection is S_{11} , showing how much of the power from the first port is reflected back. In addition, the parameter used for transmission is obtained with S_{12} measurement. This parameter shows the proportions of the electromagnetic energy transmission between the two ports. When the literature is examined, an electromagnetic measurement of such a wide band gap has not been found, especially for an agricultural waste material of the proposed type.

The purpose of this objective study is to production of alternative materials to insulation materials, regain organic waste to the industry sector and keep the environment from the adverse effect of industrial organic waste. The organic wastes that thrown through the environment was investigated to see recyclability of the waste. Therefore, organic wastes derived from pomegranate was examined. Because, pomegranate one of the main agricultural production of the Iskenderun region, which is commonly uses to produce pomegranate syrup. Due to high pomegranate syrup production capacity of the region, there are so much pomegranate seeds that thrown to the environment.

In the scope of the study, the usability of pomegranate seed, which is one of the most wasted wastes in the region, has been investigated as an insulating material. Firstly, a sample produced from pomegranate seed was prepared to determine heat conduction coefficient. Then, the electromagnetic measurement was applied on the sample to analyse the electromagnetic adsorption behaviour.

2. Material and Method

2.1 Preparing the Sample

The separated pomegranate seeds were dried under the sun in a specific area until the biological reactions were ended (Figure 1). Dried pomegranate seeds are ground to powder to make them homogeneous. In order to prepare sample form suitable for linear heat transfer coefficient measurement device (30x30 mm cylindrical format), a special stamping mould have been manufactured with lathe and the prepared pomegranate powder were pressed in this mould (Figure 2).



Figure 1. Pomegranate seeds in the drying phase

2.2 Experimental System

2.2.1 Heat Conduction Coefficient Test System

In this study, the investigation of the sample made from pomegranate seed powder was conducted with our existing heat transfer coefficient measuring device (Figure 3).



Figure 2. The final shape of sample and mould

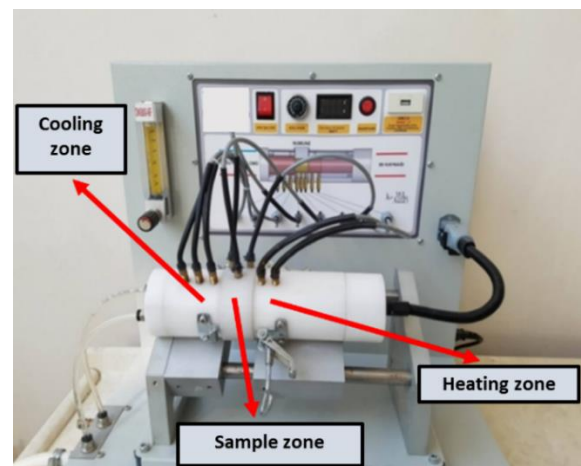


Figure 3. Experiment Device

The experimental device generally consists of three main parts;

The first is the part of the cooling water through which the cooling water passes and the heat given to the system is removed from the system. In this part, temperatures were measured at three different location in total including the water coming from the cold source, the surface where the water and sample contacted and the temperatures of the heated cooling water after the contact.

The second and the main part is the location where the sample is placed. A total of three temperature measurements are made on the sample. These are the surface temperature of the sample on the refrigerant side, the temperature of the midpoint of the sample and the surface temperatures at which the sample contacts the hot source.

The third is the hot zone within the resistance that provides heat to the system. In the heating zone, a total of two temperature measurements are made on the surface and the resistance that the hot source touches to the sample.

2.2.2 Electromagnetic Measurement Test System

The experimental setup used is shown in Figure 4. As can be seen in the figure, the horn antennas are connected to the two-port network analyser and the samples are placed in the mid-point of the antennas. The distance between the two horn antennas is chosen above the limit value in order to measure outside of the near reactive field region.

Table 1. The Technical Specifications of Heat Conduction Coefficient Test System [29]

| Measuring Ability | Linear and Radial | - |
|----------------------------|-------------------|----|
| Number of Measuring Sensor | 15 | - |
| Linear Heating Capacity | 100 | W |
| Radial Heating Capacity | 100 | W |
| Measurement Range | -20 to 200 | °C |
| Cooling System | Water | - |
| Measurement System | Digital | - |

The technical specification of heat conduction coefficient test system has been given above in Table 1.

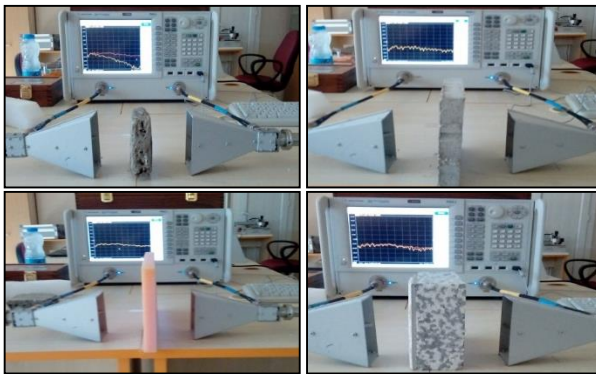


Figure 4. Magnetic measuring device

The device was calibrated over both ports before measurements were started in order to avoid losses that could result from cabling and connection devices. Since the test cables are made up of convolutional cables, the type of calibration set that is suitable for such connections was selected and the calibration was tested, with the open, closed, load states and transmission states carefully adjusted for both ports and also measurement was tested, when the device was idle.

Table 2. The Technical Specifications of the N5234A PNA-L Microwave Network Analyzer Test System

| | | |
|--------------------------|---------------|-----|
| Maximum Frequency | 43.5 | GHz |
| Dynamic Range | 122 | dB |
| Output Power | 6 | dBm |
| Number of Built-In Ports | 2 Ports | - |
| Harmonics | -33 | dBc |
| Network Analyzer Series | PNA-L Economy | - |
| Instrument Type | n/a | - |

The Technical specifications of the N5234A PNA-L microwave network analyser test system used for measuring scattering parameters have been given in Table 2.

2.3 Formulas and Acceptances

Heat conduction occurs in three main forms, conduction, convection and radiation.

Since the heat energy lost in the walls is mostly proportional to the heat conduction and the heat conduction coefficient, the transmission through the conduction is examined in this study.

Heat conduction is the transfer of heat from a hot zone to a colder zone. In rigid objects, this occurs via conduction and is theoretically calculated by Fourier's law. Fourier's law basically is described with the equation below.

$$Q_x = -kA \frac{dT}{dx} \quad (1)$$

Here, Q_x is the amount of heat (Watt) that passes vertically through a certain area in the x direction. k and A show heat conduction coefficient (W/mK) and the area (m^2), respectively. When the equation is rewritten to leave the heat transfer coefficient alone,

$$k = \frac{QL}{A(\Delta T)} \quad (2)$$

is obtained by the expression. In the test setup, the electrical resistance is used as a heat source and is indicated by the heat (Q) given to the system by the electrical resistance. The air bubbles in the prepared sample during the test and calculations are assumed to be zero. A total of 800 data have been taken from the test device. The average heat transfer coefficient has been calculated by using data at the time, when the lines in the graph flatten.

3. Research Findings

3.1 Thermal Conductivity of Sample

When the prepared sample is examined in terms of heat conduction in the experimental setup, the graph of the heat transfer coefficient change obtained in the system is given in Figure 5.

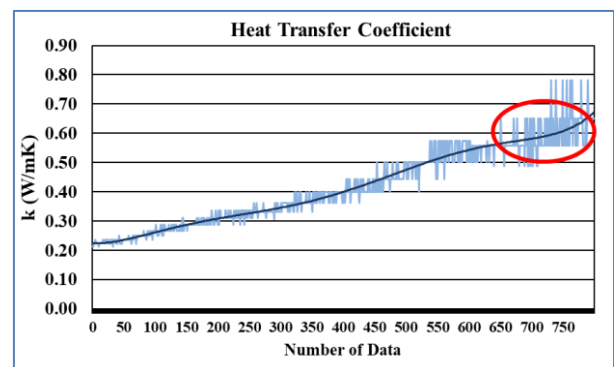


Figure 5. Alteration of the heat transfer coefficient

The data was recorded for every five seconds from the test setup and the recorded data was analysed graphically. When the data taken from the device is examined entirely, it is clearly seen that the heat transfer coefficient value not stable up to 690th data after that the system is seen in balance between 690th and 800th, where the values are near to each other and the line started to flatten. Accordingly, the heat transfer coefficient of the pomegranate seed was found as $k = 0.6115$ (W/mK) in the tests conducted under the above and on accepted conditions. There are little studies on heat transfer coefficient of pomegranate seed in literature and they found smaller heat condition coefficient than $k = 0.6115$ (W/mK) in theirs studies. The pomegranate seed sample that used in the experiment setup was made into a single piece by pressing with a cylindrical mold. However, in other studies [27, 28], the pomegranate seed sample was milled and dried to measure at different humidity and temperature in test tube without being pressed. In contrast to the pressed sample, when the measurement is made in this way, air molecules fill the gaps of the sample and cause the heat transfer coefficient to be smaller.

In addition, since the heat transfer coefficient of the pomegranate seed is smaller than the pure concrete ($k_{concrete} = 8$ W/mK) [30], it makes alternative to the concrete for using an insulation material in structure and even in insulation reinforced concrete buildings.

3.2 Electromagnetic Measurement

Experimental studies of the electromagnetic transduction of the sample were completed using a two-port vector network analyser device. This device offers S-parameters, also known as scattering parameters. Insulation materials such as carbon reinforced Eps (Expanded Polystyrene), Sponge and 18 densite Eps (Styrofoam) were compared with the concrete with added pomegranate seed for their heat transfer coefficients. At the beginning of the measurement, the device is calibrated and the effect of the added cables, adapters, equipment, etc. is eliminated. The values of the scattering parameters in the frequency range of 3-18 GHz band are shown in Figure 6 and Figure 7. The pomegranate sample was compared with the commonly used insulation materials under the same laboratory conditions.

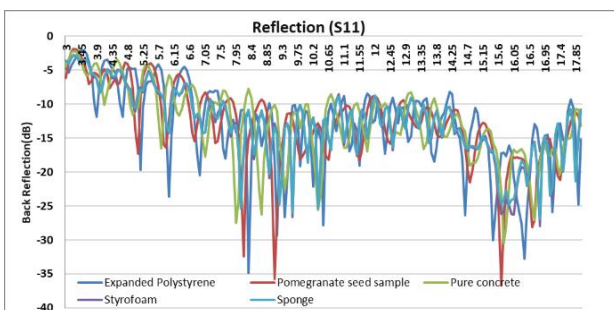


Figure 6. Alteration of reflection parameter according to frequency (GHz)

When the variation of the reflection parameter is examined, it appears that the sample does not have a meaningful effect on the reflected signal at this time. However, examining Figure 7, which shows the energy

transfer from the first port to the second port (or vice versa), the proposed sample clearly showed significant differences, especially after 6 GHz. As the values in the graph become smaller, it shows that the energy transfer between the ports decreases by that amount in dB. One can see from the figure that the proposed structure preventing the electromagnetic energy transfer and behaves like an electromagnetic absorber. Considering that there is not too much return, it appears that the sample is absorbing the signal in the frequency band being worked on. Because of this feature, the use of the proposed sample as an insulation material will provide many benefits;

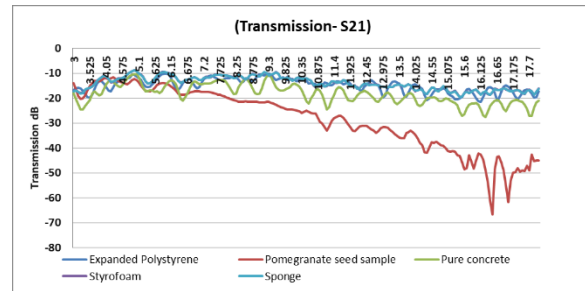


Figure 7. Alteration of Transmission Parameter according to frequency (GHz)

4. Conclusions

In this study; a new perspective on the recovery of agricultural wastes with limited use in the industry has been put forward. It is an important fact that a great amount of energy saving can be made by performing recycling of the wastes obtained in the sectors especially in agricultural areas and this energy saving has a great importance. In this experimental study conducted about the recovery of tons of pomegranate seeds which are thrown as agricultural wastes, the heat transfer coefficient obtained from these pomegranate seeds are measured ($k = 0.6115$ W/mK). This heat transfer coefficient value indicates that the use of pomegranate seed as thermal insulation material is alternative to concrete because of better heat transfer coefficient. It has been shown that it might be possible to use it as an additive material to other insulation. In addition, it has been found at the end of the conducted electromagnetic measurements that the proposed material offers considerable advantages in terms of electromagnetic insulation compared to the existing insulation materials and pure concrete. Although the reflection values did not alter much, the transmitted power was identified to decrease at very high rates especially after the frequency of 6 GHz, and it is believed that it can be advantageous to use it as an electromagnetic absorber. In today's environment, where electromagnetic radiation is very common, especially near to base stations and other places where electromagnetic pollution is high, the use of such insulating materials will provide a lot of advantages. Consequently, in the case of using electromagnetic absorption materials such as the test sample can absorb undesirable effect of the electromagnetic radiation especially in closed structures such as houses, schools, hospitals etc.

Nomenclature

| | |
|-----|------------------------------------|
| Q | : Heat quantity (W) |
| k | : Heat transfer coefficient (W/mK) |
| T | : Temperature (K) |
| A | : Area (m ²) |
| l | : Thickness (m) |

References

- Tüccar, G. and Uludamar, E., *Emission and engine performance analysis of a diesel engine using hydrogen enriched pomegranate seed oil biodiesel*. International Journal of Hydrogen Energy, 2018. **43**(38): p. 18014-18019.
- Hajjari, M., Tabatabaei, M., Aghbashlo, M., and Ghanavati, H., *A review on the prospects of sustainable biodiesel production: a global scenario with an emphasis on waste-oil biodiesel utilization*. Renewable and Sustainable Energy Reviews, 2017. **72**: p. 445-464.
- Bulut, U., and Muratoglu, G., *Renewable energy in Turkey: Great potential, low but increasing utilization, and an empirical analysis on renewable energy-growth nexus*. Energy Policy, 2018. **123**: p. 240-250.
- Koç, A., Yağlı, H., Koç, Y., and Uğurlu, İ., *Dünyada ve Türkiye'de Enerji Görünümünün Genel Değerlendirilmesi*. Engineer & the Machinery Magazine, 2018. **59**(692): p. 86-114.
- Türkiye Doğalgaz Dağıtıcıları Birliği (GAZBİR), [cited 2019 09 February]; Available from: <http://www.gazbir.org.tr/uploads/page/Dunya-ve-Turkiye-Enerji-Gorunumu.pdf>
- Enerji Tabii ve Kaynaklar Bakanlığı. [cited 2019 09 February]; Available from: <https://www.eigm.gov.tr/tr-TR/Denge-Tablolari/Denge-Tablolari>.
- Bulut, U. and Muratoglu, G., *Renewable energy in Turkey: Great potential, low but increasing utilization, and an empirical analysis on renewable energy-growth nexus*. Energy Policy, 2018. **123**: p. 240-250.
- Türkiye Petrolleri (TP). [cited 2019 09 February]; Available from: <http://www.tpao.gov.tr/tp5/docs/rapor/sectorrapor3105.pdf>.
- Ervural, B. C., Zaim, S., Demirel, O. F., Aydin, Z. and Delen, D., *An ANP and fuzzy TOPSIS-based SWOT analysis for Turkey's energy planning*. Renewable and Sustainable Energy Reviews, 2018. **82**: p. 1538-1550.
- Bilgiç, H.H., Yağlı, H., Koç, A. and Yapıcı, A., *Deneyisel bir organik Rankine Çevriminde Yapay Sinir Ağları (YSA) Yardımıyla Güç Tahmini*. Selçuk University Journal of Engineering, Science & Technology, 2016. **4**(1): p. 7-17.
- Yağlı, H., Koç, Y., Koç, A., Görgülü, A. and Tandiroğlu, A., *Parametric optimization and exergetic analysis comparison of subcritical and supercritical organic Rankine cycle (ORC) for biogas fuelled combined heat and power (CHP) engine exhaust gas waste heat*. Energy, 2016. **111**: p. 923-932.
- Yağlı, H., Koc, A., Karakus, C. and Koc, Y. *Comparison of toluene and cyclohexane as a working fluid of an organic Rankine cycle used for reheat furnace waste heat recovery*. International Journal of Exergy, 2016. **19**(3): p. 420-438.
- Yağlı, H., Karakuş, C., Koç, Y., Çevik, M., Uğurlu, İ. and Koç, A., *Designing and exergetic analysis of a solar power tower system for Iskenderun region*. International Journal of Exergy, 2019. **28**(1): p. 96-112.
- Yılmaz, M., *Türkiye'nin Enerji Potansiyeli ve Yenilenebilir Enerji Kaynaklarının Elektrik Enerjisi Üretimi Açısından Önemi*, Ankara Üniversitesi Çevre Bilimleri Derg., 2012. **4**(2): p. 33-54.
- İner, G. and Çağlar, E., *Two countries at same parallel in solar energy productions: USA and Turkey*. International Advanced Researches and Engineering Journal, 2018. **2**(3): p. 325-329.
- Gürer, C., *Atık Mermer Parçalarının Bitümlü Yol Kaplamalarında Değerlendirilmesi*, 2005. Yüksek Lisans Tezi, Afyon Kocatepe Üniversitesi, Fen Bilimleri Enstitüsü, Yapı Eğitimi Anabilim Dalı, Afyon.
- Gustavsson, J., Cederberg, C., Sonesson, U., Otterdijk, R.van. and Meybeck, A. [cited 2019 09 February]; Available from: <http://www.fao.org/3/mb060e/mb060e00.pdf>.
- Goula, A.M. and Lazarides, H.N., *Integrated processes can turn industrial food waste into valuable food by-products and/or ingredients: The cases of olive mill and pomegranate wastes*. Journal of Food Engineering, 2015. **167**: p. 45-50.
- Dönmez, İ. and Dönmez, Ş., *Ağaç kabuğunun yapısı ve yararlanma imkanları*. SDÜ Orman Fakültesi Dergisi, 2013. **14**: p. 156-162.
- Köse Ö., Koç Y., Yağlı H., Üstün İ., Kasap F., Öztürk N.A. and Koç A., *Experimental Investigation of Thermal Coefficient of the Graphene Used Concrete*. International Advanced Researches and Engineering Journal, (2019). (In Print).
- Binici, H., Gemci, R., Küçükönder A. and Solak H., *Pamuk Atığı, Uçucu Kül ve Barit İle Üretilen Sunta Panellerin Isı, Ses ve Radyasyon Geçirgenliği Özellikleri*. Yapı Teknolojileri Elektronik Dergisi, 2012. **8**(1): p. 16-25.
- Kozak, M., *Tekstil Atıklarının Yapı Malzemesi Olarak Kullanım Alanlarının Araştırılması*. Yapı Teknolojileri Elektronik Dergisi, 2010. **6**(1): p. 62-70.
- Fayaz, G., Goli, S.A.H., Kadivar, M., Valoppi, F., Barba, L., Calligaris, S. and Nicoli, M.C., *Potential application of pomegranate seed oil oleogels based on monoglycerides, beeswax and propolis wax as partial substitutes of palm oil in functional chocolate spread*. LWT-Food Science and Technology, 2017. **86**: p. 523-529.
- Talekar, S., Patti, A.F., Singh, R., Vijayraghavan, R. and Arora, A., *From waste to wealth: High recovery of nutraceuticals from pomegranate seed waste using a green extraction process*. Industrial Crops and Products, 2018. **112**: p. 790-802.
- Hora, J.J., Maydew, E.R., Lansky, E.P. and Dwivedi, C., *Chemo preventive effects of pomegranate seed oil on skin tumor development in CDI mice*. Journal of medicinal food, 2003. **6**(3): p. 157-161.
- Tüccar, G. and Uludamar, E., *Emission and engine performance analysis of a diesel engine using hydrogen enriched pomegranate seed oil biodiesel*. International Journal of Hydrogen Energy, 2018. **43**(38): p. 18014-18019.
- Mahmood, M. and Hosein, K.M., *Determination and comparison of thermal conductivity of Iranian pomegranate varieties*, in *18th National Congress on food technology: Mashhad*. p. 15-16.

28. Mukama, M., Ambaw, A. and Opara, U.L., *Thermal properties of whole and tissue parts of pomegranate (Punica granatum) fruit*. Journal of Food Measurement and Characterization, 2018. **13**(2): p. 901-910.
29. Deneysan. [cited 2019 09 February]; Available from: <http://deneysan.com/en/products/heat-transfer/ht-350-thermal-conductivity-detecting-training-set/221>.
30. Georgia State University. [cited 2019 09 February]; Available from: <http://hyperphysics.phy-astr.gsu.edu/hbase/Tables/thrcn>.



Research Article

Experimental investigation of thermal coefficient of the graphene used concrete

Özkan Köse^a , Yıldız Koç^a , Hüseyin Yağlı^a , İsmail Üstün^a , Furkan Kasap^a ,
Nurhan Adil Öztürk^a  and Ali Koç^{a,*} 

^aDepartment of Mechanical Engineering, Iskenderun Technical University, Iskenderun, Hatay, 31200, Turkey

ARTICLE INFO

Article history:

Received 13 April 2018

Revised 17 October 2018

Accepted 24 October 2018

Keywords:

Graphene

Thermal conductivity coefficient

Concrete materials

ABSTRACT

Today, fossil fuels are used primarily in energy production throughout the world. However, the ever-diminishing energy production and developing technology has encouraged energy recovery, saving or different topics. Grafen is one of the most remarkable studies in the field of nanotechnology in recent years. This nanotechnological product, considered as one of the mainstream products of future technology, has superior properties in some physical and chemical issues compared to many materials. Because of its high conductivity and durability, it continues to attract attention in energy and materials science. In this paper, the concrete samples obtained by mixing the graphene at certain ratios were compared with pure concrete (graphene free concrete) and the thermal conductivity of the grafen added concrete was determined. Finally, the thermal conductivity of the pure concrete (thermal conductivity of 1.3096 W/mK) added with 1 gr, 2 gr, 3 gr, 4 gr and 5 gr graphene were calculated as 1.6516, 1.6668, 1.6773, 1.8080 and 1.8486 (W/mK), respectively.

© 2019 Advanced Researches and Engineering Journal (IAREJ) and the Author(s).

1. Introduction

Today, fossil fuels such as coal, oil and natural gas, which are known as non-renewable energy sources, are used primarily in energy production around the World [1]. Developing technology and increasing energy consumption have encouraged the scholars to study about energy recovery and savings in the field of nanotechnology. One of the most widely studied topics on nanotechnology in recent years is the use of graphene. The graphene, which has a two-dimensional carbon atom structure, is known as a unique nano-product with a honeycomb appearance [2]. The graphene, seen as one of the mainstream products of future technology, has outstanding properties in some physical and chemical issues compared to many materials. Thanks to such superior properties of the graphene, it is possible that the structural integrity of the buildings and the interior or exterior structure of the buildings are more durable and long-life in isolation applications made by using the

graphene [3].

Moreover, if the graphene is used as isolation, it has been determined in a number of studies that it can be able to minimize adverse situations, especially due to seasonal weather variation, over time. In other words, thanks to the use of graphene in building concrete materials, it can increase the resistance of the structure against weather conditions like snow, rain, hot, cold [4,5]. Therefore, many companies in Europe have allocated a large share of their budgets to Research & Development Studies in order to support and develop grafen investigations. Although there are very few studies on the use of graphene materials, some studies are available in the literature. Zenyatta (2017), in this study on Graphene Concrete Pilot Project Developments, the Graphene mixture arising from Albany derivation has been applied to a large volume of concrete. In result of this experimental studies, it was seen that the addition of graphene into the concrete provided a faster curing in the concrete. Besides, it has shown that it can achieve a remarkable mechanical performance that

* Corresponding author. Tel.: +90 (326) 613 56 00; Fax: +90 (326) 613 56 13.

E-mail addresses: ozkan.kose@iste.edu.tr (Ö. Köse), yildiz.koc@iste.edu.tr (Y. Koç), huseyin.yagli@iste.edu.tr (H. Yağlı),

ismail.ustun@iste.edu.tr (İ. Üstün), furkankasap05@gmail.com (F. Kasap), nadil.ozturk@iste.edu.tr (N.A. Öztürk), ali.koc@iste.edu.tr (A. Koç)

ORCID: 0000-0002-9069-1989 (Ö. Köse), 0000-0002-2219-645X (Y. Koç), 0000-0002-9777-0698 (H. Yağlı), 0000-0001-8885-5510 (İ. Üstün),

0000-0003-1481-0699 (F. Kasap), 0000-0002-9551-8122 (N.A. Öztürk), 0000-0002-7388-2628 (A. Koç)

DOI: 10.35860/iarej.415181

prevents premature deterioration of concrete by tolerating external forces during natural disasters. In addition to all these, graphene material usage is thought that it will reduce the amount of cement used in construction [6]. Ahammed, N. et. al. (2015) In this study, the design, development and measurement of graphene-water (nanofluid) thermal conductivity using a hot wire technique are temporarily investigated at ambient temperatures ranging from 10 °C to 50 °C. The equipment is designed to measure thermal conductivity using a single platinum wire with a diameter of 50 µm and a length of 100 mm. Platinum micro-wire is acted as both a temperature sensor and a heating element. SDBS (sodium dodecyl benzene sulphonate) as a surfactant was dispersed in 100 ml of water for a long-time stability and a graphite was used at a low volume concentration (0.05%, 0.1% and 0.15%) smaller than 100 nm. As a result, an increase in thermal conductivity of 37.2% when compared to water at the same temperature for a 0.15% volume concentration of graphene at 50 °C was observed. Besides, another result from this study is that the average thermal conductivity increment percentage at volume concentration (e.g., 0.05% to 0.15%) at temperatures between 10 °C and 50 °C is found to be 3.3% higher than the average improvement level [7]. In a study by Australian technology minerals company Talga Resources (2017), they have worked on the ability of the grafen to improve the strength of concrete by forming graphite and graphite-added cement and concrete products. As a result of the 28-day waiting period, the increase in the bending strength and the compression strength of the reference concrete were occurred by 26% and 14%, respectively. The obtained data show that graphene will provide significant performance advantages for various industrial applications, particularly the global construction and infrastructure sectors [8]. Wicklein, B. et al. (2014), they have used frozen cellulose nanospheres, graphene oxide, and sepiolite nanorods to increase the energy efficiency of buildings and produce super insulated, fire resistant, strong anisotropic foams. As a result of the study, it was found out that foams that perform better than conventional polymer-based insulation materials have a thermal conductivity of about half (15 W/mK) of the expanded polystyrene and excellent fire resistance [9].

When the studies in the literature considered together, it is clearly seen that almost all the studies on the graphene measures the electrical resistance of the graphene. However, there are only limited studies that uses graphene in the concrete. In this study, the linear heat transfer coefficient of the graphene was investigated, inspiring from the current studies on the graphene. The Concrete samples prepared by using graphene were mixed with pure concrete (graphene free concrete) and the heat transfer coefficient was examined experimentally. The appropriateness of the use of the graphene to the concrete was investigated in terms of heat transfer. Detailed analysis of the material was made using the experimental results obtained.

2. Material and Method

2.1 Graphene Properties

In spite of having a two-dimensional structure, the graphene, which is 300 times more durable than steel, is the lightest and thinnest material known for honeypot appearance of the carbon. Grafen is known as the first two-dimensional crystal material and transmits heat at a much higher rate than copper. Graphene that is the more robust and highly flexible than steel is the thinnest shape brought the graphite to an atomic thickness like a diamond. Thanks to this flexibility, materials made from graphene can easily be folded, twisted and extended. Grafen is one of the rare materials that keeps all these features together [3]. In this study, a graphite named as GNP (3 nm-24 micron-150 m²/g) was used. The technical characteristics of the used graphene are given in Table 1.

Table 1. The technical characteristics of the used graphene

| Properties | Value | Units |
|-----------------------|----------|--------------------|
| Purity | 99.5 | % |
| Thickness | 6 | nm |
| Diameter | 24 | µm |
| Specific Surface Area | 150 | m ² /gr |
| Conductivity | 1100-100 | s/m |
| Colour | Grey | – |

2.2 Preparation of Graphene

In the scope of the experimental study, samples were examined with the help of molds prepared by using cement, water and graphene. The materials included in the samples and the usage rates of these materials are given in Table 2.

Table 2. The materials included in the samples and the usage rates of these materials

| | Cement | Water | Graphene |
|--------------------|--------|-------|----------|
| | gr | ml | gr |
| Pure concrete | 200 | 60 | 0 |
| 1. Graphene sample | 200 | 61 | 1 |
| 2. Graphene Sample | 200 | 63.75 | 2 |
| 3. Graphene Sample | 200 | 67 | 3 |
| 4. Graphene Sample | 200 | 69 | 4 |
| 5. Graphene Sample | 200 | 75 | 5 |

In the study cement clay (pure concrete) was brought to homogenous consistency with 32% water and the obtained sample was selected as a control sample. Five graphene-

cement mixtures of 1 gr, 2 gr, 3 gr, 4 gr and 5 gr were used during the experimental study. In the preparation phase of the samples, five graphene-cement mixture and pure concrete samples were comprised by varying the amount of water since the graphene's water absorption ability was fairly good, provided that the amount of cement was constant. Then the samples which were dried in the mold along one day were removed from the mold and kept in water during 28 days. The samples were taken from the water and contacted with the atmospheric air for a certain period of time for drying material surface. The samples waited in the air were kept at 45 °C for one day in an oven and taken to the drying room. The prepared test samples are shown in Figure 1.

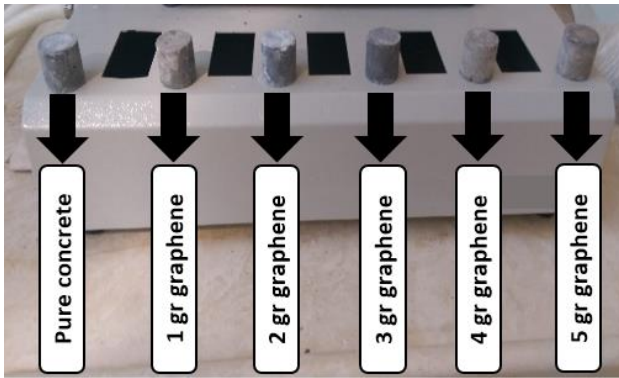


Figure 1. Samples used in the experiment

As the concrete molding is carried out at the appropriate ambient temperature (25 °C), no chemical additive material is used during the preparation of the samples. During all these preparation steps, it has been paid attention to the removal of the samples from the mold without damaging the concrete, the mixing amounts of the materials, the vibration and the presence of any foreign matter in concrete.

2.3 Description of Experimental Setup

All experimental analyses and data recording steps were carried out using a linear heat transfer coefficient measurement instrument available in our laboratory. The linear heat transfer coefficient measurement instrument used is shown in Figure 2.

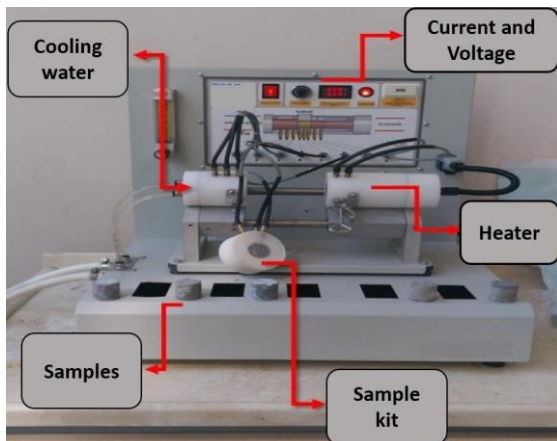


Figure 2. Linear heat transfer coefficient analysing setup

In this part, the water coming from the network is drawing heat from the hot section by getting in touch with the sample. The inlet and outlet temperature of the water entering the cooler section, the area where the water contacts with the sample is measured by the test device. Sample apparatus is the main equipment which is connected to the test device. Three different temperature measurements are made on the surface where the sample is connected. These measurements are; in the contact area where the sample is connected to the cold source, in the middle part of the sample and in the contact area to which the hot source is connected. In the heater section, heat is applied to the sample with the resistor and temperature measurement is made from two different points. All measurements made during the experiment are made automatically by the system at specified time intervals. It is recorded on the computer with the help of data control software. The MDVT data control software interface used during the operation is shown in Figure 3

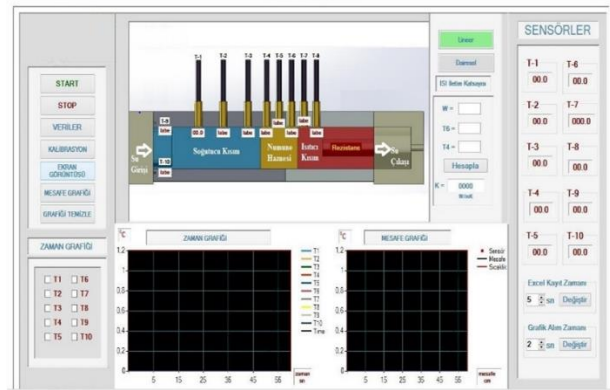


Figure 3. MDVTS data control software interface

The data control software used throughout the study performs the functions of collecting data and sending data from the centre, analysing and then displaying this data on an operator's screen.

2.4 Mathematical Model

As defined in the first law of thermodynamics, heat is transferred from the hot part to the cold part. There are three different types in which heat is transferred. These are convection, conduction and radiation. In this study, since the heat transfer is taking place through a solid body, the heat transfer equilibrium equation via conduction was theoretically used to measure the heat transfer coefficient. Heat transfer coefficient according to Fourier's law;

$$Q_x = -kA \frac{dT}{dx} \quad (1)$$

In the equation, Q_x expresses the amount of heat passing through a certain area in the x direction. A refers to the determined area. k stands for the heat transfer coefficient. Q_x is calculated by reading the voltage (V) and current (A) values from the test device;

$$Q_x = VA \tag{2}$$

The data recorded by the computer using the calculated Q_x values was regulated and k values were found for each sample.

3. Research Findings

Pure concrete (cement clay) and graphene samples between 1 and 5 gr were separately tested in MDVTS. The heat transfer coefficients were recorded to the excel program at intervals of 5 seconds for each sample. Comparison of the heat transfer coefficients of pure concrete and 1gr graphene samples is given in Figure 4.

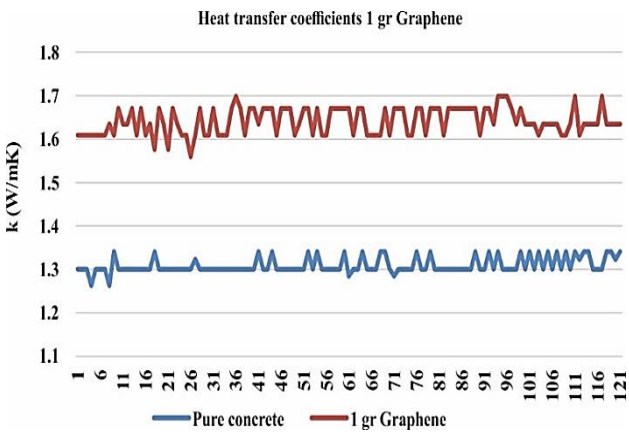


Figure 4. Comparison of heat transfer coefficients of pure concrete and 1gr grafted samples

The heat transfer coefficients of pure concrete and 1 gr graphene samples were examined in the MDVTS and data were recorded at intervals of 5 seconds. Pure concrete and 1gr graphene mixture have reached a balance between the 81st. and 91st. data. The heat transfer coefficient of pure concrete and graphene mixture were 1.30966,1 W/mK and 1.65116 W/mK, respectively. when the graphene was included in pure concrete, it was observed that the heat transfer coefficient has increased seriously. Comparison of heat transfer coefficients of pure concrete and 2 gr of graphene mixture samples are shown in Figure 5.

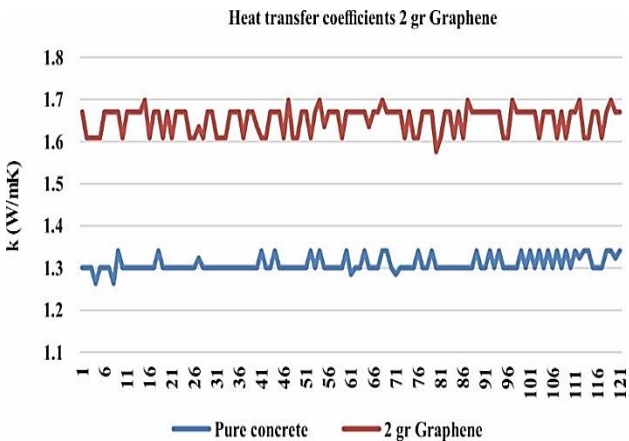


Figure 5. Comparison of heat transfer coefficients of pure concrete and 2 gr graphene mixture

When the data recorded at intervals of 5 seconds were analysed, it was seen that the heat transfer coefficient of the graphene mixture of 2 gr remained constant at between 61. and 65. data and the heat transfer coefficient of the 2 gr graphene mixture was approximately 1.66648 W/mK. Heat transfer coefficient has increased a little more when adding 2 gr graphene to the mixture. comparison of heat transfer coefficient of 3 gr graphene included pure cement is given Figure 6.

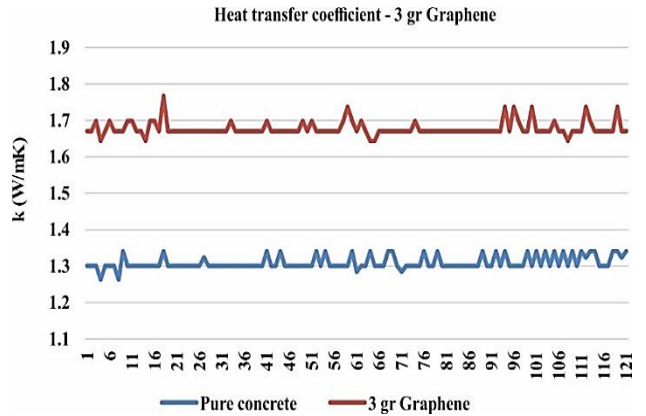


Figure 6. Comparison of heat transfer coefficients of pure concrete and 3 gr graphene mixture

The heat transfer coefficient of the graphene mixture reaching the balance between 73. and 97. points was found to be about 1.67783 W/mK. It was found that there was no significant increase in the heat transfer coefficient when the obtained data were compared with the mixture containing 2 gr of graphene. Comparison of heat transfer coefficient of 4 gr graphene included a sample with pure cement is shown Figure 7.

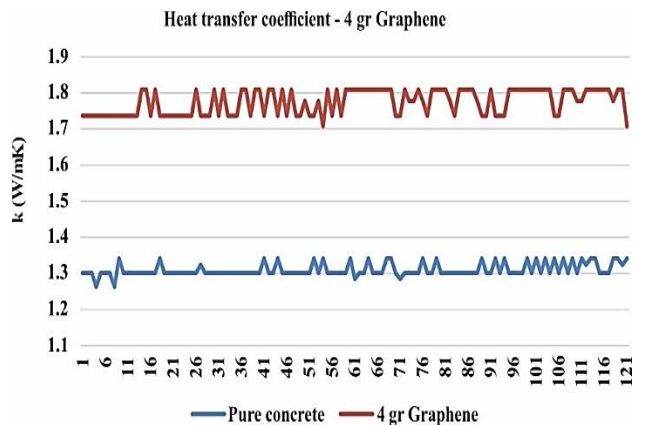


Figure 7. Comparison of heat transfer coefficient of 4 gr graphene included a sample with pure cement

The heat transfer coefficient of 4 gr graphene added sample was balanced between 57. and 73. points and approximately calculated as 1.80890 W/mK. After the amount of 3 g of graphene, a significant increase has occurred in the heat transfer coefficient. Comparison of heat transfer coefficient of 5 gr graphene included a sample with pure cement is demonstrated Figure 8.

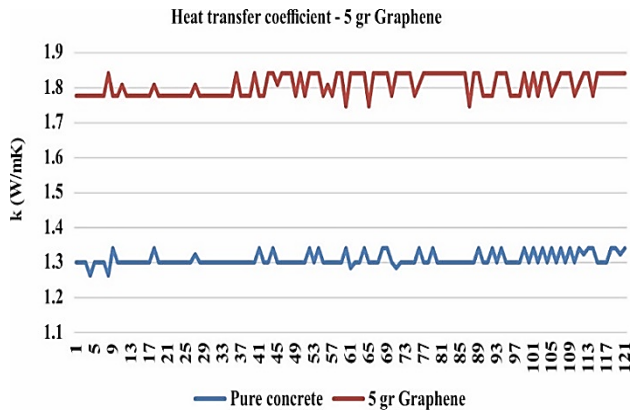


Figure 8. Comparison of heat transfer coefficient of 5 gr graphene included a sample with pure cement

5 gr of graphene included sample have reached a balance between the 77. and 89. points. The heat transfer coefficient of graphene sample is determined as 1.84846 W/mK. It was observed that the increase in the heat transfer coefficient of 5 g of graphene added sample was slower than that of the graphene sample of 4 g. Comparison of heat transfer coefficients of graphene included samples between 1 and 5 gr is displayed Figure 9.

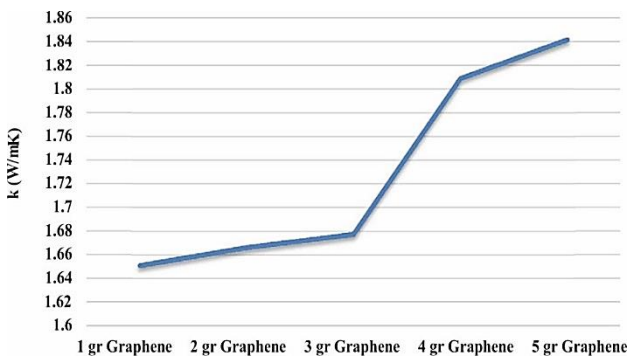


Figure 9. Comparison of heat transfer coefficients of graphene included samples between 1 and 5 gr

When the heat transfer coefficients of all graphene included concrete samples are examined in detail, it is seen that the amount of graphene has a considerable effect on the heat transfer coefficient. Although a linear increase was observed between 1 gr and 3 gr graphene, the heat transfer coefficient has increased substantially when 4 g of graphene is added to the sample. Eventually, it was observed that the rate of increase of the heat transfer coefficient decreased when 5 gr graphene was added to the sample.

4. Conclusions

In the calculations made in the experiment study, 121 data were recorded and plotted. The heat transfer coefficients of pure concrete were compared with the graphene added samples between 1gr and 5 gr. When the above graphs were taken into consideration, it was seen that the heat transfer coefficients of graphene-based samples have increased approximately between 35% and 50% compared to pure concrete. Heat transfer coefficients according to graphene amount is given Table 3.

Table 3. Heat transfer coefficients according to graphene amount

| Samples | k | Unit |
|--------------------|--------|------|
| Pure Concrete | 1.3096 | W/mK |
| 1. Graphene Sample | 1.6516 | W/mK |
| 2. Graphene Sample | 1.6668 | W/mK |
| 3. Graphene Sample | 1.6773 | W/mK |
| 4. Graphene Sample | 1.8080 | W/mK |
| 5. Graphene Sample | 1.8486 | W/mK |

The obtained results showed that as the amount of graphene in pure concrete increases, the heat transfer coefficient escalates significantly. Although the concrete structure is desired to have a high thermal resistance for many applications, it can be more appropriate to use the concrete structure with a high heat transfer coefficient in some applications. The use of the graphene-based material in the work areas where high heat transfer coefficient is required (in the fields where rapid cooling is desired) will provide serious advantages. Graphene is suitable for use on concrete walls of cooling towers used in thermal and nuclear power plants, where heat must be removed quickly and high strength is required. Besides, it is considered that the use of graphene-reinforced concrete tapes will be advantageous in order to achieve the desired rapid cooling on the concrete tape surfaces where steel billet is transferred to the rolling mill

Nomenclature

| | |
|---|--|
| k | : Heat transfer coefficient (W/mK) |
| A | : Current (Amper) |
| A | : Area (m ²) |
| V | : Voltage (Volt) |
| Q | : Energy obtained from current and voltage (J/s) |
| T | : Temperature (°C) |

References

- Koç, A., Yağlı, H., Koç, Y. and Uğurlu, İ., Dünyada ve Türkiye'de enerji görünümünün genel değerlendirilmesi. Engineer & the Machinery Magazine, 2018. 59(692): p. 86-114.
- Grafen-Nanografi Türkiye. (n.d.). [cited 2018 10 October]; Retrieved from <http://nanografi.com.tr/grafen/>
- Novoselov, K. S., Fal, V. I., Colombo, L., Gellert, P. R., Schwab, M. G., & Kim, K., A roadmap for graphene. nature, 2012. 490(7419): p. 192.
- Cao, M. L., Zhang, H. X., & Zhang, C., Effect of graphene on mechanical properties of cement mortars. Journal of Central South University, 2016. 23(4), p. 919-925.
- Monash University. [cited 2018 11 October]; Retrieved from: https://www.monash.edu/_data/assets/pdf_file/0006/356973/Graphene-Reinforced-Concrete-Composites.pdf
- Zenyatta. [cited 2018 11 October]; Retrieved from: <http://www.zenyatta.ca/article/press-release-4468.asp>
- Ahammed N., Asirvatham, L.G., Titus J., Bose J.R. and S. Wongwises, Measurement of thermal conductivity of graphene-water nanofluid at below and above ambient

temperatures. *International Communications in Heat and Mass Transfer*, 2016. **70**: p. 66-74.

8. Talgaresources. [cited 2018 11 October]; Retrieved from: http://www.talgaresources.com/irm/PDF/2056_0/GrapheneMalaysia2017Presentation.
9. Wicklein, B., Kocjan, A., Salazar-Alvarez, G., Carosio, F., Camino, G., Antonietti, M., & Bergström, L., Thermally insulating and fire-retardant lightweight anisotropic foams based on nanocellulose and graphene oxide. *Nature nanotechnology*, 2015. **10**(3), 277.



Research Article

Experimental investigation of the effect of compression pressure on mechanical properties in glass fiber reinforced organic material-based brake pads production

Sait Aras ^{a,*}  and Necmettin Tarakçioğlu ^b 

^a Selçuklu Vocational and Technical Anatolian High School, Department of Motor Vehicle Technology, Konya, 42070, Turkey

^b Selçuk University, Faculty of Technology, Department of Metallurgy and Materials Engineering, Konya, 42030, Turkey

ARTICLE INFO

Article history:

Received 30 July 2018

Revised 22 December 2018

Accepted 18 April 2019

Keywords:

Brake pads

Coefficient of friction

Compression press

Hardness

Juniperus drupacea

Wear ratio

ABSTRACT

In this study, samples which can be used as brake pads are prepared. A mixture of 50% barite by mass, 20% glass fiber, 25% phenolic resin and 5% coke powder was prepared, and 6 samples were prepared by adding juniperus drupacea nut powder (JDNP) at 10%, 25% and 40%. The samples were produced in 3 different mixing times, 2 different compaction times, 3 different compaction temperatures and 3 different compression pressures. The effect of the compression pressure on the wear rate, hardness, density and cold friction coefficient was investigated. The wear rate ranges from $0.093 \cdot 10^{-7}$ - $4.235 \cdot 10^{-7} \text{cm}^3 \cdot \text{N}^{-1} \cdot \text{m}^{-1}$. The coefficient of cold friction ranges from 0.30 to 0.48. The density is between 1.82 - 2.17g/cm^3 . The hardness values are from 85 to 117 according to the Rockwell R scale. Wear rate and cold friction coefficient values are in accordance with TS 555 standard. It has been determined that the compressive pressure is most affected by the hardness and friction coefficient. Generally, rise of pressure reduces hardness and friction coefficient. The effect of density on JDNP ratio is opposite.

© 2019, Advanced Researches and Engineering Journal (IAREJ) and the Author(s).

1. Introduction

People have to complete their needs by either moving or carrying in order to make their lives easier to get food, beverages, fuel or energy. They use different means of transportation for these needs.

The oldest known wheel remains dates from 3000 to 2500 BC [1]. Although the invention of the wheel goes back 5000 years, the history of motor vehicles is about 130 years.

People acquire the necessary energy from the internal combustion engines that burn different fuels when transporting themselves and the materials they need. This movement of the motor is transmitted by the powertrain to the wheels by adjusting the speed, direction and torque.

The vehicles produce kinetic energy while moving. The brake system turns this energy into heat energy.

The use of frictional forces in the moving bodies to produce a deceleration mechanism and to form between

the two sliding bodies in contact with each other has historically been up to the beginning of the first tests of mankind [2].

The performance of the system depends on the friction between the pads that presses against the rotating disk (or drum).

The numerical value of friction is practically always present even if it is too small to be taken into account [3]. Friction should be within certain values between the respective surfaces. A typical example is the fact that the vehicle cannot stop at the desired distance and time due to low friction in the vehicle brakes or that the brakes of the vehicle are blocked due to excessive friction [4].

The most important factor of braking performance is the stopping distance after braking. This is possible by maximum deceleration acceleration. High braking performance is related with high quality braking pads which constitutes a significant portion of the friction surfaces [5].

* Corresponding author. Tel.: +90 532 711 52 27, Fax: +90 332 241 21 79

E-mail addresses: saitaras@gmail.com (S. Aras), ntarakcioglu@selcuk.edu.tr (N. Tarakçioğlu)

ORCID: 0000-0003-2618-535X (S. Aras), 0000-0003-0742-6699 (N. Tarakçioğlu)

DOI: 10.35860/iarej.449089

Abrasion is an inevitable consequence of friction [4]. Wear; temperature, lubrication, working conditions, environment, surface roughness, material pair etc. elements are connected to a system [6]. The contact area of the two friction surfaces is called the mechanical interaction area. This area has a significant effect on wear [7].

Braking systems consist mainly of two rubbing elements fig.1. These are called lining and disc/drum. As we don't have a specific formula for the materials used in these pads, development studies for better pads are still going on [8].

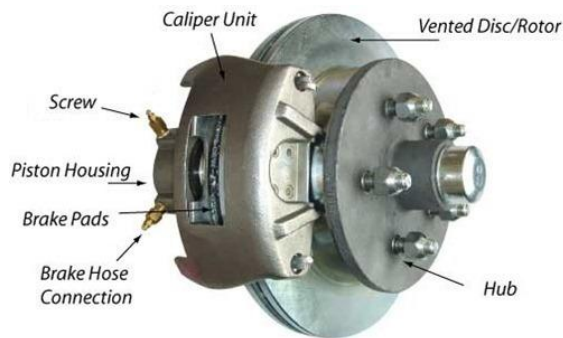


Figure 1. Disc brake unit [9]

The affecting factors to braking pads are components and producing parameters as it surged in studies of braking.

While producing brake pads hundreds of different materials in different rates are tried. Among the parameters affecting the produced brake pads are distinguishing as mixing type, duration of mixing, pressing temperature, pressing pressure, pressing time and sintering time.

Applied pressure value changes from 5 MPa to 4000 MPa in literature. If the pressure is to be applied cold, the pressure value is high, and if it is hot, it is lower.

Some of the applying pressing pressure, pressure heat, sort are given in the table 1 bellow.

Table 1. Compression pressures and temperatures in the literature

| Pressing pressure | Pressing temperature | |
|-----------------------|----------------------|------|
| 15MPa | 153°C | [10] |
| 15MPa | 150°C | [11] |
| 8MPa | 150°C | [12] |
| 15MPa | 150°C | [13] |
| 500MPa | cold pressing | [14] |
| 400MPa | room temperature | [15] |
| 1000-400-4000-600 MPa | 150-170°C | [16] |
| 5-7,5-10-12,5 MPa | 125°C | [2] |
| 150-250 bar | 150-180°C | [17] |
| 25Mpa | 150°C | [18] |
| 10, 15, 20 Mpa | 180°C | [19] |
| 100Mpa | 160°C | [20] |
| 100bar | 150°C | [8] |
| 50-100-200-300 Mpa | 150°C | [21] |

In this study the braking pad consists of barite, phenolic resin, glass fiber, coal and juniperus drupacea nut powder (JDNP). The effect of the formed pressures on the hardness, friction coefficient, density and wear rate of different pressing pressures were investigated by changing the pressing pressures to 100, 150 and 200 MPa, which are considered to affect the properties of the starting material.

2. Material and Method

While preparing samples used in research 50% barite, 20% glass fiber, 25% phenolic resin, 5% coal powder are used and to this mixture, a mass of 10%, 25%, 40% rate JDNP is added.

2.1 The sample inclusion and specifications

The barite used in this study is 5 μ m volume and obtained from "Barit Maden Türk AŞ." company. The technical specifications of barite are given in the Table 2.

Table 2. Technical specifications of barite [22]

| | | |
|-------------------------|-------------------|------------|
| BaSO ₄ | % | 91-93 |
| Density | g/cm ³ | 4,25 (min) |
| Hardness | Moh's | 3-3,5 |
| Humidity / Factory exit | % | 0,1 (max) |
| Oil absorbing value | mL/100g | 15-16 |
| Acidity value (pH) | % | 6-8 |

The resin suitable for ÇK 82790 type disc and drum lining is supplied from Çukurova Kimya Endüstrisi AŞ.

The coke was turned into powder in Selçuk University Mining Engineering Laboratory.

3 mm broken glass fiber bunch (PH2) suitable for the production of phenolic linings is used which was produced by "Cam Elyaf Sanayi AŞ. Gebze/Kocaeli". The product specifications of glass fiber are given in the table 3.

Table 3. Product specifications of glass fiber [23]

| | |
|-----------------------------|-----------------|
| Glass Type | E |
| Filament Diameter (μ) | Nom. 13 |
| Moisture Content (%) | max. 0,07 |
| Sizing Type | Silane |
| Sizing Content (%) | 0,90 \pm 0,15 |
| Flowability | Very good |
| Resin Compatibility | Phenolic |
| Chopped Length (mm) | 3 |

In Figure 2(a) juniperus drupacea nuts (JDN) are collected from nature and dried in the sun light. They were washed to get rid of soil and sand and dried again. The photos of broken nuts are in Figure 2(b). The JDN, which was subjected to dehumidification after being broken, was turned into powder Figure 2(c) at Selçuk University Mining Engineering Laboratory.

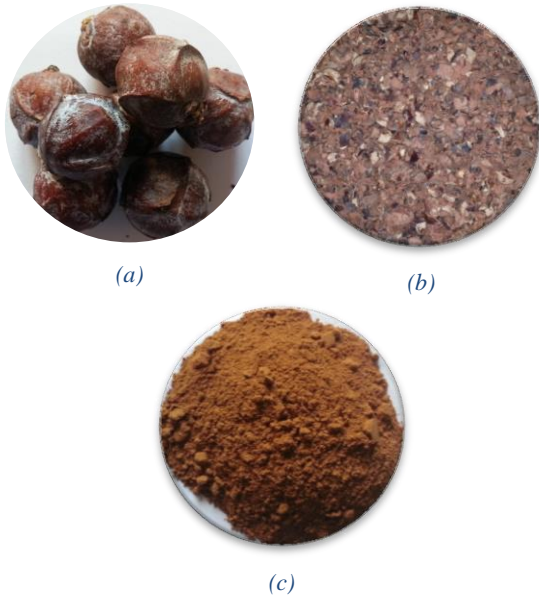


Figure 2. Pictures of juniperus drupacea nuts (JDN) [24]

All the powders were sieved in $\leq 1\text{mm}$. In order to ensure homogeneous distribution of the materials used in the sample production, all of the materials forming the samples were mixed at the mixing times specified in table 4 in the blade mixer.

The contents and parameters used in studies are given in the table 4 below.

Table 4. Sample contents and production parameters

| Sample No | Pressing | | | Mixing time (min) | JDNP (%) |
|-----------|----------------|----------------|------------|-------------------|----------|
| | Duration (min) | Pressure (MPa) | Temp. (°C) | | |
| 1 | 10 | 100 | 140 | 10 | 10 |
| 2 | 10 | 150 | 160 | 15 | 25 |
| 3 | 10 | 200 | 180 | 20 | 40 |
| 4 | 15 | 200 | 180 | 10 | 25 |
| 5 | 15 | 100 | 140 | 15 | 40 |
| 6 | 15 | 150 | 160 | 20 | 10 |

2.2 The experiments

In order to get the friction coefficient and wear rate of the produced samples, the wear test was carried out with a Turkey brand abrading device (Figure 3).



Figure 3. Wear tester

Wear rate tests were carried out using a pin-on-disc type tribo-test machine. The pin-on-disc test apparatus with disc made of grey cast iron of hardness value 19 5HB (62.5 kg.f, 5mm ball) and 180mm track diameter was used to investigate the dry sliding wear rate of the brake pad specimens in accordance with ASTM:D792 standard [25].

Load cell located on the device detects the forces axially generated under constant load after the rotation movement starts and transfers the data to the computer program. The wear rate is measured according to the mass loss principle by measuring the masses before and after the wear test; was calculated using equation (1).

$$W_a = \frac{\Delta G}{\rho \cdot M \cdot S} (\text{mm}^3 \cdot \text{N}^{-1} \cdot \text{m}^{-1}) \quad (1)$$

The hardnesses of the samples were measured on the rockwell R scale (1/2" ball 10kgf preload, 60kgf total load) in the Digirock® brand hardness tester produced by Bulut Makine Sanayi ve Ticaret Ltd.Şti (Figure 4).



Figure 4. Hardness Tester

For the calculation of sample densities, sample masses were weighed with a 1mg precision scales, sample diameters and heights were measured with digital calipers with a sensitivity of 0.01mm in three different axes and calculated with equation (2).

$$\rho = \frac{m}{\frac{\pi \cdot D^2 \cdot h}{4}} (\text{g} \cdot \text{cm}^{-3}) \quad (2)$$

In order to calculate the friction coefficient, during the wear test, the load cell data stored in the wear device were recorded on the computer momentarily. The mean cold friction coefficient was calculated by taking the average of the recorded data during the wear test.

2.3 The results of the experiments

It was found that the most wear on the pin-on-disk test to determine the wear rate was at the sample 5. It came out that it was produced 100MPa pressure, the lowest one. Another

factor is the reduced sample density, which is high for the proportion of JDNP participating in the sample. Thus, the decrease in density caused the wear rate to increase.

The least wear rate is in the number 2, where the pressing pressure is at the mid-level of 150MPa and the minimum rate of JDNP.

The wear rate values of the samples were given in the Figure 5.

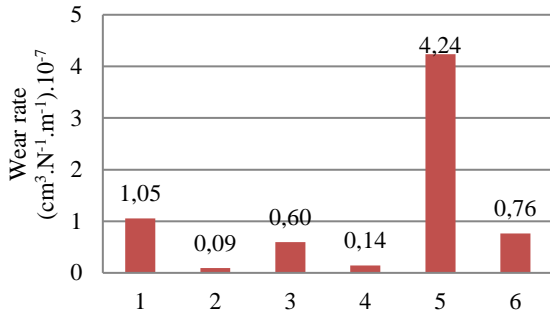


Figure 5. Wear rate graph

When the wear rate graph in fig. 5 and the table 3 are examined together, it is seen that the higher the pressing pressure, the lower the wear rate.

While the wear rate is calculated, the density is also in the denominator. The wear rate is expected to decrease while the density goes up in experiments done in the same conditions. But the density itself isn't the main factor for the wear rate. When we have a look at the graphs in 3 and 4 together, the density of sample 5 is seen low whereas the wear rate is the highest. When the properties of the sample 5, which has the highest wear rate, are examined from table 4, it will be seen that the pressing pressure and pressing temperature is the lowest and the rate of JDNP is the highest. When the wear rates and production parameters of samples 3 and 5 with JDNP at the same rate are examined together, the wear rate of sample 3 is seen to be lower. In order to reduce the wear rate in the use of high-rate JDNP, increasing the pressing pressure and pressing temperature can be a solution.

This condition can be explained by the hardness graph of fig. 7 and the graph of the mean cold friction coefficient in fig. 8, which show that the coefficient of friction of the sample 5 is the highest and that the hardness is relatively small.

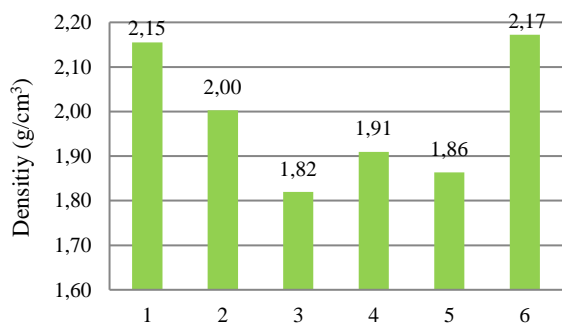


Figure 6. Density graph

High density values were found in samples with low JDNP ratio and low density values were in samples using

high JDNP. In other words, the JDNP ratio is increased, the sample density is decreasing.

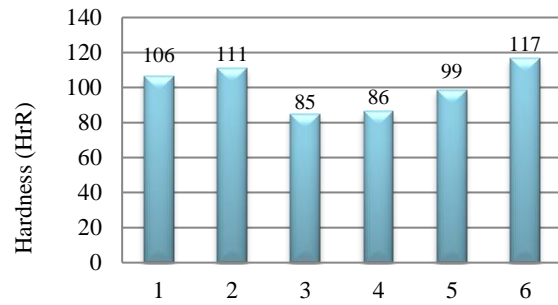


Figure 7. Hardness graph

The pressing pressure alone has not been associated with the hardness value. However, when the samples produced at the same pressing pressure are compared, the hardness of samples with a higher JDNP ratio is lower, while the hardness of samples with a lower JDNP ratio is higher.

As the pressing pressure increases, it is generally seen that the friction coefficient decreases. Figure 8 shows the average cold friction coefficient [26] values of the samples during the wear test.

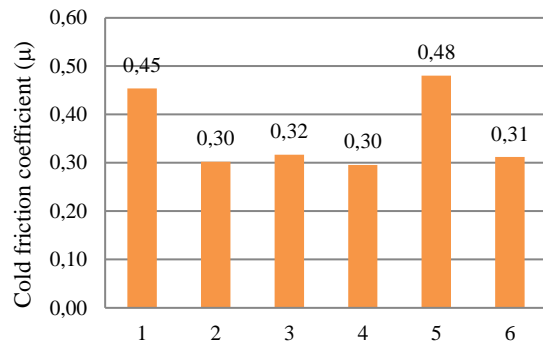


Figure 8. Average cold friction coefficient graph

3. Conclusions

The wear rate values change between $0.093 \cdot 10^{-7}$ - $4.235 \cdot 10^{-7} \text{cm}^3 \cdot \text{N}^{-1} \cdot \text{m}^{-1}$. These values are lower than the minimum wear rate specified in TS 555.

The friction coefficient ranges from 0.30 to 0.48. When compared with TS555 values, these values were found to be the E class of 4 samples, the G class friction coefficient of 2 samples, and all the samples were found to conform to the standard [27].

The density changes between 1.82 - 2.17g/cm^3 . The direct effect of pressure to density couldn't be noticed. Density and JDNP rate have reverse effect.

Hardness values range from 85-117 according to the Rockwell R scale.

The hardness values of the samples (2 and 6) produced were higher than the results of the other samples while the pressing pressure was at the medium level (150 MPa). Also, when the pressing pressure is increased to the highest (200 MPa), the produced specimens (3 and 4) are found to fall to the lowest level.

The pressing pressure mostly effected the hardness and

friction coefficient. Generally, the excess of pressing force reduces the hardness and friction coefficient.

The wear rate of the samples with low pressing pressure is higher than the wear rate of other samples.

Acknowledgment

This work was supported by Selçuk University Scientific Research Projects Coordination Unit within the scope of PhD thesis Project 16201089.

We would like to thank Selçuk University Scientific Research Projects Coordination Unit for their support.

Nomenclature

| | |
|------------|---|
| Wa | : wear rate ($\text{mm}^3 \cdot \text{N}^{-1} \cdot \text{m}^{-1}$) |
| ΔG | : mass loss (mg) |
| S | : sliding distance (m) |
| M | : loading weight (N), |
| ρ | : sample density (g/cm^3) |
| h | : sample height (cm) |
| m | : sample mass (g) |
| D | : sample diameter (cm) |
| JDN | : juniperus drupacea nut |
| JDNP | : juniperus drupacea nut powder |

References

1. Ulkemiz.com [2018 October 21]; Available from <http://www.ulkemiz.com/tekerlegin-icadi-ve-tarihsel-gelisimi>
2. Ertan, R. *Fren Balata Malzemelerinin Optimizasyonu ve Üretim Parametrelerinin Analizi*, Uludağ Üniversitesi, Fen Bilimleri Enstitüsü, Doktora Tezi, Bursa, 2008.
3. Karaoğlu, Y., *Bir Aşınma Test Cihazının Tasarımı ve İmalatı*, Sakarya Üniversitesi, Fen Bilimleri Enstitüsü, Yüksek Lisans Tezi, Sakarya, 2006.
4. Sugözü, İ., *Bor Katkılı Asbestsiz Otomotiv Fren Balatası Üretimi ve Frenleme Karakteristiğinin İncelenmesi*, Fırat Üniversitesi, Fen Bilimleri Enstitüsü, Doktora Tezi, Elazığ, 2009.
5. Domaç, G.S., *Disk Frenlerin Tasarım ve Tribolojik Açidan İncelenmesi*, Yıldız Teknik Üniversitesi, Fen Bilimleri Enstitüsü, Doktora Tezi, İstanbul, 2006.
6. Kuş, H., *Bronz Esaslı Seramik Takviyeli Fren Balatalarının Performansının Geliştirilmesi*, Gazi Üniversitesi, Fen Bilimleri Enstitüsü, Doktora Tezi, Ankara, 2014.
7. Boz, M., *Seramik Takviyeli Bronz Esaslı Toz Metal Fren Balata Üretimi ve Sürtünme-Aşınma Özelliklerinin Araştırılması*, Gazi Üniversitesi, Fen Bilimleri Enstitüsü, Doktora Tezi, Ankara, 2003.
8. Üstün, N.S., *Otomotiv Endüstrisi İçin Bir Disk Fren Balatası Üretimi ve Performansının İncelenmesi*, Süleyman Demirel Üniversitesi, Fen Bilimleri Enstitüsü, Yüksek Lisans Tezi, Isparta, 2011.
9. Makinemuh.com [2018 July 18]; Available from: <http://mesnet.makinemuh.com/otomobillerde-mekanik-fren-sistemi-nasil-calisir>
10. Kumar, M., B.K. Satapathy, A. Patnaik, D.K. Kolluri and B.S. Tomar, *Hybrid composite friction materials reinforced with combination of potassium titanate whiskers and aramid fibre: Assessment of fade and recovery performance*, Tribology International, 2011, 44(4): p. 359–367.
11. Öztürk, B., F. Arslan and S. Öztürk, *Hot wear properties of ceramic and basalt fiber reinforced hybrid friction materials*, Tribology International, 2007, 40: p. 37 – 48.
12. Kumar, M., X. Boidin, Y. Desplanques and J. Bijwe, *Influence of various metallic fillers in friction materials on hot-spot appearance during stop braking*, Wear, 2011, 270(5-6), p. 371–381.
13. Satapathy, B.K. and J. Bijwe, *Performance of friction materials based on variation in nature of organic fibres Part I. Fade and recovery behaviour*, Wear, 2004, 257(5-6), p. 573–584.
14. Albayrak, B., *Bronz Balataların Üretimi ve Performans Testleri*, Sakarya Üniversitesi, Fen Bilimleri Enstitüsü, Yüksek Lisans Tezi, Sakarya, 2009.
15. Stadler, Z., K. Krnel and T. Kosmac, *Friction and wear of sintered metallic brake linings on a C/C-SiC composite brake disc*, Wear, 2008, 265(3-4), p. 278–285.
16. Dante, R.C., F. Vannucci, P. Durando, E. Galetto and C.K. Kajdas, *Relationship between wear of friction materials and dissipated power density*, Tribology International, 2009, 42(6), p. 958–963.
17. Akagündüz, E., *Kompozit sürtünmeli fren balatalarında yerli uçucu kül katkısının raylı taşıt balata özelliklerine etkisinin incelenmesi ve kullanılabilirliğinin saptanması*, Yıldız Teknik Üniversitesi, Fen Bilimleri Enstitüsü, Doktora Tezi, İstanbul, 2014.
18. Adıgüzel, A.A., *Katı Yağlayıcı ve Aşındırıcı Bileşenlerinin Fenolik Reçine Esaslı Fren Balatalarının Mekanik ve Tribolojik Özelliklerine Etkileri*, Karadeniz Teknik Üniversitesi, Fen Bilimleri Enstitüsü, Yüksek Lisans Tezi, Trabzon, 2015.
19. Sugözü, İ., İ. Yavuz and İ. Mutlu, *Polimerik Kompozit Sürtünme Malzemelerinde Üretim Basıncının Performansa Etkisinin Araştırılması*, in IATS'09, Karabük, p. 1140-1143.
20. Demirhan, Y. Z., *Yüksek Performanslı Para-Aramid Elyaf Takviyeli Fren Balatalarının Mekanik Özelliklerinin Araştırılması*, Selçuk Üniversitesi, Fen Bilimleri Enstitüsü, Yüksek Lisans Tezi, Konya, 2017.
21. Unaldi, M. and R. Kus, *Effect of Pressing Pressure on Density and Hardness of Powder Miscanthus Reinforced Brake Pads*, Applied Mechanics and Materials, 2014, 680, p. 237-240.
22. Baritmaden [2018 July 18]; Available from: <http://www.baritmaden.com/endustriyelmineraller/belgeler/TDS.11072017.pdf>
23. Sisecam [2018 July 18]; Available from: <http://www.sisecamkimyasallar.com/sites/catalogs/en/Documents/buss-seg/Cam-Elyaf/kiprma/sisecam-PH2.pdf>
24. Aras S. and N. Tarakçioğlu, *The Usage of Some Organic Materials in Brake Pad Composition and Researching the Results*, in ICNASE'16: Kilis. p.1099-1105
25. Unaldi M. and R. Kus, *The effect of the brake pad components to the some physical properties of the ecological brake pad samples*, IOP Conference Series: Materials Science and Engineering, 2017, 191(1), p. 012032
26. TS 9076, *Karayolu Taşıtları Fren Sistemleri Fren Balataları Malzeme Sürtünme Özelliklerinin Küçük Deney Parçaları İle Değerlendirilmesi*, Ankara, 1991.
27. TS 555, *Karayolu Taşıtları Fren Sistemleri Balatalar Sürtünmeli Frenler İçin*, Ankara, 1992.



Research Article

Performance analysis of SRF-PLL and DDSRF-PLL algorithms for grid interactive inverters

Fehmi Sevilmiş ^{a,*}  and Hulusi Karaca ^a 

^a Selçuk University, Faculty of Technology, Konya-42130, Turkey

ARTICLE INFO

Article history:

Received 03 April 2018

Revised 23 April 2019

Accepted 25 June 2019

Keywords:

Grid interactive inverter

Phase locked loop

PLL

Synchronization

ABSTRACT

In grid interactive power converter applications, phase locked loop (PLL) algorithms are very important to realize grid synchronization. The performance of PLL should not be affected by adverse conditions such as voltage unbalance, harmonics, frequency and phase changes. Otherwise, synchronization errors occur between the grid interactive inverter and the grid. In this paper, two different PLL algorithms are simulated by modeling under MATLAB/Simulink. The performances of the PLLs are comparatively presented under four different grid conditions such as balanced, unbalanced, harmonics and variable frequency. In this study, synchronous reference frame-PLL (SRF-PLL) and decoupled double synchronous reference frame-PLL (DDSRF-PLL) which are mostly used, state-of-arts and effective PLL algorithms are analyzed by modeling in grid synchronization applications. It has also been demonstrated the positive and negative aspects of the PLLs based on the obtained results.

© 2019, Advanced Researches and Engineering Journal (IAREJ) and the Author(s).

1. Introduction

Phase lock loop (PLL) algorithm was first proposed by Appleton in 1923 [1]. After Appleton, Bellescize used the PLL algorithm to synchronize radio signals in 1932 [2]. Until the 1970s, the PLL could not find a wide range of applications due to the difficulty of its implementation. The PLL has begun to be largely used in modern communication systems by means of the rapid development of integrated-circuit (IC) technology in the 1970s. Later, it was used in different industrial fields such as speed control of electric motors and static power converters [3].

Nowadays, the PLL algorithm is also used as a new area to ensure synchronization in grid interactive inverters. In recent years, there has been an increase in use of the PLL in this field. The PLL must provide fast and precise synchronization between the inverter and the grid. Furthermore, it must have a good response to harmonics, imbalances, phase jump, frequency changes, and various disturbing effects in grid voltages. Therefore, PLL algorithm plays a major role for grid interactive inverters [3].

In Figure 1, block structure of the PLL is shown. This

structure automatically synchronizes the phase of the output signal to the phase of the input signal as it is a feedback system [4]. The PLL structure consists of the phase detection (PD), the loop filter (LF) and the voltage controlled oscillator (VCO) blocks. The PD block determines the phase difference between input signal (V_i) and output signal. In addition, it produces a proper error signal [5], [6]. This error signal is transferred to the LF block. The LF demonstrates the low-pass-filter (LPF) characteristic to provide stability of the system. Moreover, it typically comprises of the first-order LPF or a proportional and integral (PI) controller. In other words, the LF block specifies the dynamics of the system [7], [8]. The signal at the output of the LF block generates the output signal in the same phase as the input signal by driving the VCO. Thereby, the output signal follows the input signal [9], [10].

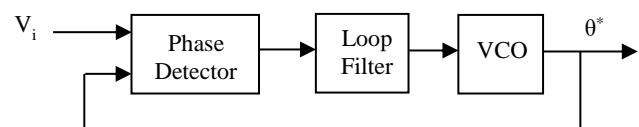


Figure 1. Block structure of the PLL

* Corresponding author. Tel.: +90-332-223-4396; Fax: +90-332-241-2179.
E-mail addresses: fehmi.sevilmis@selcuk.edu.tr (F. Sevilmiş), hkaraca@selcuk.edu.tr (H. Karaca)
ORCID: 0000-0002-6059-9583 (F. Sevilmiş), 0000-0002-5561-489X (H. Karaca)
DOI: 10.35860/iarej.412250

The aim of this paper is to compare the performances of two of the most preferred, state-of-arts and the most effective PLL algorithms under four different grid conditions such as balanced, unbalanced, harmonics and variable frequency. In this study, SRF-PLL and DDSRF-PLL algorithms have been modeled. The performances of the PLL methods have been compared based on the obtained results. The results have been presented in a comparative table and the advantages and disadvantages of these PLL algorithms have been pointed out. In this respect, according to the grid disturbances, PLL algorithm which should be preferred has been put forward.

This article is organized as follows: in the first section, the PLL algorithm is introduced and the purpose of the study is explained. In the second section, two different PLL algorithms and the block structures of each PLL algorithm are mentioned. In the third section, the PLLs with block structures are simulated in MATLAB/Simulink under different grid conditions such as balanced, unbalanced, harmonics and variable frequency, and their performances are compared. In the last section, the advantages and drawbacks of the PLLs are emphasized.

2. Phase Locked Loop Algorithms

2.1 Synchronous Reference Frame-PLL

The synchronous reference frame-phase locked loop (SRF-PLL) algorithm is used extensively in three-phase systems. In Figure 2, the block structure of SRF-PLL is shown.

The SRF-PLL operates as a feedback servo system to instantaneously detect the phase angle (θ) of the grid voltage. In this system, the three-phase grid voltages are firstly measured. Then, the measured three-phase grid voltages are transformed to the stationary frame variables (V_α, V_β) by Clarke rotation matrix given in Equation (1). After, the V_α and V_β voltages are converted to the rotating (synchronous) frame variables (V_d, V_q) by Park rotation matrix in Equation (2). The estimated phase angle (θ^*) of the grid voltage is fed back to operate the abc to dq block so that the Park rotation can be performed. That block also works like the PD block [11]-[13].

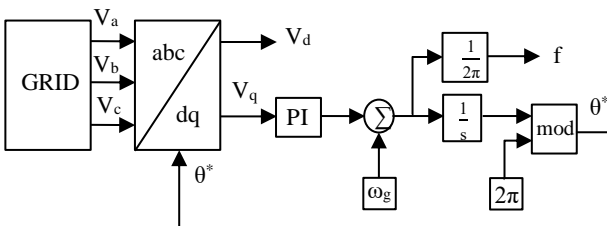


Figure 2. Block structure of the SRF-PLL

$$\begin{bmatrix} V_\alpha \\ V_\beta \end{bmatrix} = \frac{2}{3} \begin{bmatrix} 1 & -\frac{1}{2} & -\frac{1}{2} \\ 0 & \frac{\sqrt{3}}{2} & -\frac{\sqrt{3}}{2} \end{bmatrix} \begin{bmatrix} V_a \\ V_b \\ V_c \end{bmatrix} \quad (1)$$

$$\begin{bmatrix} V_d \\ V_q \end{bmatrix} = \begin{bmatrix} \cos(\theta^*) & \sin(\theta^*) \\ -\sin(\theta^*) & \cos(\theta^*) \end{bmatrix} \begin{bmatrix} V_\alpha \\ V_\beta \end{bmatrix} \quad (2)$$

In the SRF-PLL method, V_d and V_q voltages appear as DC components. In ideal grid conditions where the grid voltages are balanced and there are no harmonics or distortions, the estimated phase angle (θ^*) equals to the phase angle (θ) of the grid voltage. The estimated phase angle is the same as the phase angle of the voltage V_a of the grid. As can be seen from Equation (3) and Equation (4), V_q equals zero while V_d equals the peak value of the grid voltage. As can be understood from the equations, V_q contains information about the phase angle error of the grid. On the other hand, V_d gives the amplitude information of the grid voltage in steady-state. Besides, the SRF-PLL offers the estimated frequency (f) information [13]-[16].

$$V_q = V_m \sin(\theta - \theta^*) \quad (3)$$

$$V_d = V_m \cos(\theta - \theta^*) \quad (4)$$

In the loop filter design of the SRF-PLL, it is very important for the dynamic performance of the system that the estimated phase angle is fast locked to the phase of the grid and shows good filtering characteristics. However, in the SRF-PLL, these two conditions cannot be met at the same time. In ideal grid conditions, the high bandwidth of the filter ensures that the grid voltage and phase angle can be determined quickly and accurately [9]. If the grid voltage is disturbed by high-order harmonics, the band-width is reduced to ensure stable operation of the SRF-PLL, but in this case, synchronization time is increased. Moreover, V_d voltage cannot exactly determine. When imbalances in the grid voltage occur, reducing the band-width cannot stabilize the system. This problem can be solved by adding a simple low pass filter to the system. While the addition of low pass filter improves the stability of the system, it greatly reduces the dynamic response of the system [9], [17]-[18].

PI controller is usually used in the control algorithm of the SRF-PLL. The PI controller also works as a loop filter in the system, which controls V_q and detects the dynamics of the system. In order to determine the phase angle of the grid voltage fast and precisely, the PI parameters must be adjusted appropriately. In variable grid conditions, if the PI parameters are not adjusted properly, errors occur at the determined phase angle and the system works unstably [3], [15], [19].

While the SRF-PLL has a good response under ideal grid

conditions and variable frequency grid condition, it causes errors in determining the phase angle of the grid voltage under non-ideal grid conditions such as distorted and/or unbalanced [16], [19]. In non-ideal conditions, different filtering methods should be used [3], [4].

2.2 Decoupled Double Synchronous Reference PLL

Under unbalanced grid condition, positive sequence and negative sequence components of grid voltage occur. Since these components cannot be controlled independently in the SRF-PLL method, errors occur in synchronization between the inverter and the grid. The basis of the DDSRF-PLL algorithm is based on the conversion and independent control of the positive sequence and negative sequence components of the grid voltage. This algorithm highly removes the errors in determining the phase angle of the grid in the conventional SRF-PLL [20]. Furthermore, the DDSRF-PLL can be used in wind energy systems due to its very good response to grid frequency changes [21].

The DDSRF-PLL consists of the dq^{+1} frame rotating in positive direction (with angle θ) and the dq^{-1} frame rotating in negative direction (with angle $-\theta$). The components of the dq^{+1} and dq^{-1} frame are given by Equation (5) and Equation (6), respectively [9], [20].

$$\begin{bmatrix} V_{d^{+1}} \\ V_{q^{+1}} \end{bmatrix} = \begin{bmatrix} V_{d^{+1}}^* \\ V_{q^{+1}}^* \end{bmatrix} + \begin{bmatrix} \cos(2\theta^*) & \sin(2\theta^*) \\ -\sin(2\theta^*) & \cos(2\theta^*) \end{bmatrix} \begin{bmatrix} \overline{V_{d^{+1}}} \\ \overline{V_{q^{+1}}} \end{bmatrix} \quad (5)$$

$$\begin{bmatrix} V_{d^{-1}} \\ V_{q^{-1}} \end{bmatrix} = \begin{bmatrix} V_{d^{-1}}^* \\ V_{q^{-1}}^* \end{bmatrix} + \begin{bmatrix} \cos(-2\theta^*) & \sin(-2\theta^*) \\ -\sin(-2\theta^*) & \cos(-2\theta^*) \end{bmatrix} \begin{bmatrix} \overline{V_{d^{-1}}} \\ \overline{V_{q^{-1}}} \end{bmatrix} \quad (6)$$

As seen from the equations, coupled 2nd harmonic components (2ω) are added to positive and negative sequence components of V_d and V_q voltages. The positive and negative sequence components of the grid voltage are obtained in a decoupled manner by eliminating these coupled components.

Equation (5) and Equation (6) are rearranged to determine the decoupled components as in Equation (7) and Equation (8). In Figure 3 and Figure 4, block diagrams of these decoupled components are given.

$$\begin{bmatrix} V_{d^{+1}}^* \\ V_{q^{+1}}^* \end{bmatrix} = \begin{bmatrix} V_{d^{+1}} \\ V_{q^{+1}} \end{bmatrix} - \begin{bmatrix} \cos(2\theta^*) & \sin(2\theta^*) \\ -\sin(2\theta^*) & \cos(2\theta^*) \end{bmatrix} \begin{bmatrix} \overline{V_{d^{+1}}} \\ \overline{V_{q^{+1}}} \end{bmatrix} \quad (7)$$

$$\begin{bmatrix} V_{d^{-1}}^* \\ V_{q^{-1}}^* \end{bmatrix} = \begin{bmatrix} V_{d^{-1}} \\ V_{q^{-1}} \end{bmatrix} - \begin{bmatrix} \cos(-2\theta^*) & \sin(-2\theta^*) \\ -\sin(-2\theta^*) & \cos(-2\theta^*) \end{bmatrix} \begin{bmatrix} \overline{V_{d^{-1}}} \\ \overline{V_{q^{-1}}} \end{bmatrix} \quad (8)$$

In Figure 5, the block structure of DDSRF-PLL is given. This block structure is the extended form of the classical SRF-PLL block structure.

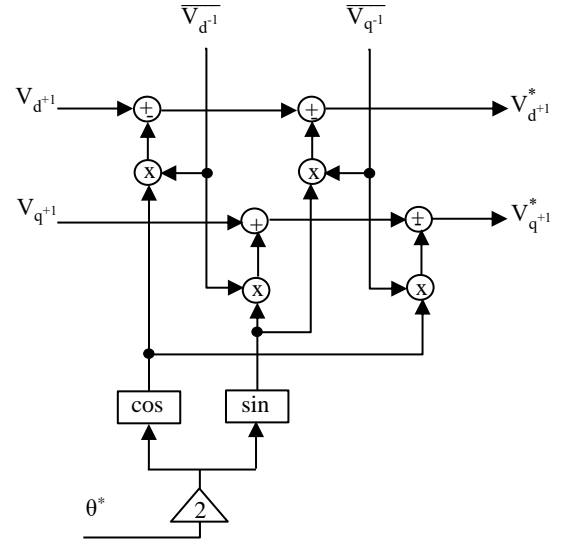


Figure 3. Block diagram of dq^{+1} decoupled components

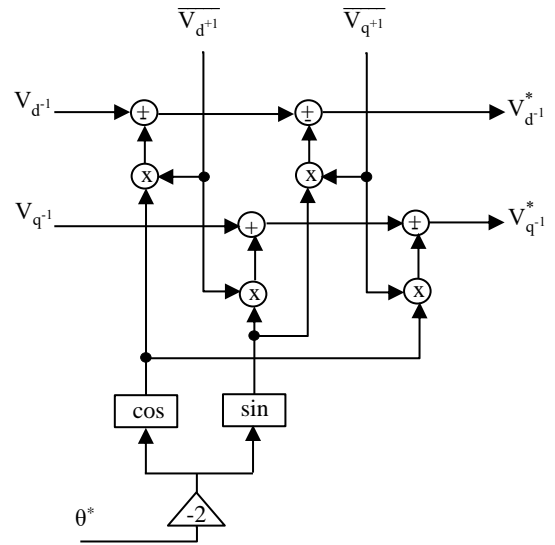


Figure 4. Block diagram of dq^{-1} decoupled components

With the DSRF-PLL algorithm, the actual amplitude value of the positive sequence voltage component is obtained exactly. The expression of the first order low-pass filter (LPF) shown in Figure 5 is given by Equation (9).

$$LPF(s) = \frac{\omega_f}{s + \omega_f} \quad (9)$$

The mathematical expression of the Park transform used for the positive sequence components ($\alpha\beta/dq^{+1}$) in Figure 5 is as in Equation (2). The mathematical expression of the Park transformation block used for the negative sequence components ($\alpha\beta/dq^{-1}$) is given by Equation (10).

$$\begin{bmatrix} V_{d^{-1}} \\ V_{q^{-1}} \end{bmatrix} = \begin{bmatrix} \cos(\theta^*) & -\sin(\theta^*) \\ \sin(\theta^*) & \cos(\theta^*) \end{bmatrix} \begin{bmatrix} V_\alpha \\ V_\beta \end{bmatrix} \quad (10)$$

Since the DDSRF-PLL is one of the state-of-the-art PLL methods, many studies have been done to enhance the DDSRF-PLL [22]-[25].

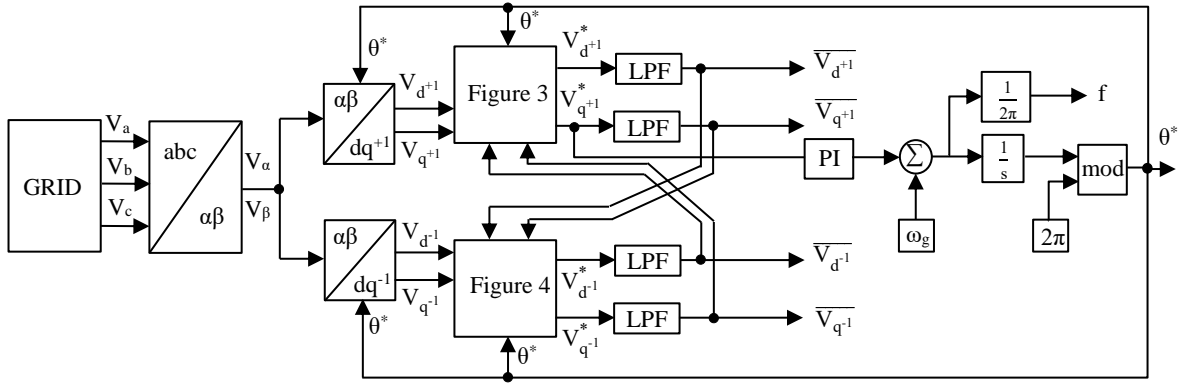


Figure 5. Block structure of the DDSRF-PLL

3. Simulation Results

In this section, the performances of phase locked loop algorithms are tested under different grid conditions. These are balanced, unbalanced, harmonics and variable frequency grid conditions. Simulations of PLL algorithms were performed in the MATLAB/Simulink environment. In the simulated PLL algorithms, the settling time was selected as 40 ms. In each PLL algorithm, PI coefficients were calculated by taking the damping ratio of the PLL loop filter as $\xi = 0.707$ and natural frequency $\omega_n = 162.63 \text{ rad/s}$. Taking these parameters into consideration, $K_p = 0.74$ and $K_i = 85.05$ were obtained.

3.1 Unbalanced Grid Condition

In the first test, the PLL algorithms have been tested under unbalanced grid condition. As shown in Figure 6, the three-phase grid voltages are set to 311 V peak value and 50 Hz grid frequency under balanced grid condition until 0.1 s. Without frequency changes, harmonics and other disturbing effects are ignored. In simulation, the unbalanced grid phase voltages were injected to the system after 0.1 s. 373 V peak value for A-phase and 285 V peak value for B-phase and C-phase are used as unbalanced grid voltages.

Figure 7 and Figure 8 show the response of the SRF-PLL and DDSRF-PLL at unbalanced phase voltages, respectively. As seen in the figures, the SRF-PLL responds faster than the DDSRF-PLL under balanced grid condition (up to 0.1 s) due to its simple construction and low process requirements. However, the SRF-PLL causes a fault in determining the grid phase angle under unbalanced grid phase voltages. In this case, maximum phase error of SRF-PLL is 0.081 rad.

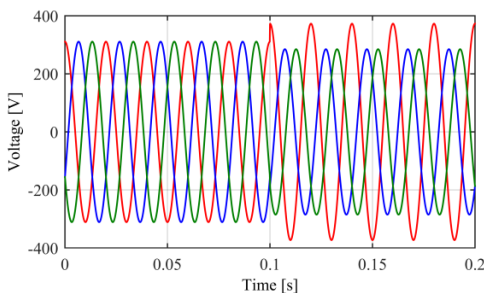


Figure 6. Three-phase unbalanced grid voltages

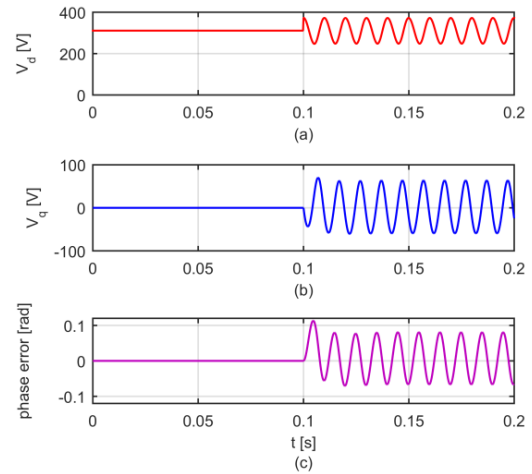


Figure 7. Response of the SRF-PLL under unbalanced grid condition (a) Change of V_d (b) Change of V_q (c) Phase error

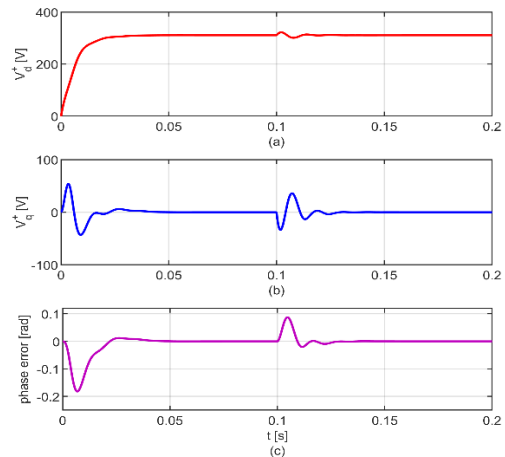


Figure 8. Response of the DDSRF-PLL under unbalanced grid condition (a) Change of V_d (b) Change of V_q (c) Phase error

In addition, since the positive sequence and negative sequence components of the grid phase voltage cannot be obtained independently, the effect of the second order harmonic component in the V_d and V_q voltages is clearly visible. In the DDSRF-PLL, as the positive sequence and negative sequence components of the grid phase voltage are obtained independently, the effects of the second order harmonic component in the V_d and V_q voltages disappear. Moreover, there is no phase error in steady state under unbalanced grid condition.

3.2 Grid Condition with Harmonics

In the second test, the responses of the PLL algorithms have been investigated by adding the fifth and seventh harmonic components to the grid voltages. The amplitudes of the added 5th and 7th harmonic components correspond to 10% (31 V) and 5% (15.5 V) of the grid voltage, respectively. The grid voltages are balanced and there is no change in the grid frequency. As shown in Figure 9, harmonics are added to the grid voltages after 0.1 s. Figure 10 and Figure 11 compare the performances of SRF-PLL and DDSRF-PLL algorithms, respectively.

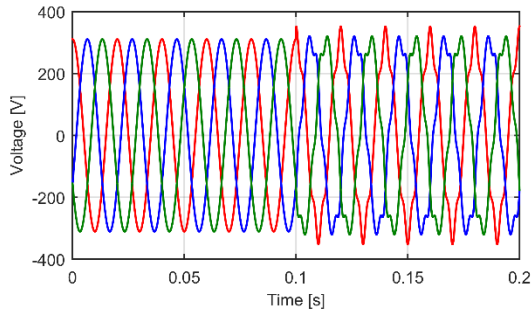


Figure 9. Three-phase harmonics grid voltages

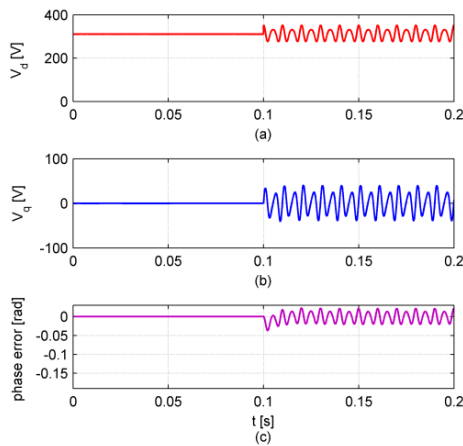


Figure 10. Response of SRF-PLL under grid condition with harmonics (a) Change of V_d (b) Change of V_q (c) Phase error

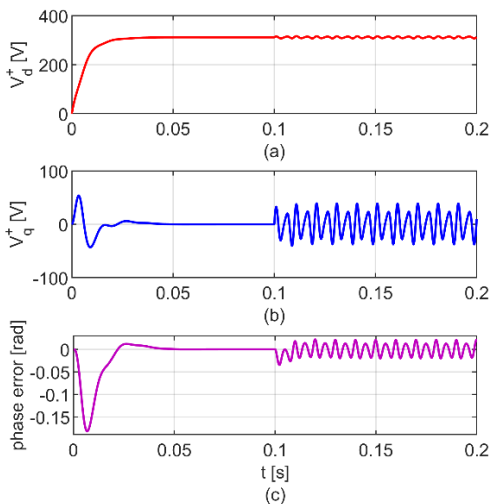


Figure 11. Response of DDSRF-PLL under grid condition with harmonics (a) Change of V_d (b) Change of V_q (c) Phase error

As can be seen from the figures, the response of the SRF-PLL and DDSRF-PLL to the harmonics is not good and causes a fault in determining the phase angle (maximum phase error = 0.021 rad). In both PLLs, when the bandwidth of the filter is reduced, their performances improve; however, the synchronization times are longer. While the estimated V_d voltage in SRF-PLL fluctuates between 273 V and 357 V, it fluctuates between 306 V and 316 V in DDSRF-PLL. Although the phase errors are the same, DDSRF-PLL estimates the V_d voltage more accurately than the SRF-PLL.

3.2 Variable Frequency Grid Condition

In the last test, the responses of the PLL algorithms have been tested under variable frequency grid condition. As can be seen in Figure 12, the frequency of the grid voltages has been increased from 50 Hz to 55 Hz at the time of 0.1 s, the grid frequency has been decreased from 55 Hz to 45 Hz at the time of 0.2 s and the grid frequency has been increased from 45 Hz to 50 Hz at the time of 0.3 s. It is assumed that the grid voltages are balanced and there are no harmonics or other disturbing effects. Figure 13 and Figure 14 show the responses of the SRF-PLL and DDSRF-PLL algorithms, respectively.

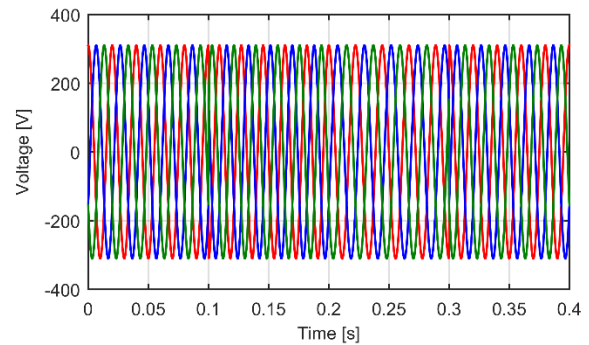


Figure 12. Three-phase variable frequency grid voltages

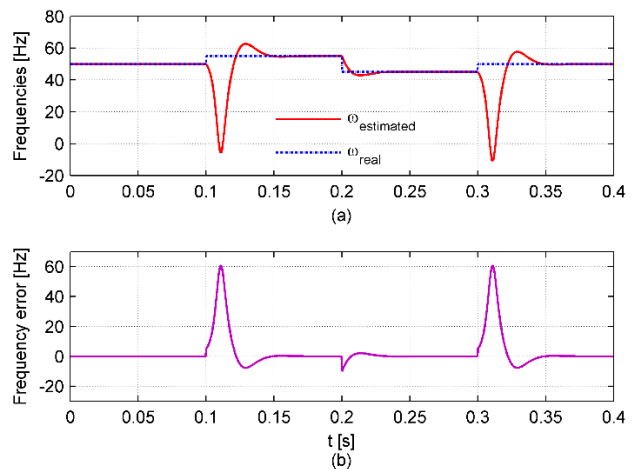


Figure 13. Response of the SRF-PLL under variable frequency grid condition (a) Real and estimated grid frequency (b) Frequency error

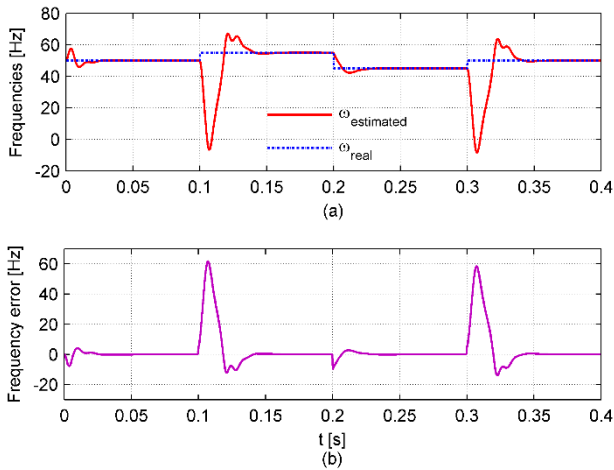


Figure 14. Response of the DDSRF-PLL under variable frequency grid condition (a) Real and estimated grid frequency (b) Frequency error

As can be understood from the figures, the performances of SRF-PLL and DDSRF-PLL against frequency changes are almost the same. In the case of the variable frequency grid, the maximum overshoot value of the SRF-PLL is 8 Hz while it is 13 Hz in the DDSRF-PLL. On the other hand, the SRF-PLL and DDSRF-PLL algorithms have an average settling time of 65 ms. There is no steady-state error in each PLL algorithms. Thus, the phase angle of the grid is determined without error in both PLL algorithms.

Finally, the PLL algorithm which should be preferred according to different grid conditions is presented in Table 1. If the grid interactive inverter is used only for a balanced and/or variable frequency grid condition, the SRF-PLL is more suitable to prefer. If the grid interactive inverter is used only for an unbalanced and/or harmonics grid condition, the DDSRF-PLL is more suitable.

Table 1. PLL preference for different grid conditions

| Grid condition | PLL preference |
|---|----------------|
| Balanced | SRF |
| Unbalanced | DDSRF |
| Harmonics | DDSRF |
| Variable frequency | SRF |
| Unbalanced + Harmonics | DDSRF |
| Unbalanced + Variable frequency | DDSRF |
| Harmonics + Variable frequency | DDSRF |
| Unbalanced + Harmonics + Variable frequency | DDSRF |

4. Conclusions

In this study, two different phase locked loop algorithms for grid synchronization are presented comparatively. The SRF-PLL and DDSRF-PLL algorithms are simulated in MATLAB/Simulink software. Based on the results obtained from these simulations, the performances of PLLs are compared under different conditions.

As a result of the findings, the SRF-PLL stands out with its simplicity, easy applicability and frequency response. However, under non-ideal grid conditions such as

unbalanced and/or harmonic grid, the stability of the system becomes worse. On the other hand, since the DDSRF-PLL algorithm can accurately obtain positive and negative sequence components and the filtering capacity is high, the response and accuracy in such adverse conditions are at a desired level. The results of comparative simulations clearly demonstrate the importance of the PLL algorithm which should be preferred according to the grid distortions.

Nomenclature

- LPF* : Low-pass filter
PI : Proportional + Integral
 V_a : A-phase voltage of grid
 V_b : B-phase voltage of grid
 V_c : C-phase voltage of grid
 V_α : Stationary frame variable
 V_β : Stationary frame variable
 V_d : Synchronous frame variable
 V_i : Voltage of input signal
 V_q : Synchronous frame variable
 θ : Phase angle of grid voltage
 θ^* : Obtained phase angle
 ω_g : Angular frequency of grid voltage

References

- Appleton, E. V., *Automatic synchronization of triode oscillators*. Proc. Cambridge Phil. Soc., 1923. **21**(3): p. 231.
- Bellesize, H. de, *La reception synchrone*. Onde Electr., 1932. **11**: p. 230-240.
- Blaabjerg, F., Teodorescu, R., Liserre, M., and Timbus, A., *Overview of control and grid synchronization for distributed power generation systems*. IEEE Transactions on Industrial Electronics, 2006. **53**(5): p. 1398-1409.
- Nicastrì, A., and Nagliero, A., *Comparison and Evaluation of the PLL Techniques for the Design of the Grid-connected Inverter Systems*, in IEEE International Symposium on Industrial Electronics (ISIE)2010: Italy. p. 3865-3870.
- Karimi-Ghartemani, M., and Irvani, M. R., *A method for synchronization of power electronic converters in polluted and variable-frequency environments*. IEEE Transactions on Power Systems, 2004. **19**(3): p. 1263-1270.
- Devi, R. J., and Kadam, S. S., *Phase locked loop for synchronization of inverter with electrical grid: a survey*. International Journal of Engineering Research & Technology (IJERT), 2015. **4**(2): p. 352-358.
- Freijedo, F. D., Doval-Gandoy, J., Lopez, O., Martinez-Penalver, C., Yepes, A. G., Fernandez-Comesana, P., Malvar, J., Nogueiras, A., Marcos, J., and Lago, A., *Grid-synchronization methods for power converters*. in 35th Annual Conference of IEEE Industrial Electronics (IECON)2009: Spain. p. 522-529.
- Amin, M. M., and Mohammed O. A., *Software phase locked loop technique for grid-connected wind energy conversion systems*. in IEEE 12th Workshop on Control and Modeling for Power Electronics (COMPEL)2010: USA. p. 1-8.
- Teodorescu, R., Liserre, M., and Rodriguez, P., *Grid converters for photovoltaic and wind power systems*. 2011, USA: John Wiley & Sons, Inc.

10. Aydemir, M., *Modelling and analysing DC/AC inverters for wind turbines*. Ms. Thesis, 2014: Turkey.
11. Timbus, A., Teodorescu, R., Blaabjerg, F., and Liserre, M., *Synchronization methods for three phase distributed power generation systems. an overview and evaluation*. in IEEE 36th Power Electronics Specialists Conference (PESC)2005: Brazil. p. 2474-2481.
12. Iov, F., and Blaabjerg, F., *Power electronics control of wind energy in distributed power systems*. in 11th International Conference on Optimization of Electrical and Electronics Equipment (OPTIM)2008: Romania. p. 29-44.
13. Sevilmiş, F., and Karaca, H., *Simulation of three-phase grid interactive inverter for wind energy systems*. in IEEE 15th International Conference on Environment and Electrical Engineering Conference Proceedings2015: Italy. p. 169-1174.
14. Xiong, F., Yue, W., Ming, L., Ke, W., and Wanjun, L., *A novel PLL for grid synchronization of power electronics converters in unbalanced and variable-frequency environment*. in 2nd IEEE International Symposium on Power Electronics for Distributed Generation Systems2010: China. p. 466-471.
15. Adzic, E., Porobic, V., Dumnic, B., Celanovic, N., and Katic, V., *PLL synchronization in grid-connected converters*. in The 6th PSU-UNS International Conference on Engineering and Technology (ICET-2013): Serbia. p. 1-5.
16. Nagliero, A., Mastromauro, R. A., Liserre, N., and Dell'Aquila, A., *Synchronization techniques for grid connected wind turbines*. in IEEE 35th Annual Conference of Industrial Electronics (IECON)2009: Portugal. p. 4606-4613.
17. Meersman, B., De Kooning, J., Vandoorn, T., Degroote, L., Renders, B., and Vandeveld, L., *Overview of PLL methods for distributed generation units*. in 45th International Universities Power Engineering Conference (UPEC)2010: Wales. p. 1-6.
18. Guerrero-Rodriguez, N. F., Rey-Boue, A. B., Rigas, A., and Kleftakis, V., *Review of synchronization algorithms used in grid-connected renewable agents*. in International Conference on Renewable Energies and Power Quality (ICREPQ)2014: Spain. p. 1-6.
19. Sevilmiş, F., *Grid synchronization of wind energy systems*. Ms. Thesis, 2016: Turkey.
20. Rodriguez, P., Pou, J., Bergas, J., Candela, J. I., Burgos, R. P., and Boroyevich, D., *Decoupled Double Synchronous Reference Frame PLL for Power Converters Control*, IEEE Transactions on Power Electronics, 2007, **22**(2): p. 584-592.
21. Rodriguez, P., Pou, J., Bergas, J., Candela, J. I., Burgos, R., and Boroyevich, D., *Double Synchronous Reference Frame PLL for Power Converters Control*, in IEEE 36th Power Electronics Specialists Conference (PESC)2005: Brazil. p. 1415-1421.
22. Nouralinejad, A., Bagheri, A., Mardaneh, M., and Malekpur M., *Improving the Decoupled Double SRF PLL for Grid Connected Power Converters*, in the 5th Power Electronics, Drive Systems and Technologies Conference (PEDSTC)2014: Iran. p. 347-352.
23. Ali, Z., Christofides, N., Hadjidemetriou, L., and Kyriakides, E., *Design of an Advanced PLL for Accurate Phase Angle Extraction under Grid Voltage HIFs and DC Offset*, IET Power Electronics, 2018, **11**(6): p. 995-1008.
24. Ali, Z., Christofides, N., Hadjidemetriou, L., Kyriakides, E., Yang, Y., and Blaabjerg, F., *Three-phase Phase-locked Loop Synchronization Algorithms for Grid-connected Renewable Energy Systems: A Review*, Renewable and Sustainable Energy Reviews, 2018, **90**: p. 434-452.
25. Vadlamudi, S. D. V. R., Jiani, D., Acosta, M. A. C., Shuyu, C., Sriram, V. B., and Tripathi, A., *Decoupled DQ-PLL with Positive Sequence Voltage Normalization for Wind Turbine LVRT Control*, in Asian Conference on Energy, Power and Transportation Electrification (ACEPT)2016: Singapore. p. 1-6.



Research Article

Optimization of assignment problems in production lines with different skilled labor levels

Hazel Durmaz ^{a,*}  and Melik Koyuncu ^b 

^a Industrial Engineering of Çukurova University, Adana, Turkey

ARTICLE INFO

Article history:

Received 24 December 2018

Revised 28 April 2019

Accepted 25 June 2019

Keywords:

Mathematical modelling

Assignment problems

Time study

ABSTRACT

In order to serve the purpose of the study, two different mathematical models which belong to production line to were developed to assign workforces to the jobs who have different skills. The assignment model had been examined on a product that produced in a specified welding line in the automotive industry. All labor levels related to the product were analyzed by time study firstly and then the collected data were analyzed. New skill levels of workers, skill matrix were determined according to skill requirements (min. and max.) of the jobs. All collected data which come from time studies and skill matrix were used as an input parameter in the mathematical model that aim to minimize the unit production cost. Reports of mathematical models showed that it is necessary to assign right skilled worker to the job to minimize the production cost and increase the efficiency online. In this case the implementation was made by selecting a product in the welding manufacturing line. In the line, there are 5 stations that have 14 jobs and 27 operators. A modeling has been carried out in which the operators can be assigned to jobs under optimum conditions, based on assignment criterias. Models of sensitivity analyzes and statistic report results obtained the importance of the differences in the level of competence and the effect on the duration of the job as well as the decrease in the labor costs by assigning the correct workforce to the right job and by assigning right conditions to the model.

© 2019, Advanced Researches and Engineering Journal (IAREJ) and the Author(s).

1. Introduction

The first developments in Operations Research emerged during World War II regarding the need for defense. The studies that started in those years with the aim of optimization have progressed to the present day. In 1947, the Simplex Optimization method was found by George Dantzig and the simplex algorithm led to improvements in linear programming [1, 2]. Although assignment problems are seen as a special type of transportation problems, they are also encountered as the most common type in linear programming models in operations research. The assignment problem, which is the common type of transportation problems, was first brought forward by Frank L Hitchcock in 1941 [3]. As a result of finding of the Simplex algorithm by Dantzing, modeling of transportation and assignment problems by linear programming and solving them by simplex algorithm have been also realized [2]. In the assignment

problems, there are (a-amount of) tasks and (b-amount of) resources; the assignment is made to the tasks (a) that will be realized by available resources (b) and a cost emerges during this assignment. It is aimed here to use each resource in a task, and to achieve a solution method including an algorithm that will ensure that the cost is minimized in a controlled manner while performing this. Alternative solution methods have been reached by developing the simplex algorithm logic and these approaches have been used in solving problems in many different areas. It has been seen that in some of these alternative methods, the duration of the operation is shortened and in also some of them, more advanced problems are dealt with. The fact that Tjalling C. Koopmans and Martin Beckmann used linear programming models to explain the role and importance of assignment problems in economic activities can be given as an example for using simplex algorithm logic in different areas and achieving alternative solutions. In this

* Corresponding author. Tel.: +90-505-664-9696.

E-mail addresses: hazeel.durmaz@gmail.com (H.Durmaz), mkoynucu@cu.edu.tr (M. Koyuncu)

ORCID: 0000-0002-8860-9835 (H.Durmaz), 0000-0003-0513-6276 (M. Koyuncu)

DOI: 10.35860/iarej.501847

study, two problems involving economic activities were discussed, and it was observed that economic results could be obtained by assigning not only divisible resources but also non-divisible resources [5].

The most commonly used solution method for assignment problems is the Hungarian Method which tries to reach the solution with the method of obtaining reduced matrices at each step by transforming the problem information into 0-1 matrix. The Hungarian Method was introduced by Khun in 1955. In the light of the knowledge he obtained while reading Konig's book on the theory of graphics and after his research on the subject, Khun found the Hungarian Solution Method [4]. Although the assignment problems are a type of transportation problems, it is encountered as a method that is widely used in the field of production and that is especially used frequently in operator and machine assignments. In 2017, Aicha Ferjani and her colleagues studied on an assignment problem in which many changes in the production sector, particularly changes in customer demands, were made to keep the system dynamic. With systems sensitive to changes, operators and machine assignments should be performable. Changes that occur affect the time of the mainstream while the assignment is made; one of these changes that affect the time of the mainstream is also the fatigue that occurs in the operators. Operators can spend more time than expected in their assigned tasks due to fatigue. In the study, in which the effect of the fatigue on the task duration was investigated, an intuitive analysis method with multiple criteria was used and a more dynamic machine operator assignment was attempted to perform. The results of Ferjani et al. showed that fatigue had an effect on the mainstream time and that the intuitive approach gave better results [6]. In the study which was carried out by Stefanie Brilon in 2010 and which was about assigning of the tasks requiring different skills to the operators whose skill levels were unknown, it was focused primarily on the performance of the operators for the task assignments to be done. The mathematical model for assigned workers was established. In the first case, the employer may assign any worker to any task that he deems appropriate. In the second case, there are workers coming from outside to the company. According to the workers coming from outside and considering the performances of the existing workers, the assignment was made by the employer. Based on Peter's principle and taking into account the characteristics of the task, the model was created by assigning the certain workers to certain tasks [7]. In the study of Moreira and Costa conducted in 2009, it was observed that the assignment problem is an area in which meta-heuristic algorithms were developed based on linear programming and better solutions could be reached [8]. By using the tabu

algorithm, which was developed using meta-heuristic algorithm, an assembly line balancing study was performed in the assignment problem. In the addressed problem, operators with disabilities were used due to the fact that social awareness of the welfare of people with disabilities was also effective, and the solution of the problem of the completion of the task at different times due to the operators assigned to the task was discussed. In the design of tabu search algorithm developed to solve these problems, it was aimed to develop an algorithm that would make assignments as simple, flexible, accurate and fast as possible. In the established mathematical model, assignments were made taking into account task priority order and takt times in business centers (aiming to minimize). It is argued that in the tabu algorithm, an established mathematical model should be simple and flexible as well as fast and providing the correct solution. The tabu algorithm was run on the problem a large number of times and it was observed that better results were obtained [8]. In their study, in a firm making cellular production, Li and colleagues [9] developed a mathematical model that took into account the variable and fixed labor cost and assigned the operators to cells by minimizing the total cost. They calculated the total production costs based on costs varying depending on different capabilities. The competencies of the operators were determined according to the 3-sigma rule by using Gaussian distribution method and by taking into account the production efficiency that the operators obtained during the time they used the machines that they could use. Then, a technical value of the competence of each operator was created according to this method. When the results were interpreted in terms of variable and fixed labor costs, it was observed that the total cost decreased as the competencies of the staff and the number of working staff with high competency increased [9]. There are many criteria for assignment problems in production systems. In the study conducted by Achraf Ammar and his colleagues in 2013 [10], first, important features of Assignment Problems in production systems were discussed. Then, analysis was carried out by taking into consideration the other characteristics which could be evaluated as criteria and which revealed the type of problem. These characteristics were flexibility of employees, number of station, movement of labor, nature of the problem (static or dynamic assignment), human thinking (e.g., learning and forgetting effects), system type (e.g., U-shaped systems and cellular organizations), and different methods used to solve the problems (e.g., mathematical approaches, simulation, multi-criteria decision making, fuzzy logic, and methods containing a combination of these approaches). There were significant findings in the analysis results. In relation to the approaches used for dynamic operator assignments, it

was remarked that although neural network simulation metamodels had been widely used in some approaches such as multiple approaches and learning methods, studies had not yet become prevalent as widely as desired, but they had an important potential [10]. Another method that has recently started to be used in assignment problems is artificial-intelligence genetic-algorithm, which is well-known and become widespread today. The study of Shaikh Nizami et al. [11] can be shown as an example for this. In this study, it is generally mentioned that the assignment problems solved by Hungarian Method can be solved by the genetic algorithm and this method is a faster and more effective tool. While using the method, the algorithm/matrix is created by using some genetic terms (e.g., genotype, chromosome, crossbreeding, selection, multiplication, mutation, etc.). By coding the objective function and constraints according to this algorithm, sequential operations are performed, and the solution is achieved [11]. In another assignment problem in which the genetic algorithm was used, a problem in which an operator could be assigned to more than one task, task-scheduling and operator-placement constraints were available, and circumstances including operator capacity constraints changed daily costs to perform tasks were dealt with [12]. In another study, the topic was the assignment model developed by Cesani and Steudel in 2005 to demonstrate the labor flexibility (based on the principles of labor sharing and labor balancing) characterized by the mobility of the operator working within the cell in cellular production systems. In this study, the focus was to investigate the effect of different work distribution strategies (For example; when only one operator is responsible for one machine or group, or when more than one operator are responsible for one machine or a group of machines) on system performance. The results of the experiment showed that the balance of workload assigned to individual operators and the level of work load shared between operators were important factors in determining the performance of the system [13]. In the study of Heimerl and Kolisch [14], assigning of multi-faceted operators to the tasks according to the knowledge/skill, loss in value and company's ability level objectives was discussed and by the established model (limited nonlinear continuous optimization model), it was attempted to reach the strategy that could be. When the performed assignments and the learning curves based on these were examined, it was concluded that faster learning made the human resources more specialized and this also led the company to have a wider quality [14]. In the study carried out by Bryan and his colleagues, the model of assigning operators to production areas was established to take into account both human and technical characteristics and their effects on system performance.

Test results showed that this model offered better task assignments than employees who only consider technical capabilities. Therefore, it supports the topic that companies allocate more space on human element in the design of production systems. [15].

In our study, the area to be examined among the assignment models is an assignment problem with different levels of labor force in production lines. A product (Damper Trailer) that came out of a welding line whose assignment model was determined in the Automotive Sector was studied. The model includes tasks done at different levels of labor force. The durations of the tasks vary according to the competence of the operators who do the tasks.

There are many important constraints that affect the objective function in assignment problems. A problem with important parameters or constraints for the automotive sector, such as the presence of different levels of labour force, the inability to assign each labor force to each task, presence of the minimum level of competence required for the operators to be employed in order to assign the operator (factors inherent in the resource process are also effective in determining competencies.), changing the time of the task done according to competence and turning this time into cost was addressed.

Two models were established using Linear Programming in order to complete the product as soon as possible and to minimize labor costs with the correct assignments when assigning labor force in production lines or products, which required different levels of labor force in the automotive sector. In the first mathematical model, it was aimed to ensure the cost minimization in the lines that had certain cycle time (takt) by assigning the operators at different levels of labour force taking in to account the level required by the task. On the other hand, in the second model, the cycle time (time) was unclear; while making cost minimization, making also line balancing was aimed by this second model in which operators at different labor force levels were assigned to the level required by the task and operators who minimized the time difference between assignments and had maximum time to do the task defined the cycle time (takt). The differences between these two models will be interpreted.





2. Data Analysis and Mathematical Modeling

2.1 Data Analysis

In the trailer welding line where the model will be installed for the damper trailer product, there are a total of 27 operators who could work throughout the factory. The competence of these operators are different from each other. For 8 different technical features to be sought in a person who would work on the trailer welding line

where all trailer vehicle variants were produced, the competency table of the persons was formed. These technical features are: making manufacturing and welding by reading technical drawings, making MAG welding, making longitudinal girder spot and its welding, making longitudinal girder completion welding, making cold straightening, making positioner spot and its welding, making the final completion welding and making flame straightening. While these technical features were examined according to the operators, 4 level of competence was determined. The specified levels of competence are displayed visually in a circle and each quarter of the circle is described as a level of competence.

Table 1. Description of the Competency Levels Used in the Competency Table

| | | |
|--------------|--|---|
| 1.Level (1L) |  | He has on-the-job training (can work with supervision). |
| 2.Level (2L) |  | He can work alone only at that station. |
| 3.Level (3L) |  | He can work alone at all stations. |
| 4.Level (4L) |  | This level is the instructor level. |

The operators whose competency levels were determined according to their technical features are shown in the competency table as follows.

Table 2. Trailer Welding Line Competency Table

| Work Abilities | A1 | A2 | A3 | A4 | A5 | A6 | A7 | A8 |
|----------------|----|----|----|----|----|----|----|----|
| Operator | | | | | | | | |
| 1.operator | 4L | 4L | | 4L | 4L | 4L | 4L | 3L |
| 2.operator | 4L | 4L | 4L | 3L | | 2L | 2L | 2L |
| 3.operator | 4L | 4L | 2L | 3L | 4L | 2L | 4L | 4L |
| 4.operator | 1L | 2L | 3L | 2L | | 1L | 2L | 1L |
| 5.operator | 3L | 4L | 1L | 4L | 4L | 2L | 3L | 4L |
| 6.operator | 1L | 2L | 1L | 1L | | 2L | 1L | |
| 7.operator | 2L | 4L | 1L | 3L | 3L | 1L | 4L | 4L |
| 8.operator | 2L | 4L | 1L | 3L | 3L | 1L | 4L | 4L |
| 9.operator | 3L | 4L | 1L | 3L | 4L | 4L | 3L | 3L |
| 10.operator | 1L | 2L | 1L | 2L | | 3L | 2L | |
| 11.operator | 1L | 3L | 1L | 3L | | 2L | 2L | 2L |
| 12.operator | 1L | 2L | 3L | 2L | | 1L | 2L | |
| 13.operator | 1L | 3L | 1L | 1L | | 2L | 2L | |
| 14.operator | 1L | 3L | 1L | 1L | | 2L | 1L | |
| 15.operator | 1L | 3L | 1L | 1L | | 3L | 1L | |
| 16.operator | 1L | 3L | 1L | 3L | | 1L | 2L | |
| 17.operator | 2L | 3L | 3L | 2L | | 1L | 1L | |
| 18.operator | 2L | 3L | 1L | 3L | 2L | 1L | 1L | |
| 19.operator | 1L | 2L | 1L | 1L | | 1L | 2L | |
| 20.operator | | 2L | | | | 1L | | |
| 21.operator | | 1L | | | | | 1L | |
| 22.operator | 1L | 2L | 1L | 1L | | 1L | 1L | |
| 23.operator | | 1L | 1L | 1L | | | | |
| 24.operator | | 1L | | 1L | | 1L | | |
| 25.operator | | 2L | | 1L | | | 1L | |
| 26.operator | | 2L | | 1L | | | | |
| 27.operator | | 2L | | 1L | | | | |

For the production of damper trailer, there are 5 stations on the Trailer Welding Line and 14 different tasks are being done in total; therefore, 14 labour force is needed. The levels of the needed labor force must be determined according to the needs of the task to be done. The following table provides information about which station and level of competency the 8 technical features in the competency table should be located at.

Table 3. Minimum Competency Requirements in the Stations According To the Technical Features in the Competency Table

| Technical Necessaries | 1.Sta. | 2.Sta. | 3.Sta. | 4.Sta. | 5.Sta. |
|-----------------------|--------|--------|--------|--------|--------|
| A1 | Min3L | Min3L | Min3L | Min3L | Min3L |
| A2 | Min3L | | Min3L | Min3L | Min3L |
| A3 | Min2L | | | | |
| A4 | | Min2L | | | |
| A5 | | Min3L | | | |
| A6 | | | Min3L | Min3L | |
| A7 | | | | | Min2L |
| A8 | | | | | Min3L |

When Table 3 and Table 2 are redesigned according to the requirements of the tasks assigned, the following table showing for which station and at which level operators have the labor force emerges. This is one of the tables that will be the basis for modeling the problem.

While time-study activities for Damper trailer product were carried out, for 14 different tasks at 5 stations, data sets were created by taking the time-study of the operator at each level.

Table 4. Competency Levels of Operators According to the Requirements of the Tasks of the Stations

| Operator | 1.Sta. | 2.Sta. | 3.Sta. | 4.Sta. | 5.Sta. |
|-------------|--------|--------|--------|--------|--------|
| 1.operator | 4L | 4L | 4L | 4L | 4L |
| 2.operator | 4L | 3L | 3L | 3L | 3L |
| 3.operator | 4L | 4L | 3L | 3L | 4L |
| 4.operator | 2L | 1L | 1L | 1L | 2L |
| 5.operator | 3L | 4L | 3L | 3L | 4L |
| 6.operator | 1L | 1L | 2L | 2L | 1L |
| 7.operator | 2L | 3L | 2L | 2L | 4L |
| 8.operator | 2L | 3L | 2L | 2L | 4L |
| 9.operator | 3L | 2L | 4L | 4L | 3L |
| 10.operator | 1L | 1L | 3L | 3L | 1L |
| 11.operator | 1L | 1L | 2L | 2L | 2L |
| 12.operator | 2L | 1L | 1L | 1L | 1L |
| 13.operator | 1L | 1L | 2L | 2L | 2L |
| 14.operator | 1L | 1L | 2L | 2L | 2L |
| 15.operator | 1L | 1L | 3L | 3L | 1L |
| 16.operator | 1L | 1L | 2L | 2L | 2L |
| 17.operator | 3L | 1L | 2L | 2L | 1L |
| 18.operator | 2L | 2L | 2L | 2L | 1L |
| 19.operator | 1L | 1L | 2L | 2L | 1L |
| 20.operator | 1L | 1L | 1L | 1L | 1L |
| 21.operator | 1L | 1L | 1L | 1L | 1L |
| 22.operator | 1L | 1L | 1L | 1L | 1L |
| 23.operator | 1L | 1L | 1L | 1L | 1L |
| 24.operator | 1L | 1L | 1L | 1L | 1L |
| 25.operator | 1L | 1L | 1L | 1L | 1L |
| 26.operator | 1L | 1L | 1L | 1L | 1L |
| 27.operator | 1L | 1L | 1L | 1L | 1L |

Table 5. Distribution of Tasks and Operators Assigned to Stations in the Model

| Stations | | | | | Total Works-Operators |
|----------|--------|--------|--------|--------|-----------------------|
| 1.Sta | 2.Sta | 3.Sta | 4.Sta | 5.Sta | |
| 2 work | 4 work | 3 work | 2 work | 3 work | 14 works |
| 2 op. | 4 op. | 3 op. | 2 op. | 3 op. | 14 operators |

The distribution of tasks and operators to be assigned at stations is as follows.

Table 4 shows the distribution of tasks to be assigned according to stations and the minimum level of competence required. All operators at different competency levels worked in 14 tasks, and a data set was created with the obtained time studies. The following table was created between the tasks and competency levels taking into account the averages obtained from this data set. The data in the table will be accepted as standard in mathematical modeling to be created.

When we match the information in Table 6 and Table 4, we can obtain the following dataset. The created data set will be used effectively in the modeling of the problem.

Table 6. The Maximum-Minimum Periods obtained for Each Task from the Operators with Different Competency

| Works | Min-Max Time Studies (minute) | | | | |
|--------|-------------------------------|-----|-----|-----|-----|
| | Max-Min | 1L | 2L | 3L | 4L |
| 1.Sta | Max | 165 | 155 | 145 | 120 |
| 1.Work | Min | 150 | 140 | 125 | 105 |
| 1.Sta | Max | 120 | 105 | 90 | 80 |
| 2.Work | Min | 105 | 95 | 80 | 70 |
| 2.Sta | Max | 115 | 105 | 90 | 80 |
| 1.Work | Min | 100 | 90 | 80 | 70 |
| 2.Sta | Max | 110 | 100 | 85 | 75 |
| 2.Work | Min | 95 | 80 | 70 | 65 |
| 2.Sta | Max | 145 | 135 | 120 | 110 |
| 3.Work | Min | 130 | 125 | 105 | 95 |
| 2.Sta | Max | 165 | 155 | 140 | 130 |
| 4.Work | Min | 140 | 135 | 120 | 105 |
| 3.Sta | Max | 170 | 155 | 150 | 130 |
| 1.Work | Min | 155 | 135 | 125 | 110 |
| 3.Sta | Max | 165 | 150 | 140 | 125 |
| 2.Work | Min | 150 | 145 | 130 | 105 |
| 3.Sta | Max | 145 | 135 | 120 | 110 |
| 3.Work | Min | 140 | 130 | 115 | 105 |
| 4.Sta | Max | 165 | 155 | 140 | 125 |
| 1.Work | Min | 150 | 145 | 125 | 105 |
| 4.Sta | Max | 160 | 155 | 140 | 125 |
| 2.Work | Min | 155 | 145 | 130 | 100 |
| 5.Sta | Max | 130 | 120 | 115 | 110 |
| 1.Work | Min | 120 | 115 | 110 | 100 |
| 5.Sta | Max | 115 | 105 | 90 | 80 |
| 2.Work | Min | 100 | 90 | 80 | 70 |
| 5.Sta | Max | 145 | 135 | 120 | 110 |
| 3.Work | Min | 140 | 130 | 115 | 105 |

Table 7. The Maximum-Minimum Periods obtained for Stations, Tasks, and Operators from the Time-Study Dataset

| Operator | Time Studies (minutes) | | | | | | |
|-------------|------------------------|--------------------|--------------------|---|--------------------|--------------------|--------------------|
| | 1.Sta 1.Work | 1.Sta 2.Work | 2.Sta 1.Work | . | 5.Sta 1.Work | 5.Sta 2.Work | 5.Sta 3.Work |
| 1.operator | max=120 min=105 | max=80 min=70 | max=80 min=70 | . | max=110 min=100 | max=80 min=70 | max=110 min=105 |
| 2.operator | max=120 min=105 | max=80 min=70 | max=90 min=80 | . | max=115 min=110 | max=90 min=80 | max=120 min=115 |
| 3.operator | max=120 min=105 | max=80 min=70 | max=80 min=70 | . | max=110 min=100 | max=80 min=70 | max=110 min=105 |
| 4.operator | max=155 min=140 | max=105 min=95 | max=115 min=100 | . | max=120 min=115 | max=105 min=90 | max=135 min=130 |
| . | . | . | . | . | . | . | . |
| 25.operator | max=165 min=150 | max=120 min=105 | max=115 min=100 | . | max=130 min=120 | max=115 min=100 | max=145 min=140 |
| 26.operator | max=165 min=150 | max=120 min=105 | max=115 min=100 | . | max=130 min=120 | max=115 min=100 | max=145 min=140 |
| 27.operator | max=165 min=150 | max=120 min=105 | max=115 min=100 | . | max=130 min=120 | max=115 min=100 | max=145 min=140 |

The information in Table 6, which were created by determining according to competency level (1, 2, 3, 4th level) of the observations taken from each operators for each task without assignment criteria, consists of standardized durations according to the level at which the operator is located at the relevant station.

The writing of the model was realized by using the tables created as a result of the analyses carried out on the data collected. The following general information related to the factory was used in the model as data.

- 07:45-17:45 working hours (10 hours)
- 60 minutes lunch break
- 15 minutes of morning tea break
- 15 minutes of afternoon tea break
- Daily Net Working Time; 510 Minutes/Day
- Hourly Labor Fee; 7 Euro/Hour
- The Available Takt Time for Damper Trailer; 150 minutes/vehicle
- Number of Operators Who Can Work in the Production of Damper Trailer; 27 Operators
- Number of Stations Required for Damper Trailer Production; 5 Stations
- Number of Tasks to Be Assigned to the Stations in the Production of Damper Trailer; 14 Tasks

- Number of Operators with Appropriate Competency Required to Be Assigned to the Stations in the Production of Damper Trailer; 14 Operators

Since damper trailer is a vehicle produced in mass production, the company aims to minimize takt time by minimizing labor unit cost. However, there are some constraints in the production. Some of these constraints are that the requirements of the task are different, the competence levels of the operators are different, and there is the inability to appoint the right person to the right task. In addition, even if the person with the right competency is assigned to the task, the time to perform the task varies according to the capacity he/she has; this time period should not exceed the time of the takt. Time studies of operators at all levels were taken for the same task. When the time studies taken from the same person for the same task were examined, it was observed that the person did the task at different times in each cycle. Therefore, for the task realization duration, a standard minimum and maximum period of time was determined among the operators who were at the same task and at the same level. While mathematical models were established, the models were written by taking the highest of these durations. This is because operators always have the possibility of completing the task at the highest time. For this reason, in order to establish the model with the correct data, modeling was performed on GAMS 23.5 program by using the maximum task completion times.

2.2 Model 1: There is a Specific Cycle (Takt) Time

Notations used in the model;

Xijk: decision variable that takes 1 if k operator is assigned to j task at i station, otherwise takes 0

Tijk: task completion time of k operator at i station for j task

Cw: 1-minute labor fee

CSi: Cycle time of i station

Di: decision variable that takes 1 if i operator is assigned to the 1st station, otherwise takes 0

Ei: decision variable that takes 1 if i operator is assigned to the 2nd station, otherwise takes 0

Fi: decision variable that takes 1 if i operator is assigned to the 3rd station, otherwise takes 0

Gi: decision variable that takes 1 if i operator is assigned to the 4th station, otherwise takes 0

Hi: decision variable that takes 1 if i operator is assigned to the 5th station, otherwise takes 0

Objective function and constraints of the model;

It was aimed that the objective function would sum and minimize the multiplications of unit labor fee and task completion time of k operator when k operator was assigned to i station for j task.

$$z = \min \sum_{i=1, \dots, m} \sum_{j=1, \dots, u} \sum_{k=1, \dots, t} Xijk \times Tijk \times Cw \tag{1}$$

1st Constraint: it is added because it is required to assign one of the operators to j task at i station (if the assignment is not made, the task cannot be performed, even the product cannot be produced, and the missing operation is seen.)

$$\sum_{k=1}^t Xijk = 1 \quad i=1, \dots, m \quad j=1, \dots, u \tag{2}$$

2nd Constraint: It is added so that task completion time of k operator assigned to j task at i station does not pass the cycle time (takt)

$$\sum_{i=1}^m \sum_{j=i}^u Xijk \times Tijk \leq CSi \quad k=1, \dots, t \tag{3}$$

3rd Constraint: Because k operator who has appropriate competency must be assigned to j task at i station, it is added so that assignments of the operators who have appropriate competencies are performed by established equations.

For example, if one of the 1, 2, 3, 5, 9 or 17th operators from the competency cluster must be assigned to the 1st task at the 1st station;

$$X111 + X112 + X113 + X115 + X119 + X1117 = 1 \tag{4}$$

The same formulization is also applied for other tasks.

4th Constraint: it is added because k operator must be assigned to one of the stations.

$$\sum_{k=1}^t Dik + Eik + Fik + Gik + Hik = 1 \tag{5}$$

$i=1, \dots, m$

5th Constraint: if k operator is assigned to i station, the other tasks in i station can be also assigned to him/her (In other words, each operator can take more than one task at the station assigned within the takt time.)

For example; in order to assign all the tasks in the 1st station to the 1st operator;

$$\begin{aligned} X111 &\leq D11 \\ X121 &\leq D11 \\ X131 &\leq D11 \\ &\vdots \\ X1N1 &\leq D11 \end{aligned} \tag{6}$$

The formulization should be also repeated for other stations and operators.

According to the solution report (Appendix-1) for the mathematical model written in GAMS 23.5, the cycle time value was found as 145 minutes. Assignments made in the Gams program are transferred to the table as follows; task completion time of a operator who assigned that task (Tijk) and the cost value comprised of paid fee for that task (Tijk x Cw) are shown in the table.

Table 8. Summary Table of the Assignments Made According to the Model-1 Solution

| Model-1 Summary Table of Assigns | | | | |
|----------------------------------|----------|------------------------|--------------|-----------------|
| Sta (i) | Work (j) | Assinged Operators (k) | Times (Tijk) | costs (Tijk*Cw) |
| 1. sta | 1.work | 17.op | 145 | 17,40 € |
| 1. sta | 2.work | 12.op | 90 | 10,80 € |
| 2.sta | 1.work | 2.op | 90 | 10,80 € |
| 2.sta | 2.work | 3.op | 75 | 9,00 € |
| 2.sta | 3.work | 18.op | 135 | 16,20 € |
| 2.sta | 4.work | 5.op | 130 | 15,60 € |
| 3.sta | 1.work | 1.op | 130 | 15,60 € |
| 3.sta | 2.work | 9.op | 125 | 15,00 € |
| 3.sta | 3.work | 6.op | 135 | 16,20 € |
| 4.sta | 1.work | 10.op | 140 | 16,80 € |
| 4.sta | 2.work | 15.op | 140 | 16,80 € |
| 5.sta | 1.work | 8.op | 110 | 13,20 € |
| 5.sta | 2.work | 4.op | 105 | 12,60 € |
| 5.sta | 3.work | 7.op | 110 | 13,20 € |

Because the task with the longest work time (1st station and 1st task) takes 145 min, although the duration of the other tasks are shorter, there will be waiting in other tasks until the end of the 145-minute task; in other words, it is the task that constitutes the bottleneck of the line. For this reason, even if all operators work under 145 min, their labor costs are paid as if they worked for 145 min and while the direct labor cost of the vehicle is loaded, 145-minute work time is taken into account.

Table 9. Results Regarding the Capacity and Financial Status of the Company When Assignments are Made According to the Model-1 Solution

| Model-1 Results of Capacity and Financial Rates | | | | | |
|---|------------------------------------|---|------------------------------------|-----------------|--------------|
| Cost Unit (Euro/Takt) | Cycle Time (max Tijk) | | Cost Unit(Cw) | Total Operators | |
| | 145 | X | 0,12 | X 14 | = 243,60 € |
| Capacity of Vehicle per Shift (Vehicle/Shift) | Shift Time 510 | / | Cycle Time (max Tijk) 145 | | = 3,52 |
| Daily Production Cost (Euro/Day) | Cost Unit 243,60 € | X | Capacity of Vehicle per Shift 3,52 | | = 857,47 € |
| Annual Production Capacity (Vehicle/Year) | Capacity of Vehicle per Shift 3,52 | X | Workday (All year) 250 | | = 880 |
| Annual Production Cost (Euro/Year) | Cost Unit 243,60 € | X | Annual Production Capacity 880 | | 214,368,00 € |

2.3 Model 2: The cycle (Takt) Time is Uncertain

The notations used in the model;

Sij: sum of the duration of the tasks assigned to the j operator at i station

Ji: {cluster of the operators who will work at i station}

Ci: Max {Siji} cycle time of i station

Xijk: decision variable that takes 1 if k operator is assigned to j task at i station, otherwise takes 0

Tijk: task completion time of k operator at i station for j task

Cw: 1-minute labor fee

Di: decision variable that takes 1 if i operator is assigned to the 1st station, otherwise takes 0

Ei: decision variable that takes 1 if i operator is assigned to the 2nd station, otherwise takes 0

Fi: decision variable that takes 1 if i operator is assigned to the 3rd station, otherwise takes 0

Gi: decision variable that takes 1 if i operator is assigned to the 4th station, otherwise takes 0

Hi: decision variable that takes 1 if i operator is assigned to the 5th station, otherwise takes 0

Objective function and constraints of the model;

The objective function was added such a way to minimize the cycle time difference between the stations.

$$Z = \min \sum_{i=1}^n |Cn - Cn - 1| \quad i=1, \dots, n \quad (7)$$

1st Constraint: it was added because it was required to assign one of the operators to j task at i station.

$$\sum_{k=1}^t Xijk = 1 \quad i=1, \dots, m \quad j=1, \dots, u \quad (8)$$

2nd Constraint: It was added because k operator whose competency level was appropriate must be assigned to j task at i station.

For example, if one of the 1, 2, 3, 5, 9 or 17th operators from the competency cluster must be assigned to the 1st task at the 1st station;

$$X111 + X112 + X113 + X115 + X119 + X1117 = 1 \quad (9)$$

The same formulization is also applied for other tasks.

3rd Constraint: Since the tasks are performed simultaneously, k operator should not be assigned to more than one task at the same time; therefore, it was added.

$$\sum_{i=1}^m \sum_{j=1}^u Xijk \leq 1 \quad k=1, \dots, t \quad (10)$$

4th Constraint: At i station, the sum of the durations of the tasks assigned to j operator constitutes Sij.

$$\sum_{i=1}^m \sum_{j=1}^u Xijk \times Tijk = Sij \quad i=1, \dots, m \quad j=1, \dots, u \quad (11)$$

5th Constraint: it was added so that (Sij)s in at i station constitute the maximum cycle time.

$$If C_i = \max(S_{ij}); \tag{12}$$

$$C_i = \max \sum_{j=1}^m |S_{ij} - S_{ij+1}| \quad j=1, \dots, u \tag{13}$$

According to the solution report (Appendix-2) for the mathematical model written in GAMS 23.5, the cycle time value was found as 140 minutes. Examining the model solution results, it is seen that X_{ijk}, which is the 0-1 decision variable, takes approximate values. In the solution, operators' assignments whose approximate values are close to 1 should be accepted as 1 and operators should be assigned to the tasks in stations. The following assignments show operators assigned to the X_{ijk} decision variable for the solution of the problem. Assignments made in the Gams program were transferred to the table as follows; the assignment values of the decision variables, the total task time assigned to the operator (S_{ij}), and the station cycle time (C_i), which takes the maximum value of the (S_{ij})s assigned to the station are shown on the table.

Table 10. Summary Table of the Assignments Made According to the Model-2 Solution

| Model-2 Summary Table of Assigns | | | | | |
|----------------------------------|----------|--------------|------------------------|---------------------------|------------------------------|
| Sta (i) | Work (j) | Assing Value | Assinged Operators (k) | Times (T _{ijk}) | Cycle Time (C _i) |
| 1.sta | 1.work | 0,7 | 2.op | 120 | C1 |
| 1.sta | 2.work | 1,0 | 12.op | 90 | |
| 2.sta | 1.work | 0,8 | 7.op | 90 | C2 |
| 2.sta | 2.work | 0,5 | 5.op | 75 | |
| 2.sta | 3.work | 0,5 | 18.op | 135 | |
| 2.sta | 4.work | 0,7 | 3.op | 130 | |
| 3.sta | 1.work | 0,6 | 1.op | 130 | C3 |
| 3.sta | 2.work | 1,0 | 9.op | 125 | |
| 3.sta | 3.work | 0,9 | 6.op | 135 | |
| 4.sta | 1.work | 0,6 | 10.op | 140 | C4 |
| 4.sta | 2.work | 0,7 | 15.op | 140 | |
| 5.sta | 1.work | 1,0 | 8.op | 110 | C5 |
| 5.sta | 2.work | 1,0 | 11.op | 105 | |
| 5.sta | 3.work | 1,0 | 4.op | 135 | |

Because the task with the longest work time (4th station and 1st and 2nd tasks) takes 140 min, although the duration of the other tasks are shorter, there will be waiting in other tasks until the end of the 140-minute task; in other words, it is the task that constitutes the bottleneck of the line. For this reason, even if all operators work under 140 min, their labor costs are paid as if they worked for 140 min and while the direct labor cost of the vehicle is loaded, 140-minute work time is taken into account.

Table 11. Results Regarding the Capacity and Financial Status of the Company When Assignments are Made According to The Model-2 Solution

| Model-2 Results of Capacity and Financial Rates | | | | | | |
|---|------------------------------------|---|------------------------------------|---|-----------------|---------------|
| Cost Unit (Euro/Takt) | Cycle Time (max T _{ijk}) | | Cost Unit (Cw) | | Total Operators | 235,20 € |
| | 140 | X | 0,12 | X | 14 | |
| Capacity of Vehicle per Shift (Vehicle /Shift) | Shift Time | | Cycle Time (max T _{ijk}) | | | 3,64 |
| | 510 | / | 140 | | | |
| Daily Production Cost (Euro/Day) | Cost Unit | | Capacity of Vehicle per Shift | | | 856,13 € |
| | 235,20 € | X | 3,64 | | | |
| Annual Production Capacity (Vehicle/Year) | Capacity of Vehicle per Shift | | Workday (All year) | | | 910 |
| | 3,64 | X | 250 | | | |
| Annual Production Cost (Euro/Year) | Cost Unit | | Annual Production Capacity | | | 214.03 2,00 € |
| | 235,20 € | X | 910 | | | |

2.4 Comparison of the Model 1 and Model 2 Results

When the assignments carried out in the models are examined, it is seen that 8 of 14 tasks are assigned to the same operator in both models. In the other 6 assignments, since the models have different objective functions, it is seen that the assignments are also different.

When we compared Table 1 and Table 2 as the financial status and capacity status of the results of the assignments made within the reference range of Model-1 & Model-2;

- Considering the actual unit costs, it was seen that an 8.4 euro gain was ensured during a Takt period and Model 2 provided a 3.45% reduction in the cost per vehicle.
- It was observed that vehicle production capacity in Model 2 increased by 13% in shift.
- It was also determined that due to the 5-minute cycle time difference between Model 1 and Model 2, Model 2 made a profit of € 7392 in 2 years; this profit corresponds to the production cost of 31 vehicles per year.

3. Sensitivity Analysis

All results from Model-1 and model-2 comparisons show that model-2 achieves more efficient results. Therefore, the sensitivity analysis will be written through Model-2. The writing and solutions of the models will be done through the GAMS program and the results will be

compared. Information about new models to be created for sensitivity analysis;

- In the new Model-2.1, the number of operators (human resource) will be increased from 27 operators to 35 operators, the number of stations will be increased from 5 stations to 6 stations, and due to the addition of the 6th station, the number of tasks will increase to 16. Therefore, the number of operators required to be assigned will also be 16.
- In the new Model-2.2, the number of operators (human resource) will be increased from 35 operators to 40 operators, the number of stations will be increased from 6 stations to 8 stations, and due to the addition of the 7th and 8th stations, the number of tasks will increase to 20. Therefore, the number of operators required to be assigned will also be 20.
- In the new Model-2.3, the number of operators (human resource) will be increased from 40 operators to 50 operators, the number of stations will be increased from 8 stations to 10 stations, and due to the addition of the 9th and 10th stations, the number of tasks will increase to 25. Therefore, the number of operators required to be assigned will also be 25.

3.1 Sensitivity Analysis 1 (New Model 2.1)

The new model (Model 2.1) constituting the 1st step of the sensitivity analysis will be established by being expended according to 6th station to which the objective function and constraints of Model 2 will be added, 2 tasks connected to this station and the new 8 operators added to 27 operators. A total of 16 operators will be required for 16 tasks. In addition to Table 3, technical requirement for manufacturing and welding by reading technical drawings at a minimum 2nd level and technical requirement for MAG welding at a minimum 2nd level are required at the 6th station. In addition to Table 6, Table 12 was obtained for 6th station. See also Apendix-3 for the competencies of new operators added.

Examining the model solution results, it is seen that Xijk, which is the 0-1 decision variable, takes approximate values. In the solution, operators' assignments whose approximate values are 0.5 and above should be accepted as 1 and operators should be assigned to the tasks in the stations. The following assignments show operators assigned to the Xijk decision variable for the solution of the problem. Assignments made in the Gams program were transferred to the table as follows; the assignment values of the decision variables, the total task time assigned to the operator (Sij), and the station cycle time (Ci), which takes the maximum value of the (Sij)s assigned to the station are shown on the table.

Table 12. Maximum-Minimum Period Table Obtained For Each Task from Time Surveys Taken From Operators of Different Abilities (6th Station-New)

| Works | New Min-Max Time Studies (minute) | | | | |
|--------|-----------------------------------|-----|-----|-----|-----|
| | MinMax | 1L | 2L | 3L | 4L |
| 6.Sta | Max | 145 | 135 | 130 | 110 |
| 1.Work | Min | 140 | 130 | 120 | 100 |
| 6.Sta | Max | 145 | 135 | 130 | 90 |
| 2.Work | Min | 140 | 130 | 120 | 80 |

Table 13. Summary Table of Assignments made according to the Sensitivity Analysis 1 Model-2.1 Solution

| Model-2.1 Summary Table of Assigns | | | | | | |
|------------------------------------|----------|--------------|------------------------|--------------|-----------------|-----|
| Sta (i) | Work (j) | Assing Value | Assinged Operators (k) | Times (Tijk) | Cycle Time (Ci) | |
| 1.sta | 1.work | 0,9 | 30.op | 120 | C1 | 120 |
| 1.sta | 2.work | 1 | 12.op | 90 | | |
| 2.sta | 1.work | 1 | 7.op | 90 | C2 | 130 |
| 2.sta | 2.work | 0,9 | 3.op | 75 | | |
| 2.sta | 3.work | 1 | 5.op | 110 | | |
| 2.sta | 4.work | 0,9 | 32.op | 130 | | |
| 3.sta | 1.work | 0,9 | 1.op | 130 | C3 | 130 |
| 3.sta | 2.work | 1 | 9.op | 125 | | |
| 3.sta | 3.work | 1 | 10.op | 120 | C4 | 140 |
| 4.sta | 1.work | 0,5 | 28.op | 125 | | |
| 4.sta | 2.work | 0,5 | 29.op | 140 | C5 | 110 |
| 5.sta | 1.work | 0,9 | 8.op | 110 | | |
| 5.sta | 2.work | 1 | 4.op | 105 | | |
| 5.sta | 3.work | 0,9 | 35.op | 110 | C6 | 135 |
| 6.sta | 1.work | 0,9 | 2.op | 110 | | |
| 6.sta | 2.work | 0,9 | 11.op | 135 | | |

Because the task with the longest work time (4th station 2nd task) takes 140 min, although the duration of the other tasks are shorter, there will be waiting in other tasks until the end of the 140-minute task; in other words, it is the task that constitutes the bottleneck of the line. For this reason, even if all operators work under 140 min, their labor costs are paid as if they worked for 140 min and while the direct labor cost of the vehicle is loaded, 140-minute work time is taken into account.

Despite the same cycle time as Model-2 (140 min), the Actual Unit Cost and the Annual Production Cost increased because 2 operators worked more. However, since the cycle time was not changed, the capacity also was not changed.

3.2 Sensitivity Analysis 2 (New Model 2.2)

The new model (Model 2.2) constituting the 2nd step of the sensitivity analysis will be established by being expended according to the 7th and 8th stations to which the objective function and constraints of Model 2.1 will be added, 4 tasks connected to these stations and the new 5 operators added to 35 operators. There will be a total of 20 tasks and 20 operators will be required. In addition to Table 3, technical requirement for making cold straightening at a minimum 2nd level at the 7th station and technical requirement for making the final completion

welding at a minimum 2nd level at the 8th station are required. In addition to Table 6, Table 15 was obtained for the 7th and 8th stations. See also Apendix-4 for the competencies of new operators added.

Table 14. Results related to the Capacity and Financial Status of the Company When Assignments are Made According to the Sensitivity Analysis 1 Model-2.1 Solution

| Model-2.1 Results of Capacity and Financial Rates | | | | | | |
|---|---------------------------------------|---|-------------------------------|---|------------------|----------------|
| Cost Unit (Euro/Takt) | Cycle Time (max Tijk) | X | Cost Unit(C w) | X | Total Operato rs | |
| | 140 | X | 0,12 | X | 16 | = 268,80 € |
| Capacity of Vehicle per Shift(Vehicle/Shift) | Shift Time 510 | / | Cycle Time (max Tijk) | | 140 | = 3,64 |
| Daily Production Cost (Euro/Day) | Cost Unit 268,80 € | X | Capacity of Vehicle per Shift | | 3,64 | = 978,43 € |
| Annual Production Capacity (Vehicle/Year) | Capacity of Vehicle per Shift 3,64 | X | Workday (All year) | | 250 | = 910 |
| Annual Production Cost (Euro/Year) | Cost Unit 268,80 € | X | Annual Production Capacity | | 910 | = 244,608,00 € |

Table 15. Maximum-Minimum Period Table Obtained for Each Task from Time Surveys Taken from Operators of Different Abilities (7th and 8th Stations-New)

| Works | New Min-Max Time Studies (minute) | | | | |
|--------|-----------------------------------|-----|-----|-----|----|
| | Max-Min | 1L | 2L | 3L | 4L |
| 7.Sta | Max | 130 | 120 | 100 | 90 |
| 1.Work | Min | 125 | 110 | 95 | 70 |
| 7.Sta | Max | 130 | 120 | 100 | 90 |
| 2.Work | Min | 125 | 110 | 95 | 70 |
| 8.Sta | Max | 120 | 110 | 100 | 90 |
| 1.Work | Min | 115 | 105 | 95 | 70 |
| 8.Sta | Max | 120 | 110 | 100 | 90 |
| 2.Work | Min | 115 | 105 | 95 | 70 |

According to the solution report belonging to the mathematical new model written in gams, the objective function value was found as 130 minutes. When the model solution results are examined, it is seen that contrary to Model-2 and Model-2.1, Xijk, which is the 0-1 decision variable, do not take approximate values, but takes exact values as desired. Operators added to the system in Model-2.2 were selected as fully competent for all stations and tasks (4th level). Therefore, looking at the model result, it is seen that since there were a sufficient number of operators suitable for the desired competencies of the tasks, a full-value assignment was done. Assignments made in the Gams program were transferred to the table as follows.

Since the task with the longest work time (the 4th task at the 2nd stations and the 1st task at the 3rd station) takes 130 min, although the duration of the other tasks are

shorter, there will be waiting in other tasks until the end of the 130-minute task; in other words, it is the task that constitutes the bottleneck of the line. For this reason, even if all operators work under 130 min, their labor costs are paid as if they worked for 130 min and while the direct labor cost of the vehicle is loaded, 130-minute work time is taken into account.

Table 16. Summary Table of Assignments Made according to the Sensitivity Analysis 2 Model-2.2 Solution

| Model-2.2 Summary Table of Assigns | | | | | |
|------------------------------------|----------|--------------|------------------------|--------------|-----------------|
| Sta (i) | Work (j) | Assing Value | Assinged Operators (k) | Times (Tijk) | Cycle Time (Ci) |
| 1. sta | 1.work | 1 | 39.op | 120 | C1 120 |
| 1. sta | 2.work | 1 | 12.op | 90 | |
| 2.sta | 1.work | 1 | 34.op | 90 | C2 130 |
| 2.sta | 2.work | 1 | 8.op | 85 | |
| 2.sta | 3.work | 1 | 5.op | 110 | |
| 2.sta | 4.work | 1 | 36.op | 130 | |
| 3.sta | 1.work | 1 | 1.op | 130 | C3 130 |
| 3.sta | 2.work | 1 | 9.op | 125 | |
| 3.sta | 3.work | 1 | 10.op | 120 | C4 125 |
| 4.sta | 1.work | 1 | 38.op | 125 | |
| 4.sta | 2.work | 1 | 37.op | 125 | C5 110 |
| 5.sta | 1.work | 1 | 3.op | 110 | |
| 5.sta | 2.work | 1 | 35.op | 80 | |
| 5.sta | 3.work | 1 | 40.op | 110 | C6 110 |
| 6.sta | 1.work | 1 | 28.op | 110 | |
| 6.sta | 2.work | 1 | 29.op | 90 | C7 90 |
| 7.sta | 1.work | 1 | 32.op | 90 | |
| 7.sta | 2.work | 1 | 30.op | 90 | C8 110 |
| 8.sta | 1.work | 1 | 7.op | 90 | |
| 8.sta | 2.work | 1 | 2.op | 110 | |

Table 17. Results related to the Capacity and Financial Status of the Company When Assignments are Made According to the Sensitivity Analysis 2 Model-2.2 Solution

| Model-2.2 Results of Capacity and Financial Rates | | | | | | |
|---|---------------------------------------|---|-------------------------------|---|------------------|----------------|
| Cost Unit (Euro/Takt) | Cycle Time (max Tijk) | X | Cost Unit(C w) | X | Total Operato rs | |
| | 130 | X | 0,12 | X | 20 | = 312,00 € |
| Capacity of Vehicle per Shift(Vehicle/Shift) | Shift Time 510 | / | Cycle Time (max Tijk) | | 130 | = 3,92 |
| Daily Production Cost (Euro/Day) | Cost Unit 312,00 € | X | Capacity of Vehicle per Shift | | 3,92 | = 1223,04 € |
| Annual Production Capacity (Vehicle/Year) | Capacity of Vehicle per Shift 3,92 | X | Workday (All year) | | 250 | = 980 |
| Annual Production Cost (Euro/Year) | Cost Unit 312,00 € | X | Annual Production Capacity | | 980 | = 305.760,00 € |

Though the cycle time decreased to 130 minutes compared to Model-2, the Actual Unit Cost and the Annual Production Cost showed a decreasing increase

because 6 operators worked more. Moreover, since the cycle time decreased, the production capacity increased.

3.3 Sensitivity Analysis 3 (New Model 2.3)

The new model (Model 2.3) constituting the 3rd step of the sensitivity analysis will be established by being expended according to the 9th and 10th stations to which the objective function and constraints of Model 2.3 will be added, 5 tasks connected to these stations and the new 10 operators added to 40 operators. There will be a total of 25 tasks and 25 operators will be required. In addition to Table 3, technical requirement for making positioner spot and its welding at a minimum 3rd level at the 9th station and technical requirement for making MAG welding at a minimum 3rd level at the 10th station are required. In addition to Table 6, Table 18 was obtained for the 9th and 10th stations. See also Apandix-5 for the competencies of new operators added.

Table 18. Maximum-Minimum Period Table Obtained For Each Task from Time Surveys Taken From Operators of Different Abilities (9th and 10th Stations-New)

| New Min-Max Time Studies (minute) | | | | | |
|-----------------------------------|---------|-------|-----|-----|-----|
| Works | Max-Min | 1L | 2L | 3L | 4L |
| | | 9.Sta | Max | 130 | 120 |
| 1.Work | Min | 125 | 110 | 95 | 70 |
| 9.Sta | Max | 130 | 120 | 100 | 90 |
| 2.Work | Min | 125 | 110 | 95 | 70 |
| 9.Sta | Max | 130 | 120 | 100 | 90 |
| 3.Work | Min | 125 | 110 | 95 | 70 |
| 10.Sta | Max | 120 | 110 | 100 | 90 |
| 1.Work | Min | 115 | 105 | 95 | 70 |
| 10.Sta | Max | 120 | 110 | 100 | 90 |
| 2.Work | Min | 115 | 105 | 95 | 70 |

According to the solution report belonging to the mathematical new model written in gams 23.5, the objective function value was found as 130 minutes. When the model solution results are examined, it is seen that contrary to Model-2 and Model-2.1, Xijk, which is the 0-1 decision variable, do not take approximate values, but takes exact values as desired and in a similar way with Model 2.2. Operators added to the system in Model-2.3 were selected as fully competent for all stations and tasks (4th level). Therefore, looking at the model result, it is seen that since there were a sufficient number of operators suitable for the desired competencies of the tasks, a full-value assignment was done. Assignments made in the Gams program were transferred to the table as follows; the assignment values of the decision variables, the total task time assigned to the operator (Sij), and the station cycle time (Ci), which takes the maximum value of the (Sij)s assigned to the station are shown on the table.

Table 19. Summary Table of Assignments Made according to the Sensitivity Analysis 3 Model-2.3 Solution

| Model-2.3 Summary Table of Assigns | | | | | | |
|------------------------------------|----------|--------------|------------------------|--------------|-----------------|-----|
| Sta (i) | Work (j) | Assing Value | Assinged Operators (k) | Times (Tijk) | Cycle Time (Ci) | |
| 1. sta | 1.work | 1 | 39.op | 120 | C1 | 120 |
| 1. sta | 2.work | 1 | 29.op | 80 | | |
| 2.sta | 1.work | 1 | 32.op | 80 | C2 | 130 |
| 2.sta | 2.work | 1 | 8.op | 75 | | |
| 2.sta | 3.work | 1 | 5.op | 110 | | |
| 2.sta | 4.work | 1 | 42.op | 130 | | |
| 3.sta | 1.work | 1 | 1.op | 130 | C3 | 130 |
| 3.sta | 2.work | 1 | 9.op | 125 | | |
| 3.sta | 3.work | 1 | 2.op | 120 | C4 | 125 |
| 4.sta | 1.work | 1 | 38.op | 125 | | |
| 4.sta | 2.work | 1 | 37.op | 125 | C5 | 110 |
| 5.sta | 1.work | 1 | 28.op | 110 | | |
| 5.sta | 2.work | 1 | 30.op | 80 | | |
| 5.sta | 3.work | 1 | 41.op | 110 | C6 | 110 |
| 6.sta | 1.work | 1 | 40.op | 110 | | |
| 6.sta | 2.work | 1 | 48.op | 90 | C7 | 90 |
| 7.sta | 1.work | 1 | 47.op | 90 | | |
| 7.sta | 2.work | 1 | 46.op | 90 | C8 | 90 |
| 8.sta | 1.work | 1 | 7.op | 90 | | |
| 8.sta | 2.work | 1 | 3.op | 90 | C9 | 90 |
| 9.sta | 1.work | 1 | 45.op | 90 | | |
| 9.sta | 2.work | 1 | 44.op | 90 | | |
| 9.sta | 3.work | 1 | 43.op | 90 | C10 | 100 |
| 10.sta | 1.work | 1 | 18.op | 90 | | |
| 10.sta | 2.work | 1 | 11.op | 100 | | |

Table 20. Results related to the Capacity and Financial Status of the Company When Assignments are Made According to the Sensitivity Analysis 3 Model-2.3 Solution

| Model-2.3Results of Capacity and Financial Rates | | | | | |
|--|-------------------------------|---|-------------------------------|------------------|----------------|
| Cost Unit (Euro/Takt) | Cycle Time (max Tijk) | | Cost Unit(C w) | Total Operato rs | |
| | 130 | X | 0,12 | X | 25 = 390,00 € |
| Capacity of Vehicle per Shift(Vehicle/Shift) | Shift Time | / | Cycle Time (max Tijk) | | |
| | 510 | | 130 | | = 3,92 |
| Daily Production Cost (Euro/Day) | Cost Unit | X | Capacity of Vehicle per Shift | | |
| | 390,00 € | | 3,92 | | = 1528,80 € |
| Annual Production Capacity (Vehicle/Year) | Capacity of Vehicle per Shift | X | Workday (All year) | | |
| | 3,92 | | 250 | | = 980 |
| Annual Production Cost (Euro/Year) | Cost Unit | X | Annual Production Capacity | | |
| | 390,00 € | | 980 | | = 382.200,00 € |

Since the task with the longest work time (the 4th task at the 2nd stations and the 1st task at the 3rd station) takes 130 min, although the duration of the other tasks are shorter, there will be waiting in other tasks until the end of the 130-minute task; in other words, it is the task that constitutes the bottleneck of the line. For this reason, even if all operators work under 130 min, their labor

costs are paid as if they worked for 130 min and while the direct labor cost of the vehicle is loaded, 130-minute work time is taken into account.

Though the cycle time decreased to 130 minutes compared to Model-2, the Actual Unit Cost and the Annual Production Cost showed a decreasing increase because 11 more workers worked. Moreover, since the cycle time decreased, the production capacity increased.

4. Results and Discussions

4.1 Results and Recommendations Related to the Assignment of the Operator who has the Right Competency to the Right Task, Training Planning, Human Resource Planning and Productivity

It was seen that in Model-2 and Model-2.1, the Xijk decision variable received a decimal value between 0 and 1, but in Model-2.2 and model-2.3, it received value of 0 or 1 as desired. When the reason of this was examined, it was observed that there was no human resource (operator) who had appropriate competency in Model-2 and model-2.1. Therefore, in the model, the assignments were done by giving decimal values to some competent operators. In Model-2.2, it was intervened in this situation; the 35, 36, 37, 38, 39 and 40th operators with the highest level of competence in all tasks were included in the model and it was ensured that the assignments were converted into 0 or 1. The same situation was carried out by including the 41, 42, 43, 44, 45, 46, 47, 48, 49, 50th operators with full competence in the model. In an enterprise, this situation means that when the model is run, if there is an assignment other than the value of 0 or 1, there is a missing labor force in the station or task where this assignment is performed. This situation must be reported to the planning department and assignment of an operator with appropriate competence should be ensured. If there is no such operator, the subject should be communicated to the Human Resources Unit, the decision to make training planning for existing operators or the decision to seek new human resources should be made. In this way, training plans and human resource needs can be objectively revealed. From a different viewpoint, because increasing the competencies of operators will create a supply, increasing the competency will also trigger for individual competition. All of these effects will result in a win-win relationship while increasing the intangible assets (intellectual capital) in the medium-term from the growth-learning perspective for the firm. In the medium and long-term, there will be many productivity gains, such as the development of operations, the decrease in cycle time, and the increase in capacity. It will be possible to observe that intangible assets (intellectual capital) transform into tangible assets for the company along with their productivity outputs. The established model pointed out that the person with

the correct competence should work in the correct operation; also, the gains that it would bring were evaluated in terms of the medium and long-term.

4.2 Results and Recommendations Related to Productivity Provided by the Cycle of Finding Bottlenecks and Continuous Recovery

It is observed that as a result of the assignments in Model-2 and model-2.1, the cycle time has remained at 140 minutes, and as a result of the assignments with the addition of competent staffs into the model-2.2, it has dropped to 130 minutes. In the model-2.3, it is seen that although it has been continued to add the competent staffs in the model, the cycle time has not improved, but remains in 130 minutes as a result of the assignments. When the reason of this is examined, for Model 2.2 and model 2.3, it is seen that the duration of the work is 130 minutes, even if the most competent operator (4th level) were assigned for “the 4th task at the 2nd Station” and “the 1st task at the 3rd Station”. In an enterprise, this should mean that when you run the model, if you want to perform productivity studies in tasks affecting the cycle time, such as improving cycle time, line balancing, and providing capacity increase, it is necessary to perform improvement in the task or tasks that affect cycle time. When the model is executed, it is pointed out to the points of the task or tasks (that is, operations) that create bottlenecks and that affect the cycle time. This indicates that an enterprise needs improvement in which product, which station, and which task of the relevant station. After the improvement, a model that provide the presentation of the data in an objective in which direct results can be obtained and comparison for before and after can be made was developed. At the same time, the necessity of using simple production techniques come into prominence. In the improvements to be made, it should be focused on the non-value added activities in the operation prior to Kaizen, improvements should be designed to eliminate them, team works should be carried out on how value added activities can be done more efficiently, measurements should be repeated after Kaizen, and the difference should be reflected to the model as a result of improvement. Simple production methods can be taken as a guide in the operation improvement studies to be carried out. In order to emphasize the necessity and importance of the improvement, it was assumed that in “Sensitivity Analysis Model-2.3”, an improvement was made on the 130-minute “4th task at the 2nd station” and “1st task at the 3rd station” which affected the cycle time. Assuming that this time was reduced from 130 minutes to 110 minutes, the same model was run again as “Sensitivity Analysis Model-2.3 Version 2”, and the following results was obtained. According to the solution report for the new

mathematical model written in gams, the objective function value was found as 125 minutes.

Table 21. Summary Table of the Assignments Made According to the Solution of Sensitivity Analysis 3 Model-2.3 Version 2

| Model-2.3 Version 2 Summary Table of Assigns | | | | | |
|--|----------|--------------|------------------------|--------------|-----------------|
| Sta (i) | Work (j) | Assing Value | Assinged Operators (k) | Times (Tijk) | Cycle Time (Ci) |
| 1. sta | 1.work | 1 | 39.op | 120 | C1 |
| 1. sta | 2.work | 1 | 29.op | 80 | |
| 2.sta | 1.work | 1 | 32.op | 80 | C2 |
| 2.sta | 2.work | 1 | 3.op | 75 | |
| 2.sta | 3.work | 1 | 43.op | 110 | C2 |
| 2.sta | 4.work | 1 | 44.op | 110 | |
| 3.sta | 1.work | 1 | 9.op | 110 | C3 |
| 3.sta | 2.work | 1 | 1.op | 125 | |
| 3.sta | 3.work | 1 | 2.op | 120 | C3 |
| 4.sta | 1.work | 1 | 37.op | 125 | |
| 4.sta | 2.work | 1 | 36.op | 125 | C4 |
| 5.sta | 1.work | 1 | 38.op | 110 | |
| 5.sta | 2.work | 1 | 30.op | 80 | C5 |
| 5.sta | 3.work | 1 | 42.op | 110 | |
| 6.sta | 1.work | 1 | 41.op | 110 | C6 |
| 6.sta | 2.work | 1 | 50.op | 90 | |
| 7.sta | 1.work | 1 | 49.op | 90 | C7 |
| 7.sta | 2.work | 1 | 48.op | 90 | |
| 8.sta | 1.work | 1 | 46.op | 90 | C8 |
| 8.sta | 2.work | 1 | 45.op | 90 | |
| 9.sta | 1.work | 1 | 47.op | 90 | C9 |
| 9.sta | 2.work | 1 | 40.op | 90 | |
| 9.sta | 3.work | 1 | 28.op | 90 | |
| 10.sta | 1.work | 1 | 5.op | 90 | C10 |
| 10.sta | 2.work | 1 | 1.op | 100 | |

As seen in the assignments of Sensitivity Analysis 3 Model -2.3 Version 2, when it was assumed that an improvement was made on the 130-minute “4th task at the 2nd station” and “1st task at the 3rd station” and when it was accepted that this time was reduced from 130 minutes to 110 minutes, as a result of the assignments, the model was able to be reduced only to 125 minute cycle time due to other works that had effects on cycle time. When the model was run, it was said that the task or tasks (that is, operations) that affect the cycle time pointed out to the points creating the bottleneck and this indicated that an enterprise needed to be improved in which product, which station, and which task of the relevant station. Looking at the assignments of the Sensitivity Analysis 3 Model-2.3 version 2, they indicate that the new improvement points are “the 2nd task at the 3rd stations”, “the 1st task at the 4th station” and the “2nd task at the 4th Station”. These operations also should be improved by making new kaizens, pre-post measurements should be done and continuous improvement cycle should be established by running the model according to new data at each time.

4.3 Results and Recommendations on Cycle Time, Number of Operators and Unit Cost

The following chart summarizes the cycle time of the established models, the number of operators needed to

perform the production during this cycle, and the production cost per vehicle when the constraints of the models are ensured.

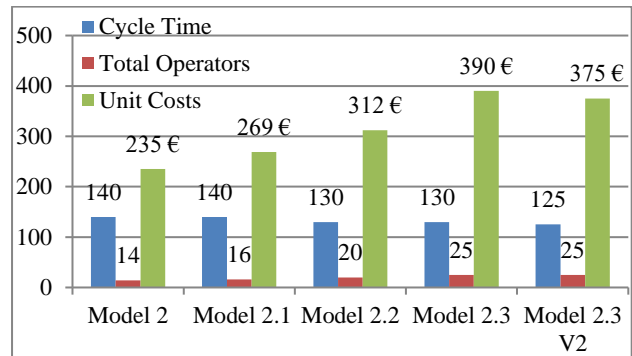


Figure 1. Results obtained on cycle time, number of operators (operators) and unit cost

- In the Sensitivity Analysis Model-2.1, with the addition of “the 6th Station 1st and 2nd tasks” to the Model-2, the number of operators increased from 14 operators to 16 operators and the cost per unit of the vehicle increased because the cycle time did not change.
- In the Sensitivity Analysis Model-2.2, with the addition of “the 7th Station 1st and 2nd tasks” and “the 8th station 1st and 2nd tasks” to the Model-2.1, the number of operators increased from 16 operators to 20 operators and the cost per unit of the vehicle increased although the cycle time changed. If the cycle time was the same, the unit cost would be 337 Euros, but it is currently 312 Euros. Reduction in cycle time provided an 8% cost recovery in cost per vehicle.
- In the Sensitivity Analysis Model-2.3, with the addition of “the 9th Station 1st, 2nd and 3rd tasks” and “the 10th station 1st and 2nd tasks” to the Model-2.2, the number of operators increased from 20 operators to 25 operators and the cost per unit of the vehicle increased because the cycle time did not change.
- In the Sensitivity Analysis Model-2.3 Version 2, with the assumed improvement in cycle time compared to the Model-2.3, it was observed that with the same sources and constraints, the unit cost became 390 euros instead of 375 euros. The decrease in cycle time provided a 4% cost recovery in cost per vehicle.

4.4 Results and Recommendations on Annual Production Capacity and Annual Production Cost

The annual production capacities and the annual production costs obtained in the established models are summarized in the charts below.

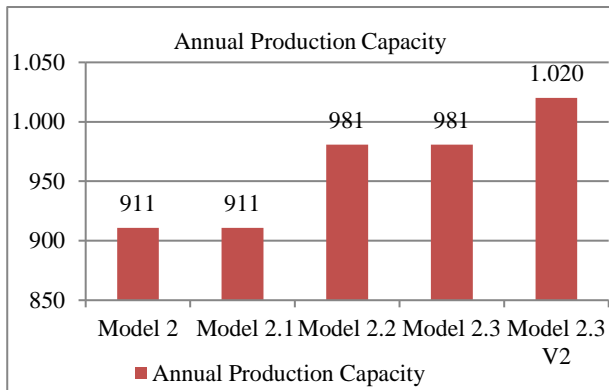


Figure 2. The obtained results on annual production capacity

- In Model-2 and Sensitivity Analysis Model 2.1, the company has the capacity to produce 911 vehicles per year since the cycle time is the same.
- In the Sensitivity Analysis Model 2.2 and Sensitivity Analysis Model 2.3, since the cycle time decreased from 140 minutes to 130 minutes, the capacity of the company increased to the capability of producing 981 vehicles per year. 8% capacity increase was observed here.

In the Sensitivity Analysis Model 2.3 Version 2, when the model was run according to the assumption that improvement was done in the operation, the capacity of the company increased to the capability of producing 1020 vehicles per year because the cycle time was reduced from 130 to 125 minutes. 4% capacity increase was observed here. A 5-minute improvement in the cycle time created an opportunity to produce 39 more vehicles in a year and 4% capacity improvement was achieved. Even if this result is based on the assumption, it reveals the ability of the model to determine the continuous improvement needs and also shows the consequences of this.

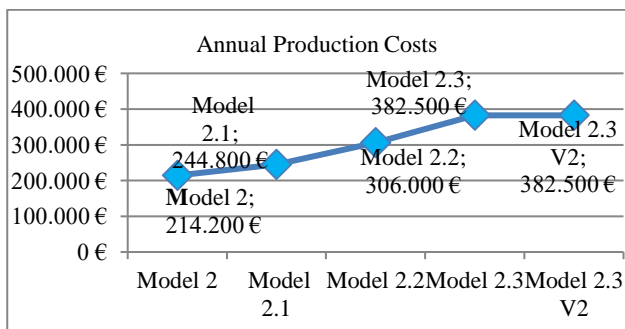


Figure 3. Results obtained on annual production cost

5. Conclusions

In the models, the annual production costs that the enterprise must bear in line with its annual production are as shown in the chart. By adding the fixed expenses and the vehicle sales figures in the annual budget to these analyses as data and by taking the variable costs from the annual production cost according to the data of the

model, the break-even analysis of the enterprise can be achieved, and by combining it with the results of the model, it can be contributed to the strategic planning and projects of the enterprise.

References

1. Hillier, F.S., Lieberman, G.J., *Introduction to Operations Research*, 2010, New York:McGraw-Hill,Inc.
2. Nash, J., *The Dantzig simplex method for linear programming*. Computing in Science & Engineering, 2000. p.29-31.
3. Hitchcock, F., *The Distribution of a Product from Several Sources to Numerous Localities*. Studies in Applied Mathematics, 1941. p.224-230.
4. Kuhn, H. W., *The Hungarian Method for the Assignment Problem*. Naval Research Logistics Quarterly, 1955. (2): p.1-2.
5. Koopmans, C. and Beckmann, M., *Assignment Problems and the Location of Economic Activities*, *Econometrica*, 1957. 25(1): p. 53-76.
6. Ferjani, A., Ammar, A., Pierreval, H., Elkosantini, S., *A simulation-optimization based heuristic for the online assignment of multi-skilled workers subjected to fatigue in manufacturing systems*, *Computers & Industrial Engineering*, 2017. p. 663-674.
7. Brilon, S., *Job Assignment with Multivariate Skills*, Preprints of the Max Planck Institute for Research on Collective Goods, 2010.
8. Moreira, M., and Costa, A., *A minimalist yet efficient tabu search algorithm for balancing assembly lines with disabled workers*, *XLI SBPO Pesquisa Operacional na Gest3o do Conhecimento*, 2009: p. 660-671.
9. Li, Q., Gong, J., Tang, J. and Song, J., *Simulation of The Model of Workers Assignment in Cellular Manufacturing based on the Multifunctional Workers*, *Chinese Control and Decision Conference*, 2008.
10. Ammar, A., Pierreval, H., Elkosentini, S., *Worker Assignment Problems in Manufacturing Systems: A Literature Analysis*, Rabat-Morocco IESM Conference, 2013.
11. Nizami, S., Khan, F., Khan, N., Inayatullah, S., Inayatullah, S., *A New Method for Finding the Cost of Assignment Problem Using Genetic Algorithm of Artificial Intelligence*, *International Journal of Latest Trends in Computing*, 2011. 2(1): p.135.
12. Kotwal, J. and Dhope, T. *Solving Task Allocation to the Worker Using Genetic Algorithm*, *International Journal of Computer Science and Information Technologies*, 2015. 6 (4): p.3736-3741
13. Cesani, V. and Steudel, H., *A study of labor assignment flexibility in cellular manufacturing systems*, *Computers & Industrial Engineering*, 2005. 48: p.571-591.
14. Heimerl, C. and Kolisch, R., *Work assignment to and qualification of multiskilled human resources under knowledge depreciation and company skill level targets*, *International Journal of Production Research*, 2010. 48(13): p.3759-3781.
15. Norman, B., Tharmmaphornphilas, V., Needy, K., Bidanda, B. and Warner, R., *Worker assignment in cellular manufacturing considering technical and human skills*, *International Journal of Production Research*, 2002. 40(6): p. 1479-1492